Terms and Conditions of Use of Digitised Theses from Trinity College Library Dublin

Copyright statement

All material supplied by Trinity College Library is protected by copyright (under the Copyright and Related Rights Act, 2000 as amended) and other relevant Intellectual Property Rights. By accessing and using a Digitised Thesis from Trinity College Library you acknowledge that all Intellectual Property Rights in any Works supplied are the sole and exclusive property of the copyright and/or other IPR holder. Specific copyright holders may not be explicitly identified. Use of materials from other sources within a thesis should not be construed as a claim over them.

A non-exclusive, non-transferable licence is hereby granted to those using or reproducing, in whole or in part, the material for valid purposes, providing the copyright owners are acknowledged using the normal conventions. Where specific permission to use material is required, this is identified and such permission must be sought from the copyright holder or agency cited.

Liability statement

By using a Digitised Thesis, I accept that Trinity College Dublin bears no legal responsibility for the accuracy, legality or comprehensiveness of materials contained within the thesis, and that Trinity College Dublin accepts no liability for indirect, consequential, or incidental, damages or losses arising from use of the thesis for whatever reason. Information located in a thesis may be subject to specific use constraints, details of which may not be explicitly described. It is the responsibility of potential and actual users to be aware of such constraints and to abide by them. By making use of material from a digitised thesis, you accept these copyright and disclaimer provisions. Where it is brought to the attention of Trinity College Library that there may be a breach of copyright or other restraint, it is the policy to withdraw or take down access to a thesis while the issue is being resolved.

Access Agreement

By using a Digitised Thesis from Trinity College Library you are bound by the following Terms & Conditions. Please read them carefully.

I have read and I understand the following statement: All material supplied via a Digitised Thesis from Trinity College Library is protected by copyright and other intellectual property rights, and duplication or sale of all or part of any of a thesis is not permitted, except that material may be duplicated by you for your research use or for educational purposes in electronic or print form providing the copyright owners are acknowledged using the normal conventions. You must obtain permission for any other use. Electronic or print copies may not be offered, whether for sale or otherwise to anyone. This copy has been supplied on the understanding that it is copyright material and that no quotation from the thesis may be published without proper acknowledgement.

Molecular Algorithms in Thyroid Neoplasia

A thesis submitted for the degree of

Doctor of Philosophy

by

Paul Smyth, BSc. (Hons)

University of Dublin, Trinity College

November 2004

Supervisor: Dr. Orla Sheils

Declaration

I declare that, except where otherwise acknowledged, this thesis is entirely my own work, and has not been submitted previously for a PhD degree at this or any other university. I agree that the library may lend or copy this thesis on request.

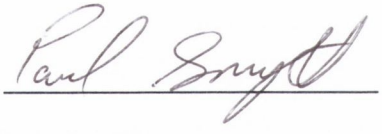

Paul Smyth

For my mother, Marian.

I firmly believe that any man's finest hour, the greatest fulfilment of all that he holds dear, is the moment when he has worked his heart out in a good cause and lies exhausted on the field of battle – victorious.

– Vince Lombardi

CONTENTS

List of Figures

Acknowledgements

I would like to thank all those who in some way or another have helped, cajoled and guided me during the researching and writing of this thesis. I would like to thank those who distracted me from it even more. There are far too many individuals to name but I shall endeavour and apologies to anyone I missed – it was probably intentional!!!!

To begin with I would like to thank Prof. John O'Leary, the man who makes it all happen. His enthusiasm for his students and their research astounds me to this day. May he may reign long over his impressive and ambitious department and research unit who provided me with an embarrassment of riches with which to conduct my research. Dr. Sheils – the woman from whom I took the red pill those many years ago. I owe you a debt of gratitude that I can never repay. From a salary to her acute proof-reading skills (!!!), the trips abroad to her kind advice and guidance, she has never failed to deliver yet. I could go on and on but thank you Orla. Now how do I get out of Wonderland and how deep is this rabbit hole anyhow? Thanks also go out to Prof. Eamon Sweeney for his valued input and advice when I was just starting out.

Next, my partners in crime – the past and present members of the Histopathology department. In chronological order: Niamh Murphy, original member of the molecular Montessori club. Thanks for all the laughs and especially your little anecdotes. Oz doesn't know how lucky it is. Stephen Finn, the other original member. What can I say? Smartest man I've ever known and like a father to me. My (very) limited pathology knowledge is attributable to you, at least what I can remember after the many legendary

nights spent out with you that are now a part of St. James's folklore. His lovely wife Esther, *the* asker of questions. For all your advice on issues of the fairer sex, pastel colours, JCBs and nights out along with your husband – thank you. Richard Flavin, MC extraordinaire – another drinking buddy, master of the Púca and a hell of a roommate in Amsterdam. His skills also include pathology!!!! The latest addition to our motley crew, Susanne (with an 's') Cahill, a fellow scientist and Swords native. Thank you for the (many) shared bus and luas rides and for keeping me up to date with more celebrity gossip than a man should ever know. To another Amsterdam adventurer and frequent drinking buddy – Amanda Murphy, thank you also.

A big thank you goes out to those that worked in the Coombe Women's Hospital especially Cara Martin and my boys, the gone but not forgotten, Ivan Silva and Richard Shattock, ex- and current New Yorkers respectively. To all those (far too many to name) who have worked in the routine Histopathology lab and their chief, Ronan Ward, I thank you all for your assistance and frequent lease of space!!!!!

There are some people from further afield that I wish to thank for their input and assistance. From IPATIMUP in Porto, Portugal – Dr. Paula Soares and Prof. Manuel Sobrinho-Simões for their technical input and advice. Speaking of technical input, I would like to thank all of the following who at some point have worked for Applied Biosystems and have provided a wealth of technical knowledge, advice and troubleshooting: Steve Picton, Adam Corner, David Howells and more recently Chris Streck.

As for civilians, I'd like to thank my old biotech buddies, Brian, Nick and Diarmuid for the memorable years both in college and after, and for never *ever* discussing work or theses. Dave and Dara who still don't understand to this day what I do. To all the guys of the Dublin Rebels American Football Club for calling me the smartest thing ever to hit them and for the frequent absentee Mondays following away trips!!!

Finally, I wish to thank my family. They may not have had as much input into this thesis as those mentioned so far but they have been a consistent source of support and encouragement, not to mention a convenient punch bag at times!!! To Dave and Amy for putting up with the biggest brother ever and our mother Marian, our pillar of strength and, as I have come to realise over the years, a true friend. This thesis would never have happened were it not for her. And lastly, but not least, thanks to my long-suffering girlfriend Jennie for sticking with me through thick and thin. For all the love and support you have given me, frequent taxi service, and for managing the *entire* purchase of our new house – you are truly an angel.

List of Abbreviations

A	adenosine
AD	allelic discrimination
AJ	adherens junction
ANOVA	analysis of variance
AP	alkaline phosphatase
APC	adenomatous polyposis coli
ATC	anaplastic thyroid carcinoma
bp	base pair
C	cytosine
CAM	cellular adhesion molecule
cDNA	complementary/copy DNA
CO_2	carbon dioxide
cRNA	copy RNA
C_T	threshold cycle
DIG	digoxigenin
DMEM	Dulbecco's Modified Eagle's Medium
DMSO	dimethylsulphoxide
DNA	deoxyribonucleic acid
dNTP	deoxynucleoside triphosphate
E	glutamic acid
EDTA	ethylenediaminetetraacetic acid
EGFR	epithelial growth factor receptor

ERK	extracellular-signal-regulated kinase
FA	follicular adenoma
FCS	foetal calf serum
FDR	false discovery rate
FFPE	formalin fixed paraffin embedded
FNA(B)	fine needle aspiration (biopsy)
FTC	follicular thyroid carcinoma
G	guanine
GAPDH	glyceraldehyde phosphate dehydrogenase
GDNF	glial-cell line derived neurotrophic factor
GDP	guanine diphosphate
GTP	guanine triphosphate
H & E	hematoxylin and eosin
hCG	Human chorionic gonadotropin
HGF/SF	hepatocyte growth factor/scatter factor
HT	Hashimoto thyroiditis
IVT	in vitro transcription
JNK	c-Jun N-terminal kinase
Kb	kilobases
LB	Luria Betani
LCM	laser capture microdissection
LOH	loss of heterozygosity
MAPK	mitogen activated protein kinases

MEN	multiple endocrine neoplasia
MGB	minor groove binder
$MgCl_2$	magnesium chloride
mRNA	messenger RNA
MTC	medullary thyroid carcinoma
MuLV	Murine Leukaemia Virus
NFQ	non-fluorescent quencher
NGF	nerve growth factor
NORM	normal/non-malignant tissue
NTC	no template control
PBS	phosphate buffered saline
PCR	polymerase chain reaction
PI3K	phosphatidylinositol 3-kinase
PTC	papillary thyroid carcinoma
RET	rearranged during transfection
RNA	ribonucleic acid
RPMI	Roswell Park Memorial Institute
RT	reverse transcription
S/N	signal to noise ratio
SNP	single nucleotide polymorphisms
T	thymidine
T_3	triiodothyronine
T_4	thyroxine

TBG	thyroxine-binding globulin
TE	tris-EDTA
Tm	melting temperature
TNS	Trypsin neutralising solution
TSH	thyroid stimulating hormone
UV	ultraviolet
V	valine

Publications

Smyth P, Sheils O, Finn S, Martin C, O'Leary J, Sweeney EC. Real-time quantitative analysis of E-cadherin expression in ret/PTC-1-activated thyroid neoplasms. Int J Surg Pathol 2001; 9: 265-72.

Smyth P, Finn S, O'Leary J, Sheils O. Real-time analysis of beta- and gamma-catenin mRNA expression in ret/PTC-1 activated and nonactivated thyroid tissues. Diagn Mol Pathol 2003; 12: 44-9.

Finn SP, Smyth P, O'Leary J, Sweeney EC, Sheils O. Ret/PTC chimeric transcripts in an Irish cohort of sporadic papillary thyroid carcinoma. J Clin Endocrinol Metab 2003; 88: 938-41.

Finn SP, Smyth P, O'Regan E, Cahill S, Flavin R, O'Leary J, Sheils O. Array comparative genomic hybridisation analysis of gamma-irradiated human thyrocytes. Virchows Arch 2004; 445: 396-404. Epub 2004 Jul 17.

Smyth P, Finn S, Cahill S, O'Regan E, Flavin R, O'Leary JJ, Sheils O. ret/PTC and BRAF act as distinct molecular, time-dependant triggers in a sporadic Irish cohort of papillary thyroid carcinoma. Int J Surg Pathol 2005; 13: 1-8.

Summary

Papillary thyroid carcinoma is the most common thyroid malignancy, with an incidence of <100 cases per year in Ireland and 16,000 cases per year in the U.S. Incidence is increasing with a global estimate of half a million new cases this year. However, benign thyroid nodules are far more frequent and distinguishing between them and malignant nodules is a common diagnostic problem. It is estimated that 5-10% of people will develop a clinically significant thyroid nodule during their lifetime. Although the introduction of fine needle aspiration (FNA) 30 years ago made identifying PTC more reliable, clinicians often have to make decisions regarding patient care on the basis of equivocal information.

The molecular pathogenesis of PTC is poorly characterised with only a few chromosomal or genetic abnormalities being described. V600E BRAF mutations and ret/PTC oncogene rearrangements are the most common. The purpose of this project was to evaluate molecular algorithms in thyroid neoplastic and inflammatory disease. The assessment was carried out using molecular techniques including TaqMan® PCR for both expression and genotyping, and microarray technology.

The effect of ret/PTC-1 oncogene rearrangement on expression levels of the cellular adhesion molecules E-cadherin and its ligands β- and γ-catenin was investigated. Variable down-regulation of adhesion molecules was demonstrated in thyroid carcinoma. Follicular lesions had significantly altered expression levels to papillary lesions. Expression levels of E-cadherin in Hashimoto's thyroiditis were comparable to those in

ret/PTC-1 positive papillary carcinomas suggesting not only an association between ret activation and the loss of cellular adhesion but, more significantly an association between papillary thyroid carcinoma and Hashimoto thyroiditis.

The incidence and temporal trends of BRAF mutation in thyroid cancer in the Irish population in conjunction with ret/PTC-1 was investigated. Heterozygous T1799A mutations were detected in 15 of 34 (44%) PTCs tested. No significant association between BRAF mutation and ret/PTC-1 was demonstrated. A significant temporal trend was observed, with ret/PTC chimera detected for the most part pre-1997 and BRAF mutations being more prevalent post-1997. Our results suggest that some environmental/etiological agent(s) may have influenced the pathobiology of thyroid tumour development, among the population examined, over time.

Finally, gene expression profiles for several thyroid cell lines were compared using a whole genome microarray system. A variety of cell lines were analysed which were characteristic of various papillary and anaplastic thyroid carcinomas harbouring genetic abnormalities consistent with those found *in vivo*. Genes involved in cell structure and motility and the extracellular matrix were consistently found to be differentially expressed between compared groups. This, coupled with the discovery of over-expressed histones in some groups, led to speculation that these genes may be responsible for the structural peculiarities of certain types of PTC. Escape of apoptosis was also a consistent theme with its inducers and inhibitors frequently found to be down- and up-regulated respectively. Individual genes from inter-group comparisons were also evaluated.

Chapter 1

Introduction

1.1 History of the thyroid

The occurrence of goitre was a common observation in Europeans over two millennia ago, especially to those living in the Alps (Merke, 1984). They did not know, however, that this condition was related to the thyroid gland, or in fact that the thyroid actually existed. The ancient Greeks called the swelling in the neck a *bronchocele* ("tracheal outpouch"). This term was still being used in the 19th century despite the fact that the thyroid had been discovered and named over 200 years previously. The gland was thought to round out and beautify the neck, thus explaining why women had larger glands than men. The many functions it was thought to serve include lubricating the larynx, serving as a vascular shunt to maintain blood flow to the brain and the formation of blood.

It took until the Renaissance period for the thyroid to be identified and characterised. It is presumed that da Vinci found it circa 1500. Vesalius termed it the laryngeal glands in 1543. Anatomists had definitely identified it in humans by the early 17th century and realised that its enlargement caused swelling in the neck. The glands more familiar modern term arose in 1656, when Thomas Wharton named it after the Greek for "shield-shaped", not by virtue of its own shape but because of the shape of nearby thyroid cartilage (Wharton, 1664).

Alpine travellers' observations of cretinism can be traced back as far as the 13th century, but clinically relevant descriptions did not appear until the 16th, when Paracelsus and Platter made the connection between goitre and cretinism (Cranefield, 1962). This was

the extent of human knowledge of thyroid physiology and disease until the 19th century. Prior to this, medical theories of the origin of disease were crude to say the least. An imbalance of the four humors: blood, phlegm, green bile and black bile, was thought to cause sickness in an individual. It was believed that goitre was caused by an excess of phlegm. Treatment was quite empiric and several remedies were proposed, usually comprising of mixtures of seaweed and marine sponge. These "treatments" were quite familiar to medieval Europeans, who were thought to have learned of them from the Chinese who had been using such substances to treat goitre for over a thousand years.

Iodine was discovered in the residue of burnt seaweed by Courtois in 1812. Subsequently, Coindet, a physician working with goitrous people in Geneva, considered iodine to be the active ingredient of the empiric remedies. In 1820, he gave iodine as a potassium salt to his patients. Their goitres shrank remarkably (Coindet J-F, 1820). Unfortunately, he also saw severe toxic effects in patients (not his own) who took too much of the miraculous remedy, which consequently fell into disfavour. Despite this, iodine continued to be administered for other disorders, including scrofula, tuberculosis and even syphilis (Lugol, 1829). Coindet had probably described the earliest case of iodine-induced thyrotoxicosis, although the true nature of the disorder was not recognised for decades.

At the time, most believed goitres to be caused by some outside influence such as a toxin, bacterium or parasite present in the food chain/water supply. Few accepted the theory that diseases could be caused by an inherent lack of something in the body. The issue was not resolved until the 1920s when iodine was found to prevent goitre in schoolgirls in Akron,

Ohio (Marine et al., 1920). Even post-1920, the concept of iodine replacement therapy never became widespread due to the thyrotoxicosis taboo that remained attached to it. This negativity resulted in continued goitre and the associated cretinism. The usefulness of iodine as a prophylactic agent has still, to this day, not been implemented universally. The International Council for the Control of Iodine Deficient Disorders currently attempts to ensure that everyone receives adequate amounts of iodine worldwide.

In his published Meath Hospital lectures (Graves, 1835), Dublin doctor Robert Graves and his student Stokes described a group of women with goitre, palpitations and exophthalmos. Both believed the illness to be cardiac in origin. The descriptions were not well known on the European continent, so when Basedow described similar patients in 1840 (Basedow, 1840), he was thought to be the first to describe the illness. Graves' and Basedow's disease subsequently became synonymously known as the former. At the time though, the disease was not thought to be connected to the thyroid. However, by the end of the 19th/beginning of the 20th century, there was a shift in medical thinking toward a thyroid origin for goitre. Partial/full thyroidectomies were being performed without excessive fatalities with the survivors being relatively "cured". It was at the turn of the century that thyroidtoxicosis was also finally understood.

Hypothyroidism was recognised clinically even later than hyperthyroidism. It was initially defined in London in the 1870s and was termed myxoedema because of the swollen skin (oedema) and its excess content of mucin (myx-). Once again it was misdiagnosed as a neurologic or skin disorder. Full understanding of the condition did not

come until 1888 (Ord, 1888) following observations that patients with total thyroidectomies were similar to those with myxedema.

Despite the increased level of understanding, a treatment proved elusive. At the time, Brown-Sequard was working on the subject of organotherapy - the use of tissue extracts for the treatment of diseases. Although his work with testicular extracts proved promising, most of the treatments failured. Until that is, Murray began to inject sheep thyroid extract into myxedema patients in 1891 (Murray, 1891), resulting in an unlikely cure. A year subsequently, the injections were disposed of and patients merely had to ingest ground or fried sheep thyroid.

The active ingredient in thyroid extracts remained a mystery, even though Baumann discovered iodine in the thyroid gland in 1895. It took another 20 years for Kendall and his associate Osterberg of the Mayo Clinic isolated bioactive crystalline material from thyroid extract on Christmas Day, 1914, which they subsequently named thyroxin (Kendall, 1915). However, Kendall was wrong about the molecule's structure and never succeeded in synthesising the active molecule. In 1926, Harington figured out the correct structure and a year later synthesised the molecule and renamed it thyroxine (Harington, 1926, 1927).

Kendall patented his extracted thyroxine and sold it commercially, but it was by far more expensive and not as effective as desiccated thyroid. Harington's synthesised treatment was also too costly. Therefore, administration of desiccated thyroid remained standard

treatment for myxedema until the successful synthesis of thyroxine in high yields as a salt in 1949 led to its use therapeutically to modern times. Although both men suspected there to be a second hormone at work in the thyroid, neither of them ever found it. That accolade went to Harington's later associate in London's National Institute for Medical Research, Pitt-Rivers who, in 1952 discovered and synthesised triiodothyronine (Gross, 1952). A group in Paris duplicated the work almost simultaneously and the presence of a second thyroid hormone was confirmed.

1.2 Thyroid embryonic development

The thyroid is the earliest recognisable endocrine glandular structure in mammalian development. Between the second and eleventh week of gestation, the thyroid begins to develop from three pharyngeal bodies: the median anlage and two lateral anlagen. The gland begins thyroid hormone production by the 12th week of foetal life.

The median anlage develops first from an invagination of the developing pharyngeal endoderm located at the base of the tongue and is visible during gestational days 16 and 17. The thyroid diverticulum continues to expand ventrally but remains attached to the pharyngeal floor via the thyroglossal duct. The rudimentary thyroid then begins to expand laterally, leading to the formation of the characteristic bilobed structure. It then enlarges further, becomes lobulated and bifurcates prior to its descent in front of the hyoid bone to its final resting position anterior to the trachea by about 7 weeks. The descended thyroid expands and enlarges further, both laterally and caudally. The thyroglossal duct normally atrophies in gestational weeks 7-10 following descent.

The lateral thyroid develops from the fourth or fifth branchial pouches as the medial thyroid anlage makes its descent. These ultimobranchial bodies eventually separate from the pharyngeal pouches after the 7th week of gestation and fuse with the lateral parts of the medial thyroid. The connection from the lateral lobes to the pharynx is lost and cells from the differentiating medial anlage surround tissue derived from the lateral anlage. The merging of the anlage is usually complete by 8 – 9 weeks of gestation at which time the thyroid has assumed its definitive form.

The ultimobranchial bodies/lateral anlagen are thought to give rise to the calcitonin-producing C cells as well as follicular cells. Persistence of ultimobranchial body remnants, known as solid cell nests, can be seen in up to 30% of sectioned adult thyroids and 88% of foetal/neonatal glands.

The gland is initially composed of a solid mass of endodermal cells. However, epithelial cells are identifiable by 10 weeks and colloid synthesis commences by week 13. Follicles appear by the 14th week. Thyroglobulin is detectable from a relatively early stage – even prior to colloid formation. Its synthesis seems independent of thyroid-stimulating hormone (TSH), as this is not detectable in the pituitary gland until week 12. Thyroxine-binding globulin (TBG) is detectable by week 10 and increases to term.

1.3 Anatomy and normal structure/function

The thyroid lies on the anterior and lateral aspects of the trachea just below the cricoid cartilage. It is attached by a loose connective tissue capsule. Both superior and inferior parathyroid glands may be found close to the posterior of the thyroid, or within the thyroid itself, but their position varies. On gross examination, the adult thyroid gland is an encapsulated structure consisting of two lobes, each measuring about 2-2.5cm wide and 4-5cm long. The lobes are connected in the midline by the isthmus. 50% of thyroids have a pyramidal lobe, derived from the distal portion of the thyroglossal duct, extending upwards from the isthmus. The thyroid has a rich intraglandular capillary network that is supplied by the superior and inferior thyroidal arteries.

The gland is firm and light brown to red in colour. It weights approx. 1-2g at birth and gradually increases to 10-15g at puberty. Adult weights vary enormously from 15-35g depending on numerous factors including age, gender, activity, geography, hormonal status, individual size and iodine uptake. Much larger glands can be observed in goitre cases. Its weight is always higher in women and the gland varies in size with the menstrual cycle. The gland may atrophy with age and resemble its pubertal weight.

Thyroid sections have a lobular appearance due to the presence of thin fibrous septa. Microscopically it is composed of lobules, each containing 20-40 evenly dispersed follicles. Thyroid follicles are spheroid structures measuring 50-500μm in diameter. They are lined with cuboidal-to-low columnar epithelium which is filled with thyroglobulin-containing colloid (see Fig 1.1). The thyrocytes are highly polarised with a basal nucleus

and are surrounded by basement membrane, the components of which include laminin and type IV collagen. Groups of calcitonin-producing, neuroendocrine parafollicular cells (C cells) may be observed among the follicular cells, particularly in the upper zones of the gland, or in the confines of the basement membrane. C cells however make up less than 0.1% of the total thyroid cellular mass.

The thyroid is one of the most responsive organs in the human body and can respond to many stimuli. During puberty, pregnancy or bouts of hyperactivity, the gland increases in size and becomes more active, resulting in transient hyperplasia. In response to trophic agents from the hypothalamus, TSH is released by thyrotrophs in the anterior pituitary into the blood. The TSH causes the thyrocytes to pinocytise colloid and convert thyroglobulin to thyroxine (T_4) and triiodothyronine (T_3) (see Fig 1.2). This results in shrinkage of the colloid and the thyrocytes can become tall and columnar, sometimes forming infolded buds or papillae. T_4 and T_3 are subsequently released into the systemic circulation and are bound to plasma proteins such as TBG for transport to peripheral tissues. When the thyroid hormones are released at the ultimate destinations, they enter cells and interact with nuclear receptors. These receptors alter gene expression profiles in catabolic pathways and ultimately increase the basal metabolic rate. When the particular stress abates, involution of the thyroid histological changes occurs and a normal histology will be observed once again.

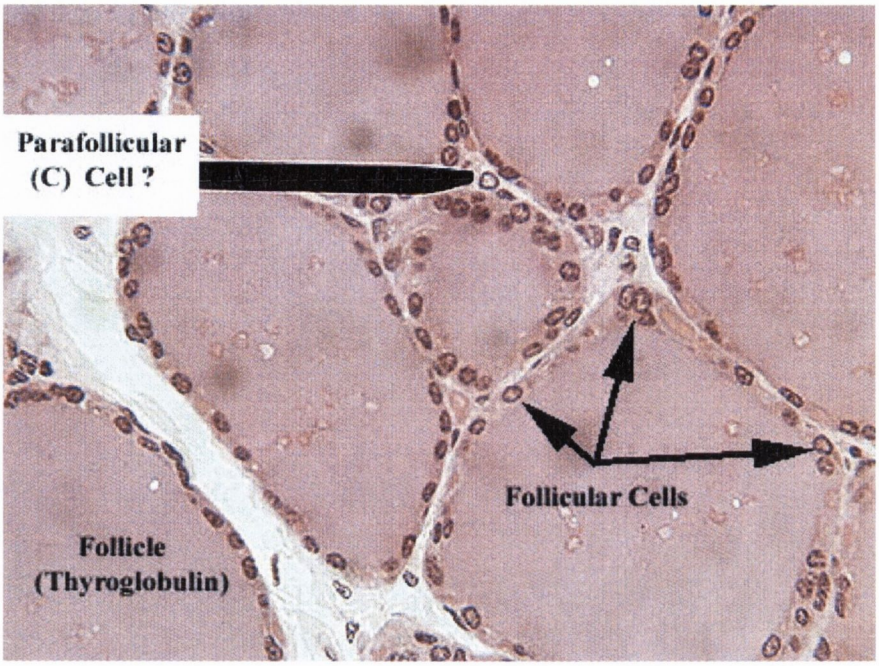

Figure 1.1 Normal microscopic histology of the thyroid.

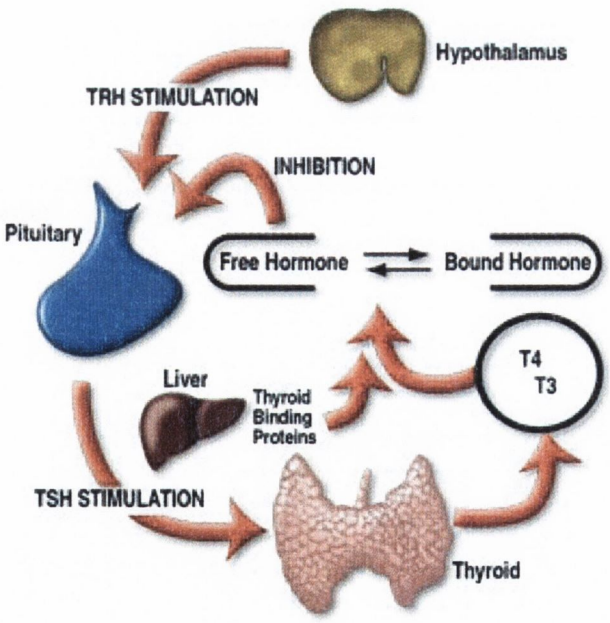

Figure 1.2 Synthesis of thyroid hormones and their regulatory pathways.

1.4 Thyroid disease states

Although the main focus of this thesis is on papillary thyroid carcinoma and Hashimoto thyroiditis, other disease states will be described to put both primary diseases in context. For the purpose of this thesis, the diseases of the thyroid gland have been divided into 4 groups: hyperthyroidism, hypothyroidism, thyroiditis and neoplasia. These will now be discussed individually.

1.4.1 Hyperthyroidism

Hyperthyroidism is a term generally assigned to describe thyrotoxicosis, a hypermetabolic state caused by elevated levels of T_3 and T_4, even though both terms technically describe two different illnesses. By far the most common cause of hyperthyroidism is Grave's disease, which accounts for ~80% of cases. This is then followed by toxic multinodular goitre and toxic adenoma as additional common causes. Rarer causes include TSH-secreting pituitary adenomas and iodine-induced hyperthyroidism. The terms primary and secondary hyperthyroidism are often used to describe hyperthyroidism arising from an intrinsic thyroid abnormality and that arising from processes outside of the thyroid, such as the above mentioned TSH-secreting pituitary adenomas. Damage to the thyroid caused by radioiodine therapy may induce transient hyperthyroidism. Hyperthyroidism can also occur in patients with hydatidiform moles or choriocarcinomas. Human chorionic gonadotropin (hCG) is the thyroid stimulator that causes hyperthyroidism in patients with trophoblastic tumours.

As for symptoms, patients typically show weight loss with an accompanying increase in appetite. They are nervous, hyperkinetic and emotionally labile. Patients with hyperthyroidism can have an increase in cardiac output resulting in tachycardia, palpitations and arrhythmias. Ocular changes can also occur with the manifestation of a wide, staring gaze with lid lag due to sympathetic overstimulation of the levator palpebrae superioris. Many patients are intolerant of heat, have warm skin and sweat excessively. Fatigue, diarrhoea, muscular weakness and visible enlargement of the thyroid are also common symptoms.

1.4.2 Hypothyroidism

Hypothyroidism is a collective term assigned to any structural or functional derangement that interferes with the production of sufficient amounts of thyroid hormone. The insult therefore can occur anywhere in the hypothalamic-pituitary-thyroid axis (see Fig 1.2). As with hyperthyroidism, hypothyroidism can be divided into primary and secondary categories, depending on whether the disorder arises from an intrinsic abnormality in the thyroid or as a result of hypothalamic or pituitary disease.

The primary variety can be caused by a simple lack of thyroid mass. A developmental abnormality would result in such a lack of function. A large resection/thyroidectomy for the treatment of hyperthyroidism or a primary tumour can result in hypothyroidism. Radiation can also ablate thyroid tissue, be it radioiodine treatment for hyperthyroidism or exogenous irradiation of the neck. The most common cause of hypothyroidism in

iodine-sufficient areas is chronic autoimmune thyroiditis (Hashimoto thyroiditis). This condition is described in section 1.4.3.1. Heritable biosynthetic defects, severe dietary iodine deficiency and antithyroidal drug therapy (such as methimazole and propylthiouracil) can result in hypothyroidism. Non-thyroidal drugs such as lithium can also contribute to the disease.

Secondary hypothyroidism is typically caused by hypopituitarism with reduced TSH secretion. Similar results can be caused by the destruction of the hypothalamus such as a tumour or inflammation, leading to a deficiency of TRH.

The development of hypothyroidism in infancy or early childhood is referred to as cretinism. Previously, this illness was fairly common in areas such as the Himalayas and certain parts of Africa where iodine dietary deficiency was endemic. However, with the recent iodine supplementation of food it has become less common. The infant may appear normal at birth, but soon develops signs of mental retardation and neuromuscular abnormalities. There is retarded growth and coarse facial features with a protruding tongue owing to the deposition of mucopolysaccharides. The severity of mental retardation in the child is influenced by the time at which thyroid deficiency occurs in utero.

In older children/adults hypothyroidism causes myxedema. The symptoms of myxedema vary and depend on the extent of hormone deficiency. Initial symptoms include general fatigue and mental sluggishness. Patients become listless, cold intolerant and are

frequently overweight. The skin and hair become dry and accumulation of matrix substances leads to coarse facial features, enlargement of the tongue and hoarsening of the voice.

1.4.3 Thyroiditis

The term thyroiditis, or inflammation of the thyroid gland, is given to a diverse group of disorders that are all characterised by some degree of thyroid inflammation. Autoimmune thyroid disease occurs clinically in approx. 1% of the population. Some of the more common and clinically significant types of thyroiditis will now be discussed.

1.4.3.1 Hashimoto thyroiditis

This type of thyroiditis is the most common cause of hypothyroidism in iodine sufficient areas. It is primarily a disease of middle-aged women, with a peak incidence between 45 and 60 years and a female to male ratio between 10:1 and 20:1. The disease is characterised by gradual loss of thyroid function due to autoimmune destruction of the thyroid gland. It is believed to be caused by a defect in T cells which recognise processed thyroid antigens. This T cell activation can then induce the formation of CD8+ cells which are cytotoxic to thyroid cells and stimulate B cell secretion of autoantibodies against a variety of thyroid antigens such as thyroglobulin, thyroid peroxidase, TSH receptor and iodine transporter.

Hashimoto thyroid patients typically present with a firm, painless goitre with some degree of hypothyroidism. Glands generally weigh less than 100g but weights in excess of 200g may be observed. The goitre is normally symmetric and diffuse but may raise suspicion of neoplasm. Patients are also at increased risk of developing B-cell lymphomas. Histologically, there is extensive infiltration of the parenchyma by a mononuclear inflammatory infiltrate containing lymphocytes, plasma cells and often germinal centres (see Fig 1.3). Thyroid follicles are small with little or no colloid, and are lined in many areas by enlarged, eosinophilic and granular epithelial cells termed Hürthle cells. Fibrosis is common but generally does not extend beyond the capsule of the gland. There is a less common fibrous variant (~10%) with associated severe hypothyroidism, marked fibrosis and extensive loss of thyroid tissue. The fibrous variant is more common in men than the classic variety, which occurs more often in women.

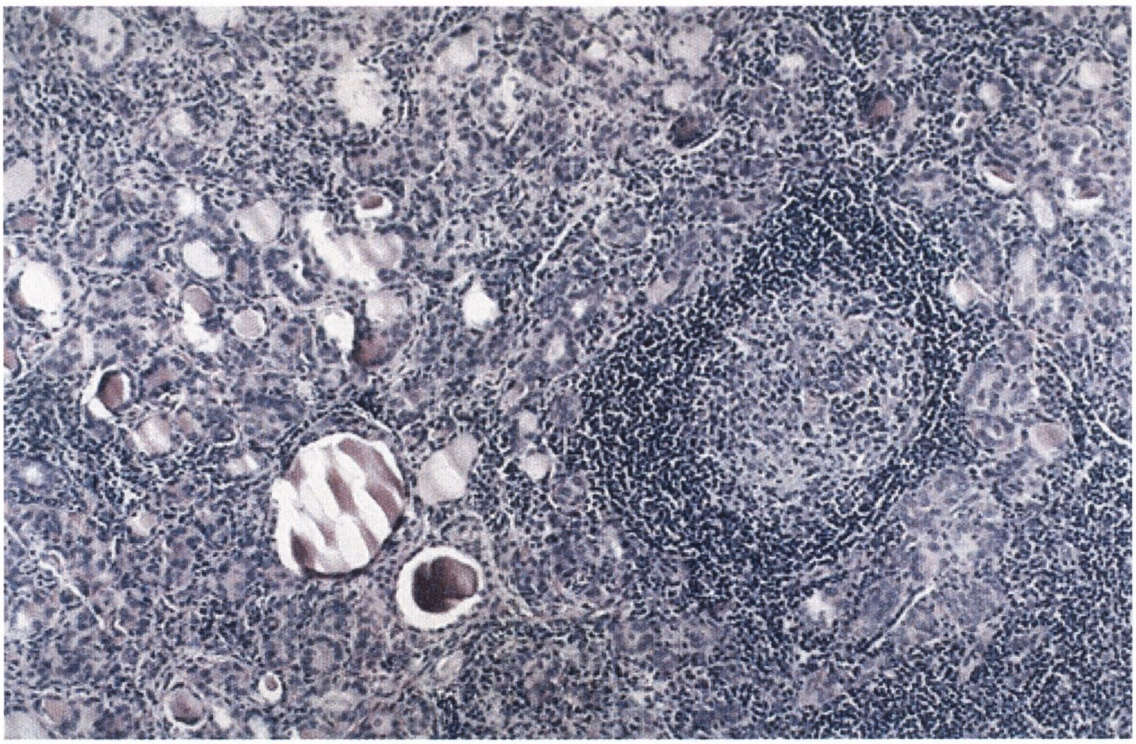

Figure 1.3 Low-power photomicrograph of Hashimoto thyroiditis.

1.4.3.2 Subacute lymphocytic thyroiditis

Subacute lymphocytic thyroiditis, which is also known as painless thyroiditis, is a cause (albeit uncommon) of hyperthyroidism. It usually comes to clinical attention due to a mild hyperthyroidism, goitrous enlargement or both. It often occurs postpartum and may recur in successive pregnancies. It is more common in women than men.

The origin of this disease and its place in the spectrum of thyroiditis is unclear. Some consider it a variant of Hashimoto thyroiditis, others, a precursor. Subacute thyroiditis also has elevated levels of autoantibodies to thyroid antigens such as thyroglobulin and thyroid peroxidase. Histologically, there is a multifocal inflammatory infiltrate composed of small lymphocytes and patchy disruption and collapse of thyroid follicles. There may be some degree of germinal centre formation, but without atrophy. There is no Hürthle cell change or fibrosis.

1.4.3.3 Granulomatous thyroiditis

This rare disease is also known as DeQuervain thyroiditis. It is most common in 30 to 50 year olds with a HLA-B35 subtype, and is once again more likely to affect women than men (3 to 5:1). Granulomatous thyroiditis is believed to be caused by a viral infection. Patients present with a painful thyroid enlargement, general fever and malaise, and many will have a recent history of an upper respiratory infection. It is suggested that a viral infection leads to a corresponding viral antigen being presented by macrophages in the context of HLA-B35. This leads to the formation of cytotoxic T cells that damage the

thyroid follicular cells. Because the immune response is not self-perpetuating, the process is limited and most patients become euthyroid after a few months. Occurrence is seasonal and tends to peak during summer months.

Histologically, scattered follicles are entirely disrupted and replaced by neutrophils forming microabscesses early in the disease. Later, the more characteristic features occur consisting of aggregations of lymphocytes, histiocytes and plasma cells around damaged thyroid follicles. Multinucleate giant cells enclose fragments of colloid (see Fig 1.4). In the latter stages of the disease, chronic inflammatory infiltrate and extensive fibrosis may replace the foci of injury.

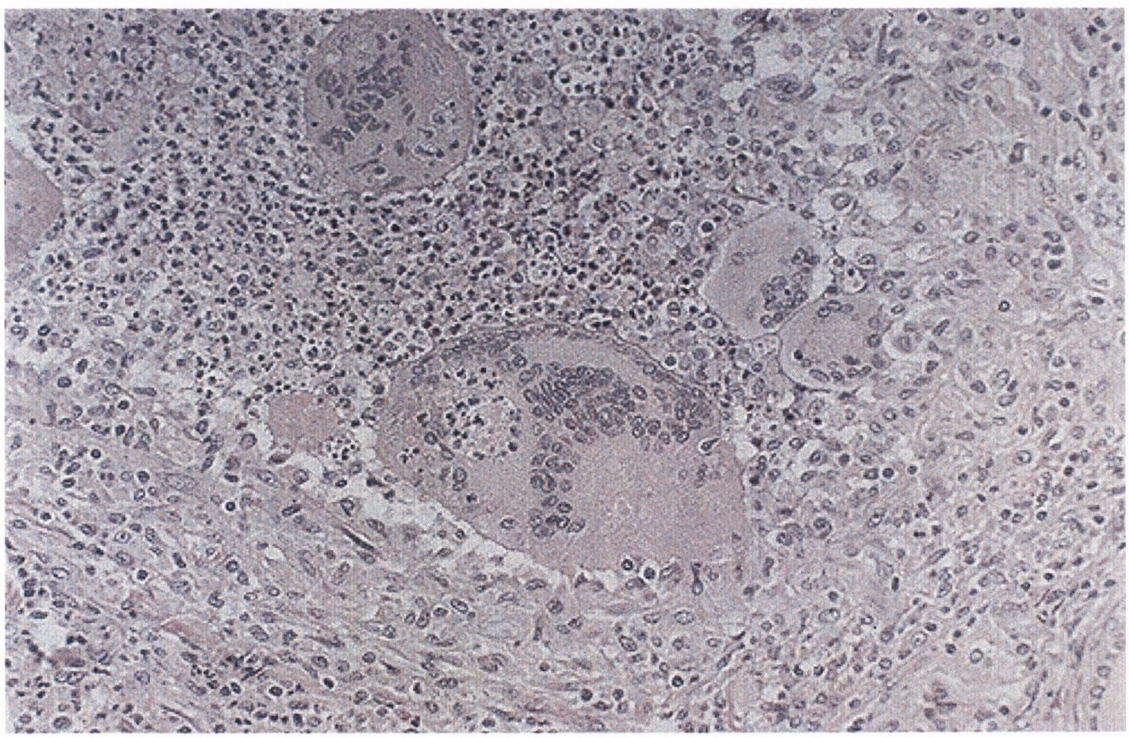

Figure 1.4 Granulomatous thyroiditis with its associated multinucleated giant cells.

1.4.4 Neoplasms of the thyroid

Thyroid cancers account for a small proportion of all thyroid masses and account for less than 0.5% of all cancer deaths. However, thyroid nodules occur frequently, with their incidence being about 2 to 4% in iodine sufficient populations. Nodules are 4 times more frequent in females and their incidence increases with age. The possibility of cancer in patients with thyroid nodules is therefore an important issue. Fortunately, the vast majority of nodules prove to be benign lesions such as nodular hyperplasias and simple cysts. When nodules prove to be neoplastic, the majority of these (>90%) turn out to be adenomas. Less than 1% of solid thyroid nodules reveal a diagnosis of carcinoma. Of those that do, most are indolent with a 90% survival rate even at 20 years. The following sections detail the major thyroid neoplasms, both adenoma and carcinoma, in their various forms and variants.

1.4.4.1 Adenoma

With rare exceptions, adenomas of the thyroid are derived from follicular epithelium and may be referred to as follicular adenomas. They are an encapsulated neoplasm composed of a collection of follicular epithelium that usually shows a uniform architecture. Clinically, they can be difficult to distinguish from both follicular hyperplasia at one end of the spectrum, and follicular carcinoma at the other end.

Histologically, follicular adenomas display a vast variety of patterns depending on the degree of follicle formation and their corresponding colloid content. Varieties include trabecular, microfollicular, macrofollicular, normofollicular and Hürthle cell. Despite

their different patterns however, they all behave similarly. The follicles are typically smaller than those of surrounding parenchyma. The lesions have a thin capsule which contrasts to the thicker variety observed in follicular carcinomas. In the absence of trauma (such as fine needle aspiration biopsy (FNAB)), mitotic activity and necrosis are both low. Variation in nuclear size may be observed and atypical cells are often present. The most important aspect of histological evaluation remains the elimination of malignant potential. For this reason the capsule must be carefully examined for evidence of invasion and for the presence of vascular invasion. Although the presence of nuclear atypia, mitotic activity and necrosis may be indicative of malignancy, these features are not truly diagnostic.

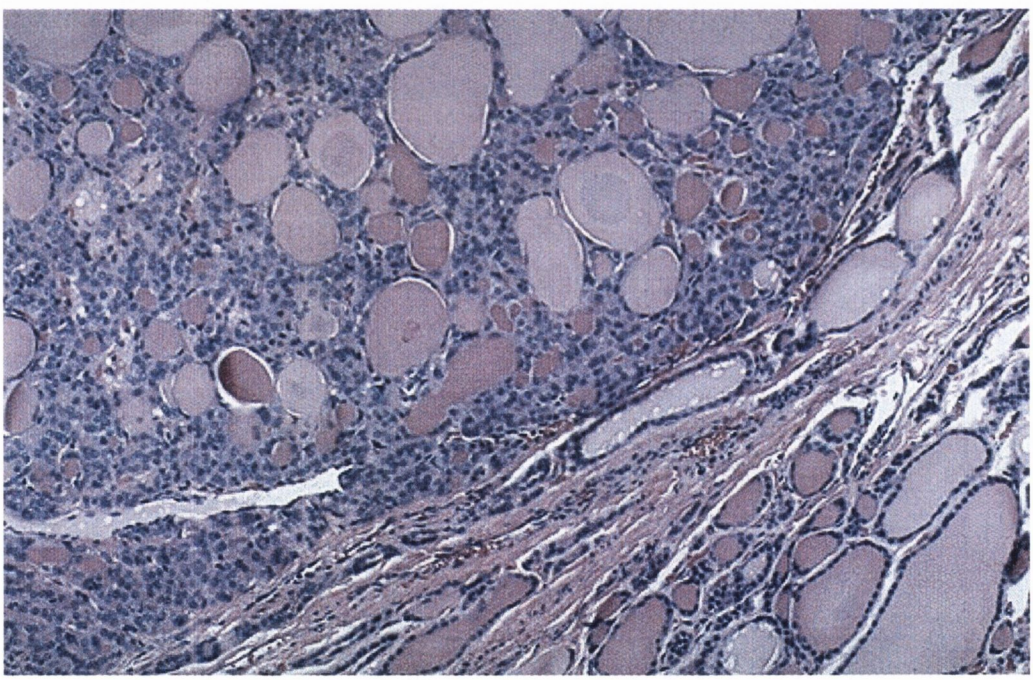

Figure 1.5 Follicular adenoma of the thyroid.

1.4.4.2 Papillary thyroid carcinoma

PTC is the most common type of thyroid malignancy (75-85%). They can occur at any age but the mean year of diagnosis is 40 years old. Females are more commonly affected than males. Most thyroid malignancies in children are of this type. A high incidence of PTC is found in patients with Gardner syndrome and Cowden disease. The association of radiation, in particular during childhood, with the development of PTC is well documented. The prognosis for patients with PTC is more favourable than that of FTC but worsens with increasing age at diagnosis.

Most PTCs present as thyroid nodules or as a mass in a cervical lymph node. The gross appearance of PTC is more variable than other follicular neoplasms. They can be solitary or multifocal lesions and can be encapsulated or infiltrate surrounding parenchyma. Lesions can contain areas of fibrosis and calcification and are often cystic.

Microscopically, classic PTC has very distinctive hallmarks marking it apart from other thyroid neoplasms. Most PTC possess branching papillae (see Fig. 1.7) with a characteristic core and epithelium. The core consists of dense, darkly eosinophilic connective tissue in which focal calcification occurs, resulting in psammoma bodies. The presence of psammoma bodies in a histological sample is strongly suggestive of occult PTC. The epithelium covering the papillae consists of well-differentiated, orderly, cuboidal to columnar cells. The nuclei of these cells have finely dispersed chromatin condensed at the nuclear membrane and often show longitudinal grooving and inclusions. These changes combine to give the nuclei an optically clear appearance, giving rise to the

designation ground-glass or "Orphan Annie" nuclei (see Fig. 1.7). Another prominent feature of PTC is dense fibrosis and scarring. An expanding number of variants of PTC have been described and are addressed in the following section.

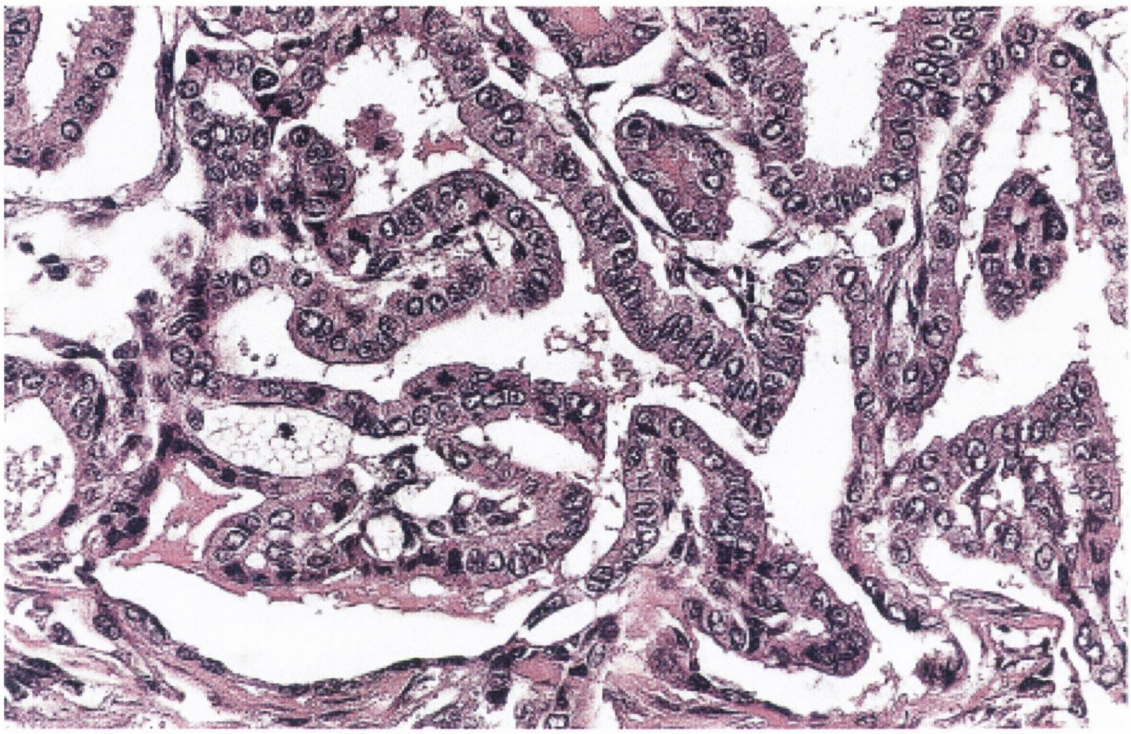

Figure 1.6 Classic PTC illustrating branching papillae and nuclear features.

Papillary microcarcinoma

Papillary microcarcinomas are found frequently in thyroids removed for other reasons and in autopsy studies. Unlike other thyroid carcinomas it is more common in men than women. Most measure less than 1cm in diameter and some have a stellate appearance. Some have been found to be encapsulated. Metastasis is rare and prognosis is extremely good.

Follicular variant

The prevalence of this lesion is unknown due to the fact that it is often misdiagnosed as FTC. They have the same prognosis as classic PTC, with metastases that are nodal, not distant and often show papillary morphology as opposed to the follicular morphology of the primary tumour. Follicular variant of PTC is characterised by a predominantly follicular architecture associated with the nuclear changes observed in classic PTC (see Fig. 1.8). They are similar to classic PTC in that they are infiltrative and generally not encapsulated.

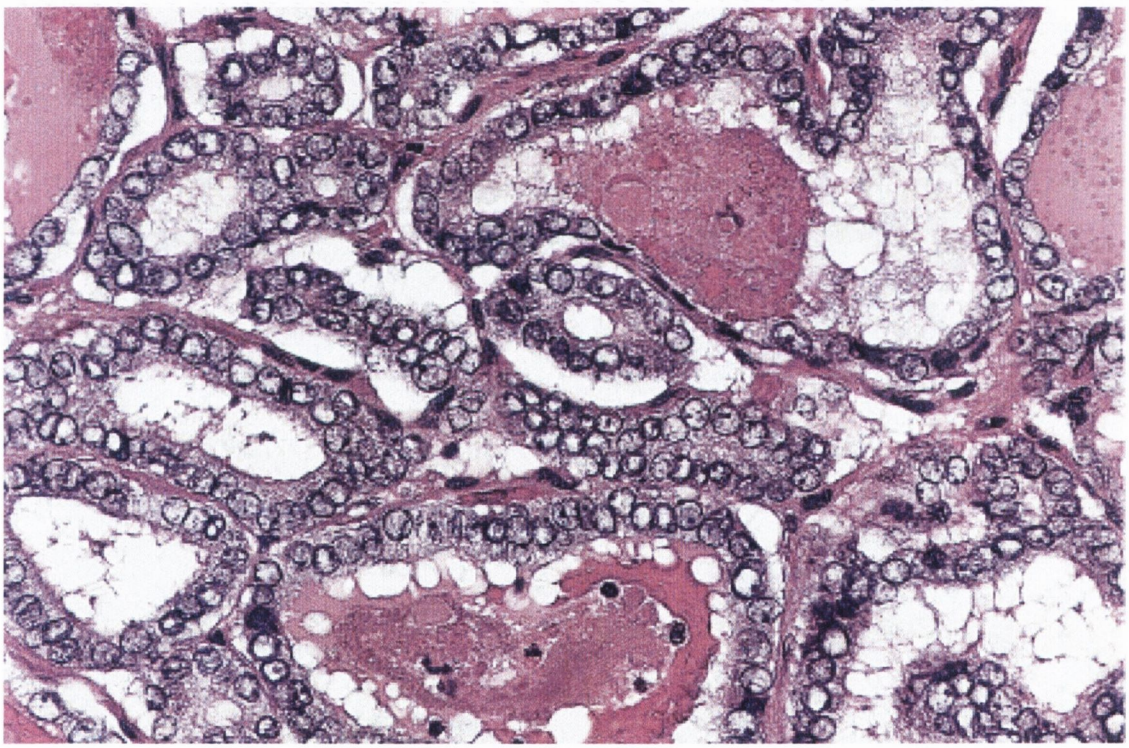

Figure 1.7 Follicular variant of PTC

Encapsulated variant

This variant accounts for approx. 10% of all papillary neoplasms. Tumours are confined to the thyroid gland and are *completely* encapsulated. Morphology and nuclear features are identical to those described in the classic or follicular variants. The incidence of distant metastasis or tumour death is exceedingly rare and prognosis is excellent. These lesions were previously known as papillary adenomas.

Tall and columnar cell variants

Tall cell variant is an unusual type of PTC and is often more aggressive than its classic family member. The tumour consists of tall, columnar cells (twice as tall as they are wide) with intensely eosinophilic cytoplasm covering the papillary structures. Tumours are large with vascular invasion and are often responsible for local and distant metastases and the clinical course is said to be more aggressive. The pattern of growth is highly papillary although the nuclei lack the features observed in other papillary carcinomas. There is often florid lymphocytic infiltration of the stroma. This variant tends to affect men and older patients (>20 years older) than that of classic PTC.

In the columnar cell variant there is prominent nuclear stratification and the cytoplasm is clear as opposed to acidophilic (see Fig. 1.9.). This entity, although very rare, initially was thought to have very poor prognosis. Recent work suggests it may have a more indolent prognosis.

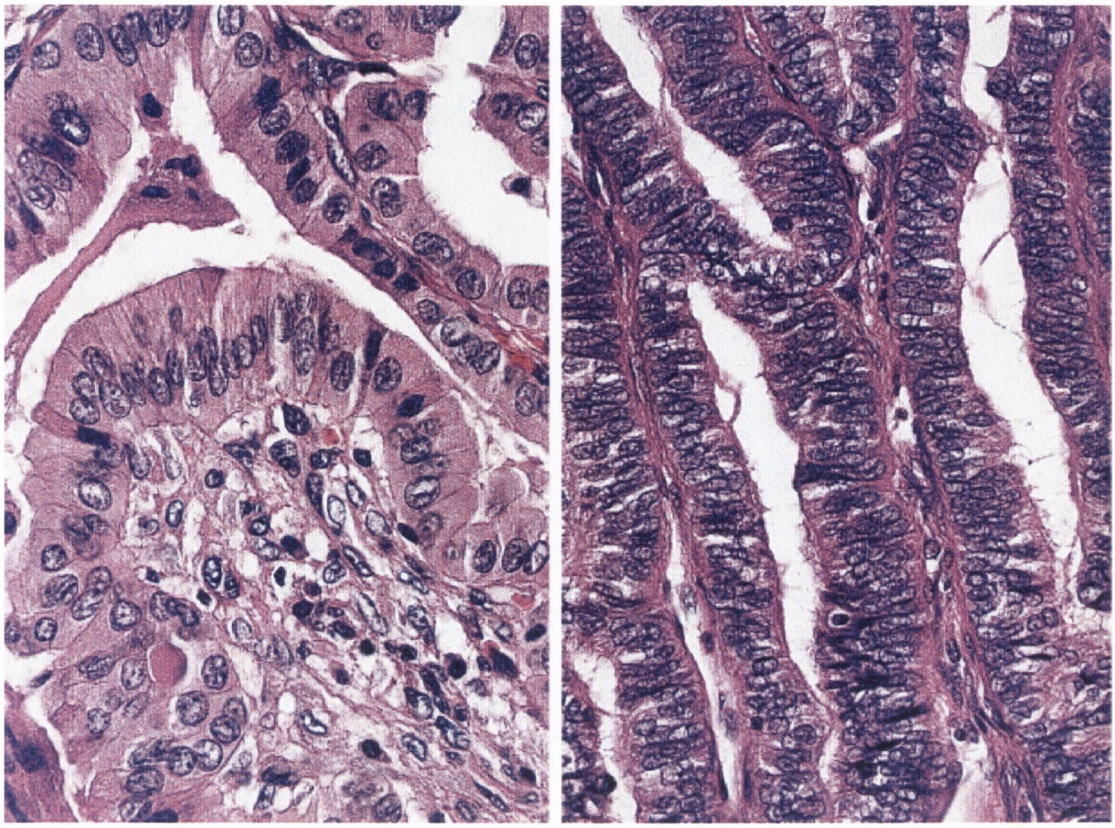

Figure 1.8 Tall cell (L) and columnar cell (R) variants of PTC

Solid variant

Papillary carcinomas can exhibit a solid growth pattern. The pattern is usually focal with no more than 25% of the tumour growth being of this type. A diagnosis of solid variant is only applied if greater than 50% of the neoplasm displays this pattern. These lesions are more common in children and although usually rare, have been reported in up to 30% of PTC resulting from the nuclear accident at Chernobyl. Histologically, classic PTC nuclei should be seen. Its prognosis is unclear with contradictions in the literature but is generally thought to be less favourable than classic PTC, especially in children.

Oncocytic variant

This variant consists of oxyphilic/oncocytic cells with the nuclear features of PTC. Its diagnosis can be further complicated by the fact that the growth pattern can be papillary or follicular and the tumour can be encapsulated or invasive. These multiple variables result in a high number of diagnostic combinations for the investigating pathologist (i.e. papillary encapsulated oncocytic variant of PTC or follicular invasive oncocytic variant of PTC, etc.).

Diffuse sclerosing variant

This variant occurs more frequently in younger patients and is often mistaken for Hashimoto thyroiditis. It is characterised by the involvement of one or both lobes, dense sclerosis, an abundance of psammoma bodies, extensive solid foci, squamous metaplasia, extensive lymph vessel permeation and heavy lymphocytic infiltration. Survival rates are lower than that of classic PTC and nodal, lung and brain metastases are common.

Cribriform-morular variant

This variant is associated with mutations of the APC gene and is therefore generally syndromic, although somatic cases can occur. It is usually found in young women. Tumours have a cribriform pattern of growth with morular formations.

1.4.4.3 Follicular thyroid carcinoma

By its definition, follicular thyroid carcinoma (FTC) is a malignancy derived from the follicular epithelium of the thyroid. FTC represents approx. 15% in its incidence rate of all thyroid malignancies and is second only to papillary thyroid carcinoma (PTC). Its incidence in areas of endemic goitre and iodine deficiency is elevated. FTC, as with most thyroid malignancies, is most often seen in females and patients are usually older (~10 years) than those of papillary carcinoma, with a peak in the forties and fifties. Its incidence worldwide is somewhat blurred due to the fact that many still incorrectly diagnose follicular variant of PTC as FTC. FTCs typically present as slowly enlarging, painless nodules. Unlike PTC, they have little tendency to invade lymphatic vessels and more commonly metastasise using vascular channels with spread to bone, lungs, liver and elsewhere.

Grossly, FTC is grey-tan-pink, fleshy and is sometimes semi-translucent when large colloid-filled follicles are present. Fibrosis and calcification are common observations. Histologically, most FTCs resemble normal thyroid with uniform cells forming small follicles containing colloid. Some may be dominated by Hürthle cells and others may seem less differentiated. The nuclear features of PTC and psammoma bodies are absent. There is frequent extensive invasion of surrounding thyroid parenchyma.

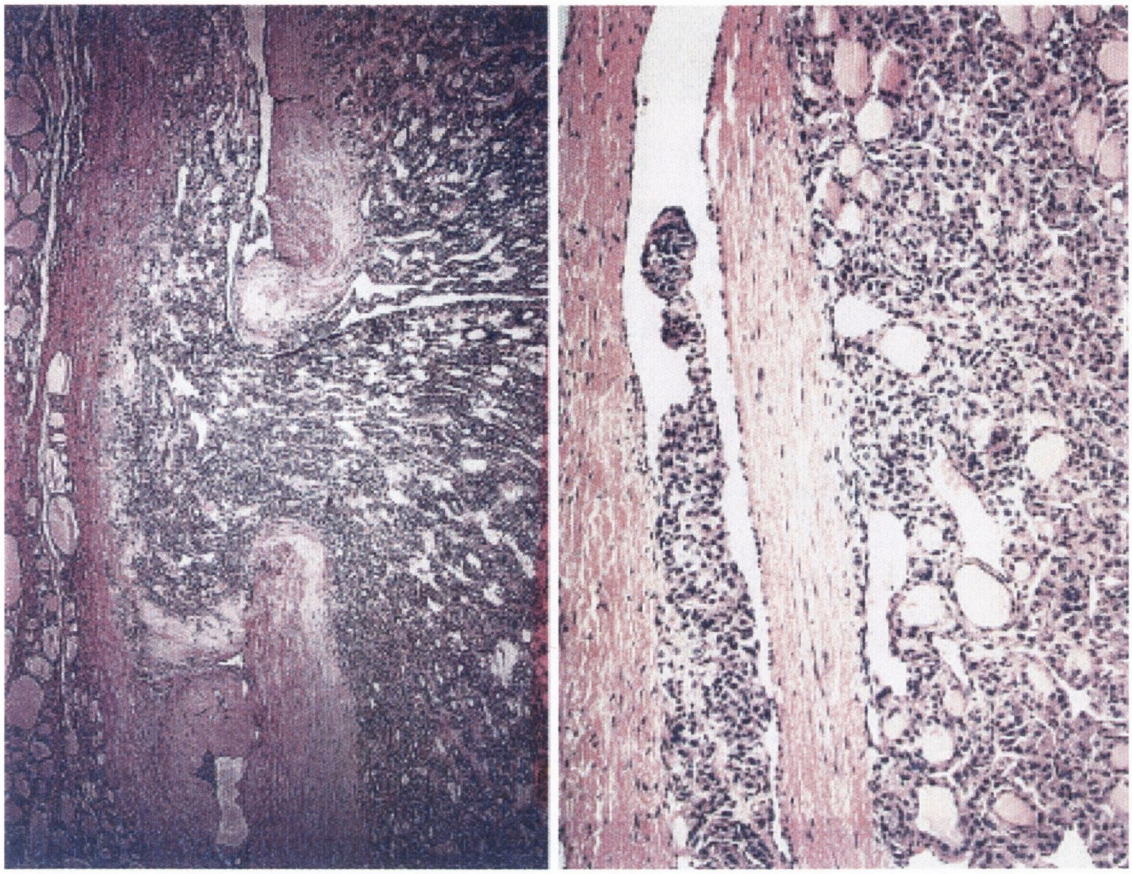

Figure 1.9 Encapsulated FTC demonstrating capsular and vascular invasion

FTCs are divided into 2 variants: encapsulated FTC and widely invasive FTC. The former carries a relatively good prognosis with little chance of metastasis and a low mortality rate. Patients with widely invasive FTC usually develop metastatic disease and the mortality rate much higher at 20-50%.

1.4.4.4 Insular/poorly differentiated carcinoma

These tumours are of follicular origin and are given their own category due to the fact that they have survival rates between those of well-differentiated and anaplastic carcinomas. Their incidence varies with geographic location. Patients are usually older than those with well-differentiated lesions.

Lesions are typically large with multifocal necrosis. They are not normally encapsulated and often invade into surrounding thyroid tissue and even into perithyroid tissue. Histologically, poorly differentiated carcinoma is characterised by the presence of solid nests (insulae) of cells that are separated by a loose network of connective tissue. Cells are small with round nuclei and scant cytoplasm. Tumour necrosis is a feature and occurs in a peritheliomatous pattern (see Fig. 1.10). Vascular invasion and mitotic activity are often observed.

Lesions are aggressive and spread via lymphatic and vascular routes. Metastases are most commonly found in node, lung and bone.

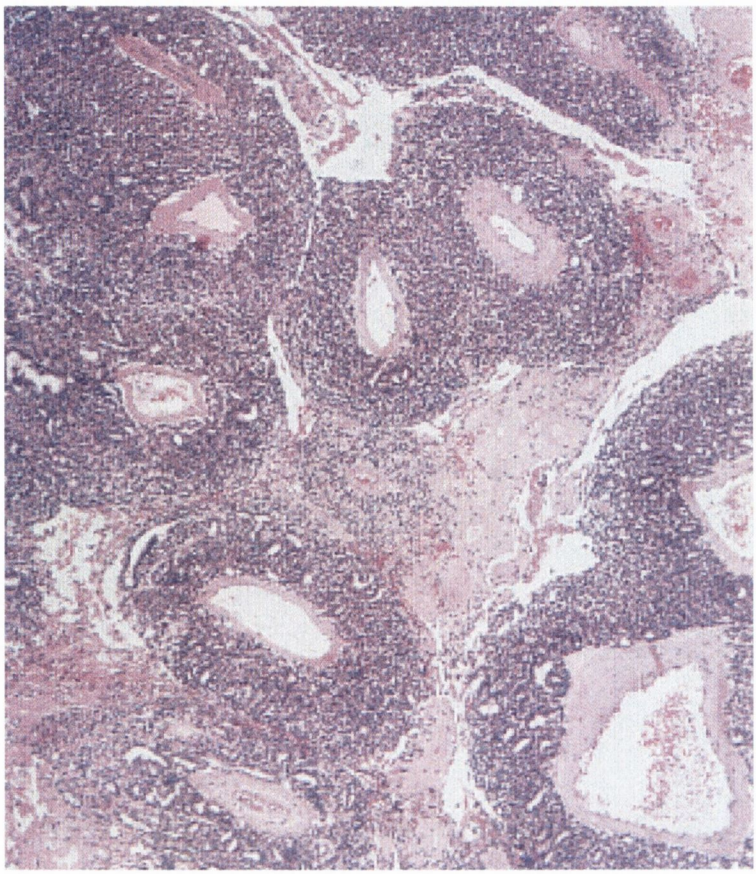

Figure 1.10 Poorly differentiated carcinoma of the thyroid

1.4.4.5 Anaplastic thyroid carcinoma

Anaplastic thyroid carcinomas (ATC) are undifferentiated tumours of thyroid follicular epithelium. They are high-grade neoplasms with highly aggressive courses and death usually occurs within 3 months of diagnosis. They are usually seen in elderly women (>60 years old). Patients frequently have a history of goitre, prior or concurrent well-differentiated carcinoma (in particular PTC). This has lead to the assumption that ATC is a progression of well-differentiated carcinoma, consequent with additional genetic insults.

ATCs present as rapidly enlarging neck masses. Most have already spread to adjacent neck structures and/or the lungs at presentation. Lesions are often associated with extensive hemorrhage and necrosis. Microscopic appearance varies considerably although there are 3 main morphologies observed: giant cell, spindle cell and squamoid ATC. Many cases show a variety of cell types but tumours are generally composed of bizarre, mitotically active cells. There is extensive tissue destruction due to follicular invasion and lesions may be almost completely necrotic.

1.4.4.6 Medullary thyroid carcinoma

Medullary thyroid carcinomas (MTCs) are tumours derived from calcitonin-producing parafollicular cells (C cells). They are rare tumours, accounting for less than 10% of all thyroid malignancies. The tumours are sporadic in 80% of cases with the remainder occurring in the setting of multiple endocrine neoplasia (MEN) type IIA or IIB, or as familial tumours without MEN. Sporadic and MEN lesions are aggressive, tend to metastasise via the bloodstream and have a 5-year survival rate of only 50%.

Large lesions may contain areas of necrosis and hemorrhage. Histologically, MTCs are composed of polygonal to spindle shaped cells, which can form nests, trabeculae and even follicles. Nuclei have a "salt and pepper" chromatin pattern and there are often differences in nuclear size.

1.5 Molecular pathology of thyroid cancer

Carcinogenesis is widely accepted as a multi-step process requiring certain genetic events to convert normal cells to transformed cells. It is believed that a typical cancer requires 6 to 7 deleterious genetic events over a period of 20 to 40 years to manifest. Thyroid carcinogenesis follows this progression model. The genes responsible for neoplastic change can be categorised into broad functional groups: oncogenes and tumour suppressor genes.

Oncogenes result from mutations in, or over-expression of, proto-oncogenes, resulting in their uncontrolled activation. Proto-oncogenes have dedicated normal cellular functions and are typically cell surface receptors or members of their corresponding signal transduction pathways. Tumour suppressor genes result from loss of heterozygosity (LOH) at a particular allele. Comparison of genomic and tumour DNA is used to identify tumour suppressor genes in LOH studies on cancer.

The majority of mutations in thyroid tumours are somatic, however germline mutations do exist. They occur in familial cancer syndromes such as MEN II. Germline mutations typically predispose individuals to thyroid malignancy, which is precipitated by additional somatic mutations. Typical genes involved in thyroid tumorigenesis are described below.

1.5.1 ret/PTC

The most common genetic alterations detected in papillary thyroid carcinomas are those pertaining to the ret/PTC group of oncogenes. Fusco et al. (1987) initially isolated a novel oncogene from PTCs and their lymph node metastases by demonstrating transforming activity using DNA transfection analysis on NIH 3T3 cells. It was subsequently demonstrated that this oncogene (then called PTC) was in fact a rearranged form of the RET proto-oncogene (Grieco et al., 1990).

1.5.1.1 RET proto-oncogene

The RET proto-oncogene (10q11.2) is a member of the receptor tyrosine kinase family of proteins which are typically cell surface molecules responsible for signal transduction of mitotic/differentiation stimuli (see Fig 1.11). Its ligands are neurotrophic factors of the glial-cell line derived neurotrophic factor (GDNF) family, including GDNF, neurturin, artemin and persefin. The receptor is expressed in a tissue and developmental stage-specific manner, but primarily in neural crest and urogenital precursor cells. Gene ablation studies have shown it to be essential in the development of the enteric nervous system and kidney during embryogenesis (Schuchardt et al., 1994; Taraviras et al., 1999; Enomoto et al., 2001).

RET (REarranged during Transfection) was initially cloned as a chimeric oncogene during a classic NIH 3T3 transformation assay (Takahashi et al., 1985). Mutations (both germline and somatic) in the RET proto-oncogene are associated with several diseases including multiple endocrine neoplasia, types IIA and IIB (MEN2A and MEN2B),

Hirschsprung disease, and medullary thyroid carcinoma. Like most receptor tyrosine kinases, RET has the ability to activate a variety of signalling pathways, including Ras/Raf/MEK/ERK, phosphatidylinositol 3-kinase (PI3K)/AKT, p38 MAPK and c-Jun N-terminal kinase (JNK) pathways.

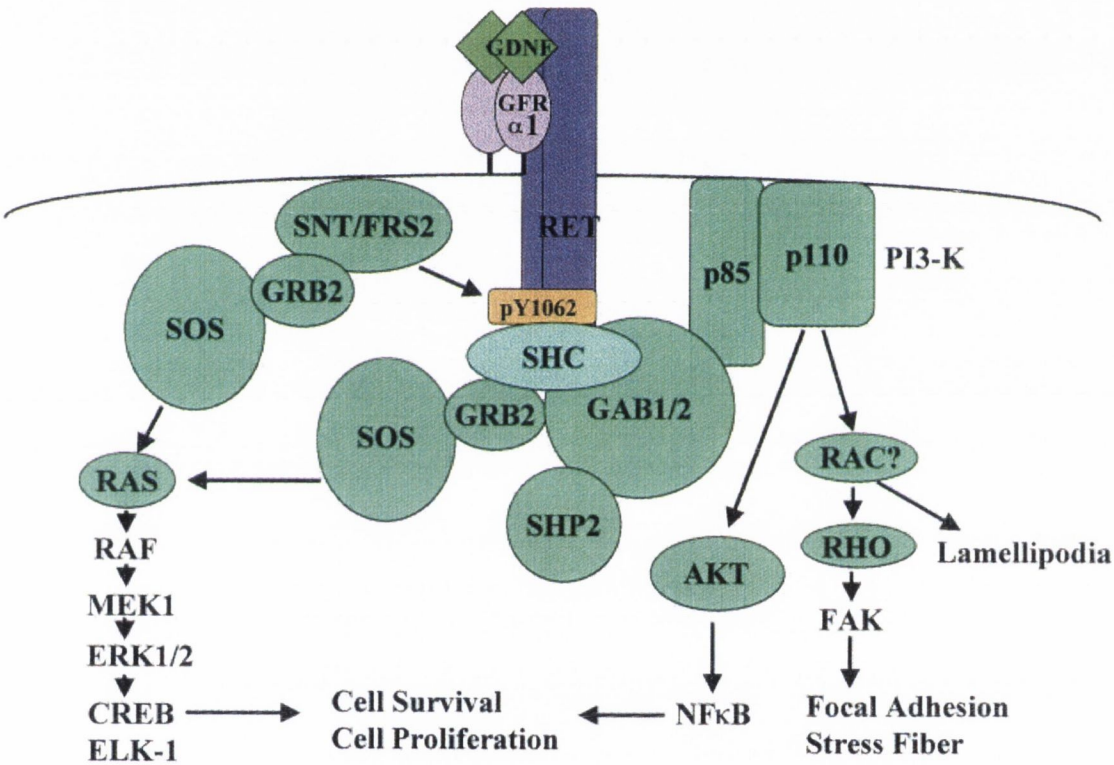

Figure 1.11 RET signalling

Figure illustrating the multitude of pathways that RET can use to effect its stimulus by GDNF, including the Ras/Raf/ERK/MEK pathway (adapted from Takahashi M. The GDNF/RET signaling pathway and human diseases. *Cytokine Growth Factor Rev.* 2001 Dec;12(4):361-73).

1.5.1.2 ret/PTC oncogenes and thyroid cancer

The ret/PTC oncogenes are the activated forms of the RET proto-oncogene. They are formed as a result of gross chromosomal rearrangements which result in the fusion of the tyrosine kinase domain of RET to another donor gene and until recently were thought to be exclusive to papillary thyroid carcinoma (Sheils et al., 2000). The membrane-anchoring and extracellular ligand-binding domains of RET are lost as a result of this fusion, while the 5' sequences that donate their promoters become juxtaposed to the RET tyrosine kinase domain. In their native form, each protein acting as a donor in the generation of a RET chimera, is ubiquitously expressed. Thus, all ret/PTC oncogenes are i) ubiquitously expressed due to the inheritance of a new 5' promoter, ii) cytoplasmic due to the loss of their transmembrane domains and iii) constitutively activated due to oligomerisation of the oncoprotein and subsequent tyrosine phosphorylation leading to ligand-independent tyrosine kinase activity.

Nine variants of ret/PTC have been described to date in papillary carcinoma. The variants, their respective gene fusion partners and the chromosomal rearrangement leading to their creation are listed in table 1. ret/PTC-1 is by far the most commonly observed variant, accounting for approximately 70% of all ret/PTC oncogenes detected.

Studies have shown sporadic ret/PTC detection rates to vary from 2.5% to as high as 85% depending on geographical location and the detection methods used (Santoro et al., 1992; Zou et al., 1994; Sugg et al., 1996; Chua et al., 2000; Sheils et al., 2000). The typical detection rate for most western countries is a more moderate 10-35% however. Consistent

high prevalences of ret/PTC rearrangements (60-70%) have been observed in PTC among children in the areas affected by the Chernobyl nuclear disaster (Fugazzola et al., 1995; Klugbauer et al., 1995; Nikiforov et al., 1997; Rabes et al., 2000). In contrast to sporadic adult PTCs, ret/PTC-3 is by far the most prevalent rearrangement detected in these children (3:1 ratio of ret/PTC-3 to ret/PTC-1).

The different types of ret/PTC rearrangements are thought to reflect phenotypic differences in neoplastic thyroid cells. ret/PTC-3 rearrangements are more often associated with the solid/follicular variant of PTC, whereas ret/PTC-1 are more common in the classic papillary type (Thomas et al., 1999; Finn et al., 2003). Moreover, ret/PTC-1 and ret/PTC-3 appear to be associated with post-Chernobyl PTCs of long and short latency, respectively (Smida et al. 1999).

RET rearrangement	Fusion partner	Causative event
ret/PTC-1	H4 (D10S170)	paracentric inversion 10q
ret/PTC-2	PRKAR1A	10;17 translocation
ret/PTC-3	NCOA4 (ELE1)	paracentric inversion 10q
ret/PTC-4	NCOA4 (ELE1)	paracentric inversion 10q
ret/PTC-5	GOLGA5	10;14 translocation
ret/PTC-6	TIF1A	10;7 translocation
ret/PTC-7	TIF1G	10;1 translocation
ret/PTC-8	KTN1	10;14 translocation
ret/PTC-9	RFG9	10;18 translocation

Table1.1 ret/PTC rearrangements

Table illustrating some of the most common ret/PTC rearrangements, their corresponding fusion partners and the proposed means of fusion (including the normal chromosomal location of the donor gene).

1.5.2 TRK

The proto-oncogene *trk* is similar to *ret* in that it encodes a cell surface tyrosine kinase receptor. It binds nerve growth factor (NGF) and is involved in the cytoskeleton. Its native expression is restricted to nerve ganglia and like *ret*, its oncogene is activated by chromosomal rearrangements that result in a chimeric protein. Similar to the ret/PTC paradigm, the 3' tyrosine kinase domain of *trk* becomes juxtaposed to the 5' promoter region of a ubiquitously expressed gene resulting in constitutively active tyrosine kinase

activity. The 5' donor genes are non-muscular tropomyosine (TPM3) gene, translocated promoter region (TPR) gene and TRK-fused gene (TFG) resulting in TRK-T1, TRK-T2 and TRK-T3 respectively.

As is the case with ret/PTC, the *trk* oncogenes are restricted to PTC. Their prevalence however is much lower, with detection rates generally less than 10%.

1.5.3 RAS

The RAS proteins, which consist of 3 subtypes (H-, K- and N-RAS), are a group of 21kDa G-proteins that function in signal transduction pathways by hydrolysing GTP to GDP. The native proteins exist in two states: an inactive form which is bound to GDP and an active form which is anchored to the inner plasma membrane and has GTPase activity. Their function is to modulate extracellular signalling from receptor tyrosine kinases such as EGFR to a cascade of mitogen activated protein kinases (MAPKs). The ultimate products in this cascade act upon nuclear transcription factors such as c-*fos* and c-*jun*.

The *ras* oncogenes are a result of point mutations within a few select codons: 12 and 13 in the GTP-binding domain and 59 and 61 in the GTPase domain (Namba et al., 1990; McCormick et al., 1994). The result of these mutations is constitutive activation and hence an inappropriate nuclear transcriptional signal. *Ras* oncogenes are the most prevalent oncogenes in human cancers, being detectable in up to 30% of all cancers.

The role of *ras* mutations in thyroid tumour progression is unclear with conflicting literature. It is believed however that ras mutations are more commonly found in FTC than PTC and in tumours arising in iodine-deficient areas. Activated *ras* has been reported previously across the entire spectrum of thyroid disease from thyroid nodules to ATC with varying detection rates (Lemoine et al., 1987; Wright et al., 1989; Said et al., 1994; Ezzat et al., 1996). It is thought that the prevalence in carcinomas is higher than that in benign tumours (Lemoine et al., 1987; Karga et al., 1991). *Ras* mutations are thought to indicate poor prognosis in PTC (Hara et al., 1994).

1.5.4 BRAF

Following on from RAS proteins are the RAF kinase proteins, a family of homologous cytoplasmic serine/threonine protein kinases which are regulated by ras binding. RAF kinases are proto-oncogenes that function in the mitogen-activated protein kinase/extracellular-signal-regulated kinase (MAPK/ERK) pathway, an important membrane to nucleus signalling module. The pathway is involved in all of the characteristics that define cancer cells: immortalisation, mitogen-independent growth, insensitivity to inhibitory signals, invasion and metastasis, angiogenesis, evasion of apoptosis and even resistance to therapy. The pathway is thought to be implicated in up to 30% of all human neoplasms.

Three RAF isoforms exist: A-RAF, B-RAF and C-RAF (RAF-1). Of these BRAF is the most extensively studied. Mutations adjacent to the activating component of the kinase domain mimic phosphorylation of the protein leading to elevated, RAS-independent

kinase activity. The most common of these mutations is a T1799A missense mutation resulting in a valine to glutamic acid substitution at amino acid position 600 (V600E). Mutations in the BRAF gene have been described in a variety of human neoplasms with its highest incidence in melanoma and nevi (~80%) (Pollack et al., 2002; 2003).

Recent results suggest that BRAF mutations are common events in PTC with detection rates being higher than those of ret/PTC. The mutations have not been detected in any other type of thyroid neoplasm apart from poorly differentiated/undifferentiated carcinoma arising from PTC. BRAF mutations and ret/PTC oncogenes have also been generally shown to be mutually exclusive. These issues and RAF kinases in general are discussed in detail in chapter 5.

1.5.5 MET

MET is the tyrosine kinase transmembrane receptor for hepatocyte growth factor/scatter factor (HGF/SF). HGF/SF is a powerful mitogen and stimulus for thyroid proliferation. The oncogene can be constitutively activated by several methods including overexpression, gene amplification and mutational change. MET overexpression is usually found in PTC and ATC and to a lesser extent in FTC (Di Renzo et al., 1991). It is not normally detectable in benign/normal tissues. *Met* activation may occur via a paracrine mechanism, as C cells are known to secrete HGF/SF. The relationship between *met* expression and tumour aggressiveness/metastasis is currently unclear.

1.5.6 MYC

The c-*myc* proto-oncogene encodes a transcription factor for genes involved in growth and differentiation. C-*myc* expression normally declines with cell cycle progression and is shut off completely following full differentiation and growth arrest. It is also thought to play a role in apoptosis. Oncogenic activation leads to up-regulation of MYC, which has been detected in many human cancers including thyroid (Terrier et al., 1988).

1.5.7 p53

Mutations of the tetrameric nuclear phosphoprotein transcription factor p53 are probably the most common genetic aberrations found to date in human cancer. The tumour suppressor gene (17p13) is an archetypal checkpoint regulator. Its main functions are cell cycle arrest to allow damaged DNA repair and inducing damaged cells to undergo apoptosis prior to division. p53 inactivation is typified by loss of one allele followed by point mutation of the remaining allele. p53 mutations are considered late events in the sequence of human carcinogenesis.

The prevalence of p53 mutations in PTC varies depending on tumour type (Zou et al., 1993). Mutations are found at a much higher level in poorly/undifferentiated thyroid carcinoma due to the fact that it is a late event (Fagin et al., 1993).

1.5.8 PTEN

PTEN (10q23.3) is a protein tyrosine phosphatase and exerts its tumour suppressor effect by antagonising tyrosine kinase activity. It is known to act on the phosphoinositide 3-kinase (PI3K) and the Akt/PKB pathways. The gene is deleted in Cowden syndrome (CS), an autosomal dominant condition characterised by the formation of hamartomas in several organs and a high risk of breast and thyroid cancer.

Somatic PTEN mutations are rare in primary thyroid tumours, however hemizygous deletion has been found to occur in 10-20% of adenomas and carcinomas. Hemizygous deletions can be detected in up to 60% of ATC.

1.6 Aims and objectives

The overall aim of this study was to search for prognostic markers in papillary thyroid carcinoma. Specific objectives were:

i) to examine expression of the cellular adhesion molecule, E-cadherin, in various thyroid tumour types and Hashimoto thyroiditis in the context of ret/PTC-1 positivity.

ii) to examine the expression of E-cadherin's ligands, β- and γ-catenin, in various thyroid tissue types in the context of ret/PTC-1 positivity.

iii) to assess the frequency of the T1799A BRAF mutation in a panel of thyroid tissues and its relation to ret/PTC oncogenes.

iv) to analyse the expression profile of thyroid carcinoma cell lines in order to describe the pathobiology of thyroid carcinoma and identify potential biomarkers and therapeutic targets.

1.7 References

Basedow C. Exophthalmus durch hypertrophie des Zellgewebes in der Augenhohle. Wochenschr Heilkd 1840; 6: 197,220.

Chua EL, Wu WM, Tran KT, McCarthy SW, Lauer CS, Dubourdieu D, Packham N, O'Brien CJ, Turtle JR, Dong Q. Prevalence and distribution of ret/ptc 1, 2, and 3 in papillary thyroid carcinoma in New Caledonia and Australia. J Clin Endocrinol Metab 2000; 85: 2733-9.

Coindet J-F. Decouverte d'un nouveau remede contre le goitre. Ann Chim Phys 1820; 15: 49.

Cranefield P. The discovery of cretinism. Bull Hist Med 1962; 36: 489.

Di Renzo MF, Narsimhan RP, Olivero M, Bretti S, Giordano S, Medico E, Gaglia P, Zara P, Comoglio PM. Expression of the Met/HGF receptor in normal and neoplastic human tissues. Oncogene 1991; 6: 1997-2003.

Enomoto H, Crawford PA, Gorodinsky A, Heuckeroth RO, Johnson EM Jr, Milbrandt J. RET signaling is essential for migration, axonal growth and axon guidance of developing sympathetic neurons. Development 2001; 128: 3963-74.

Ezzat S, Zheng L, Kolenda J, Safarian A, Freeman JL, Asa SL. Prevalence of activating ras mutations in morphologically characterized thyroid nodules. Thyroid 1996; 6: 409-16.

Fagin JA, Matsuo K, Karmakar A, Chen DL, Tang SH, Koeffler HP. High prevalence of mutations of the p53 gene in poorly differentiated human thyroid carcinomas. J Clin Invest 1993; 91: 179-84.

Finn SP, Smyth P, O'Leary J, Sweeney EC, Sheils O. Ret/PTC chimeric transcripts in an Irish cohort of sporadic papillary thyroid carcinoma. J Clin Endocrinol Metab 2003; 88: 938-41.

Fugazzola L, Pilotti S, Pinchera A, Vorontsova TV, Mondellini P, Bongarzone I, Greco A, Astakhova L, Butti MG, Demidchik EP, et al. Oncogenic rearrangements of the RET proto-oncogene in papillary thyroid carcinomas from children exposed to the Chernobyl nuclear accident. Cancer Res 1995; 55: 5617-20.

Fusco A, Grieco M, Santoro M, Berlingieri MT, Pilotti S, Pierotti MA, Della Porta G, Vecchio G. A new oncogene in human thyroid papillary carcinomas and their lymph-nodal metastases. Nature 1987; 328: 170-2.

Graves R. Clinical lectures delivered by Robert J. Graves, M.D., at the Meath Hospital during the session of 1834-5. Lond Med Surg 1835; J 7: 516.

Grieco M, Santoro M, Berlingieri MT, Melillo RM, Donghi R, Bongarzone I, Pierotti MA, Della Porta G, Fusco A, Vecchio G. PTC is a novel rearranged form of the ret proto-oncogene and is frequently detected in vivo in human thyroid papillary carcinomas. Cell 1990; 60: 557-63.

Gross J, Pitt-Rivers R. The identification of 3:5:3'-L-triiodothyronine in human plasma. Lancet 1952; 1: 439.

Hara H, Fulton N, Yashiro T, Ito K, DeGroot LJ, Kaplan EL. N-ras mutation: an independent prognostic factor for aggressiveness of papillary thyroid carcinoma. Surgery 1994; 116: 1010-6.

Harington C. Chemistry of thyroxine. III. Constitution and synthesis of thyroxine. Biochem J 1927; 21: 169.

Karga H, Lee JK, Vickery AL Jr, Thor A, Gaz RD, Jameson JL. Ras oncogene mutations in benign and malignant thyroid neoplasms. J Clin Endocrinol Metab 1991; 73: 832-6.

Kendall E. The isolation in crystalline form of the compound which occurs in thyroid: its chemical nature and physiologic activity. JAMA 1915; 64: 2042.

Klugbauer S, Lengfelder E, Demidchik EP, Rabes HM. High prevalence of RET rearrangement in thyroid tumors of children from Belarus after the Chernobyl reactor accident. Oncogene 1995; 11: 2459-67.

Lemoine NR, Mayall ES, Wyllie FS, Farr CJ, Hughes D, Padua RA, Thurston V, Williams ED, Wynford-Thomas D. Activated ras oncogenes in human thyroid cancers. Cancer Res 1988; 48: 4459-63.

Lugol JGA. Memoire sur l'emploi de l'iode dans les maladies scrophuleuses. Paris, 1829.

Marine D, Kimball OP. Prevention of simple goitre in man. Arch Intern Med 1920; 25: 661.

McCormick F. Activators and effectors of ras p21 proteins. Curr Opin Genet Dev 1994; 4: 71-6.

Merke F. History and iconography of endemic goitre and cretinism. Lancaster, UK: MTP Press Ltd., 1984.

Murray G. Note on the treatment of myxoedema by hypodermic injections of an extract of the thyroid gland of a sheep. BMJ 1891; 2: 796.

Namba H, Gutman RA, Matsuo K, Alvarez A, Fagin JA. H-ras protooncogene mutations in human thyroid neoplasms. J Clin Endocrinol Metab 1990; 71: 223-9.

Nikiforov YE, Rowland JM, Bove KE, Monforte-Munoz H, Fagin JA. Distinct pattern of ret oncogene rearrangements in morphological variants of radiation-induced and sporadic thyroid papillary carcinomas in children. Cancer Res 1997; 57: 1690-4.

Ord W. Report of a committee of the Clinical Society of London nominated December 14, 1883, to investigate the subject of myxoedema. Trans Clin Soc Lond 1888; 21(supp).

Pollock PM, Harper UL, Hansen KS, Yudt LM, Stark M, Robbins CM, Moses TY, Hostetter G, Wagner U, Kakareka J, Salem G, Pohida T, Heenan P, Duray P, Kallioniemi O, Hayward NK, Trent JM, Meltzer PS. High frequency of BRAF mutations in nevi. Nat Genet 2003; 33: 19-20.

Pollock PM, Meltzer PS. A genome-based strategy uncovers frequent BRAF mutations in melanoma. Cancer Cell 2002; 2: 5-7.

Rabes HM, Demidchik EP, Sidorow JD, Lengfelder E, Beimfohr C, Hoelzel D, Klugbauer S. Pattern of radiation-induced RET and NTRK1 rearrangements in 191 post-chernobyl papillary thyroid carcinomas: biological, phenotypic, and clinical implications. Clin Cancer Res 2000; 6: 1093-103.

Said S, Schlumberger M, Suarez HG. Oncogenes and anti-oncogenes in human epithelial thyroid tumors. J Endocrinol Invest 1994; 17: 371-9.

Santoro M, Carlomagno F, Hay ID, Herrmann MA, Grieco M, Melillo R, Pierotti MA, Bongarzone I, Della Porta G, Berger N, et al. Ret oncogene activation in human thyroid neoplasms is restricted to the papillary cancer subtype. J Clin Invest 1992; 89: 1517-22.

Schuchardt A, D'Agati V, Larsson-Blomberg L, Costantini F, Pachnis V. Defects in the kidney and enteric nervous system of mice lacking the tyrosine kinase receptor Ret. Nature 1994; 367: 380-3.

Sheils OM, O'Leary JJ, Uhlmann V, Lattich K, Sweeney EC. ret/PTC-1 Activation in Hashimoto Thyroiditis. Int J Surg Pathol 2000; 8: 185-189.

Smida J, Salassidis K, Hieber L, Zitzelsberger H, Kellerer AM, Demidchik EP, Negele T, Spelsberg F, Lengfelder E, Werner M, Bauchinger M. Distinct frequency of ret rearrangements in papillary thyroid carcinomas of children and adults from Belarus. Int J Cancer 1999; 80: 32-8.

Sugg SL, Zheng L, Rosen IB, Freeman JL, Ezzat S, Asa SL. ret/PTC-1, -2, and -3 oncogene rearrangements in human thyroid carcinomas: implications for metastatic potential? J Clin Endocrinol Metab 1996; 81: 3360-5.

Takahashi M, Ritz J, Cooper GM. Activation of a novel human transforming gene, ret, by DNA rearrangement. Cell 1985; 42: 581-8.

Takahashi M. The GDNF/RET signaling pathway and human diseases. Cytokine Growth Factor Rev 2001; 12: 361-73.

Taraviras S, Marcos-Gutierrez CV, Durbec P, Jani H, Grigoriou M, Sukumaran M, Wang LC, Hynes M, Raisman G, Pachnis V. Signalling by the RET receptor tyrosine kinase and its role in the development of the mammalian enteric nervous system. Development 1999; 126: 2785-97.

Terrier P, Sheng ZM, Schlumberger M, Tubiana M, Caillou B, Travagli JP, Fragu P, Parmentier C, Riou G. Structure and expression of c-myc and c-fos proto-oncogenes in thyroid carcinomas. Br J Cancer 1988; 57: 43-7.

Thomas GA, Bunnell H, Cook HA, Williams ED, Nerovnya A, Cherstvoy ED, Tronko ND, Bogdanova TI, Chiappetta G, Viglietto G, Pentimalli F, Salvatore G, Fusco A, Santoro M, Vecchio G. High prevalence of RET/PTC rearrangements in Ukrainian and Belarussian post-Chernobyl thyroid papillary carcinomas: a strong correlation between RET/PTC3 and the solid-follicular variant. J Clin Endocrinol Metab 1999; 84: 4232-8.

Wharton T. Adenographia: sive glandularum totius corporis descriptio. Noviomagi (now Nijmegen): Andreas ab Hoogenhuyse, 1664.

Wright PA, Lemoine NR, Mayall ES, Wyllie FS, Hughes D, Williams ED, Wynford-Thomas D. Papillary and follicular thyroid carcinomas show a different pattern of ras oncogene mutation. Br J Cancer 1989; 60: 576-7.

Zou M, Shi Y, Farid NR. Low rate of ret proto-oncogene activation (PTC/retTPC) in papillary thyroid carcinomas from Saudi Arabia. Cancer 1994; 73: 176-80.

Zou M, Shi Y, Farid NR. p53 mutations in all stages of thyroid carcinomas. J Clin Endocrinol Metab 1993; 77: 1054-8.

Chapter 2

Materials and methods

2.1 Introduction

This chapter is a comprehensive account of all the methodologies employed in this thesis, accompanied by background information on some of the newer techniques. Several of the techniques are used in a number of chapters. Where this occurs, the full description of the technique is restricted to this chapter, with specifics (e.g. primer/probe sequences) appearing in their relevant chapters only.

2.2 Laser capture microdissection

Laser capture microdissection was carried out on formalin fixed paraffin embedded (FFPE) material using the PixCell®II LCM System (Arcturus Engineering, Inc., CA, USA). Briefly, 4-7μm FFPE histological sections were cut and stained with a standard hematoxylin and eosin (H&E) stain. Upon drying they are placed on the PixCell®II microscopic stage and the following protocol is observed:

- Enable the laser via the keyswitch located on front of controller.
- Remove the CapSure® cassette module from the PixCell®II platform. It should slide out smoothly over the detents.
- Press down on the flanges of the cassette module. Press the end locking pins in to hold the plate down in the load position.
- Slide a CapSure® cartridge, which holds four film carriers, into the cassette module until it hits a stop. The cassette loads from one end only.
- If more than four caps are required, load a second cartridge in the same manner, making sure there is no space between the two loaded cartridges.

- Press down on the flanges of the loaded cassette. Retract the locking pins and gently raise the cassette to its loaded position.
- The cartridge is now ready to be loaded into the PixCell®II.
- Slide the loaded CapSure® cassette module to any detent position.
- After LCM, when the CapSure® cartridges are empty, press down on the plate and lock into position by pushing the locking pins in. Carefully slide out the spent cartridges and discard.
- Move the joystick to the vertical position. This centres the translation stage, on the optical axis and ensures proper registration of the sample slide relative to the capture area. This also maximises the transfer area available for microdissection.
- Turn off the vacuum chuck via the switch located on the front of the controller.
- Place the slide on the translation stage, covering the vacuum chuckhole. Manually position it to locate the transfer area in the centre of the field of view.
- Choose the appropriate objective for the desired magnification. Turn on the vacuum chuck.
- Adjust illumination control.
- Adjust focus control.
- Rotate the CapSure® placement arm over the tissue sample.
- Insert the visualiser by pressing the silver plunger button located above the joystick.
- Adjust the microscope light source to obtain a good image on the monitor.

- To perform a microdissection, retract the visualiser by pressing the tab located below the plunger button, and re-adjust the microscope light source.
- Slide the CapSure® cassette module to a detent position, making sure there is a CapSure® cap at the load line.
- Rotate the placement arm to the cap pick-up position. The arm will automatically line up with the cap.
- Raise the placement arm vertically to remove the cap from the cassette module.
- Rotate the placement arm to transfer position over the slide. Release the placement arm. The cap will automatically lower onto the slide. Upon contact with the slide, the placement arm will seat the cap properly on the sample.

When the laser is enabled, an aiming beam is visible on the monitor.

- Select the laser spot size with the 'Spot Size Adjust' located on the left of the laser tower.
- Use the joystick or the XY controls to aim the laser beam on the capture region.

Use the front panel digital controls on the controller to adjust laser parameters. Typical values are:

Spot Size	Power	Duration
<7.5 µm	40mW	450µs
~15 µm	25mW	1.5ms
~30 µm	20mW	5ms

- Fire the laser by pressing the remote thumb switch or the 'fire' button on the front of the controller.
- There is an audible beep when the laser fires. The activated portion of the transfer film will be visible as a ring of film fused to the tissue.
- Use the joystick to move to other areas in the tissue and capture other cells of interest.
- To remove the captured tissue, lift the placement arm in a smooth but swift motion.
- With the cap in place, lift and rotate the placement arm to the unload platform.
- Lower the placement arm onto the unload platform – dropping the cap into the extraction slot.
- Rotate the placement arm to the rest position. The cap will be extractred form the arm and suspended in the unload platform.
- Slide the cap insertion tool onto the unload platform. Make sure the open end of the insertion tool faces the suspended cap and the groove fits over the guide rail.
- Slide the insertion tool down the groove until the cap is engaged.
- Remove with cap attached.
- Insert cap into 0.5ml reagent tube.
- Press down firmly to ensure an even seal.

Continue extraction according to appropriate protocol.

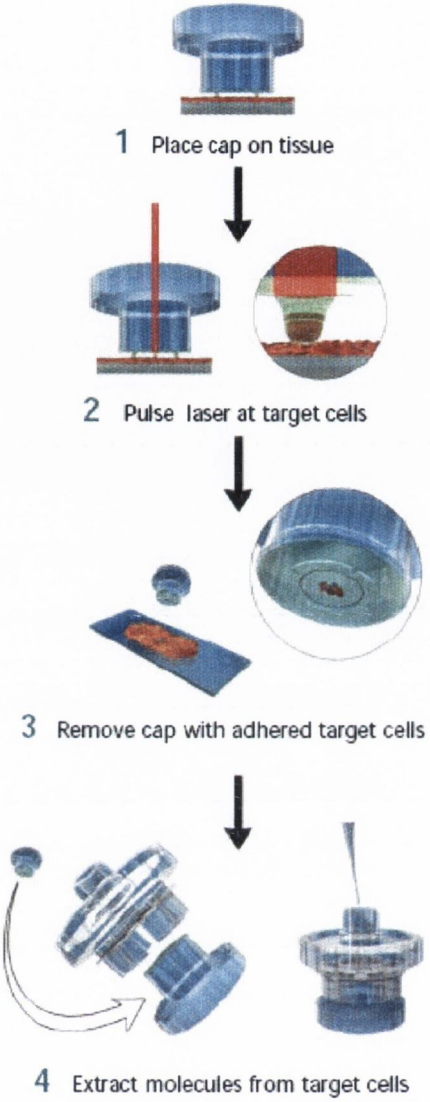

Figure 2.1 The laser capture microdissection process

2.3 Tissue culture of thyroid carcinoma cell lines

Several thyroid cell lines were grown throughout this thesis, both for the purposes of analysis of the cells themselves and for the provision of controls for other areas of the thesis.

2.3.1 Cell lines

Nthy-ori 3-1 (ECACC, Wiltshire, UK) is a normal thyroid follicular epithelial cell line. The cell line is derived from normal thyroid tissue of an adult that has been transfected with a plasmid encoding for the SV40 large T gene. This cell line is used as a normal reference throughout this thesis.

TPC-1 is a cell line derived from a papillary thyroid carcinoma. This cell line expresses the ret/PTC-1 oncogene and is used as a control in TaqMan® experiments.

B-CPAP (DSMZ, 38124 Braunschweig, Germany) is a human thyroid carcinoma cell line that was established from the thyroid tissue of a 76-year-old woman with metastasising PTC in 1992. This cell line is a homozygous mutant for the BRAF T1799A mutation.

8505C (DSMZ, 38124 Braunschweig, Germany) is a cell line that was established from the primary tumor of a 78-year-old woman with thyroid carcinoma (undifferentiated carcinoma, histologically a largely papillary adenocarcinoma with some spindle, polygonal and giant cells). It has a CG to GC transversion at the first base of p53 gene codon 248, and LOH studies show it to have allelic deletion of the

p53 gene. The 8505C cell line also harbours the homozygous BRAF T1799A mutation.

Other cell lines used include: HTH74, an undifferentiated thyroid carcinoma cell line with wild-type BRAF; KAT4, an undifferentiated thyroid carcinoma cell line with heterozygous BRAF T1799A mutation; and KAT10, a papillary thyroid carcinoma cell line with heterozygous BRAF T1799A mutation.

2.3.2 Culture and passage

All cell lines were grown to confluence in a humidified atmosphere containing 5% CO_2 at 37°C in the following plating medium: RPMI 1640 with 2mM L-glutamine, 10% Foetal calf serum (FCS), Penicillin (100U/ml) and Streptomycin (100µg/ml). The exception to this was TPC-1, which replaced RPMI 1640 with DMEM.

Medium was removed and confluent monolayers were washed with sterile PBS. Trypsin/EDTA was added and flasks were returned to the 37°C incubator. Flasks were examined by phase microscopy every 2-3min to assess cell detachment. Flasks were lightly tapped to encourage the release of cells from the plastic surface. When >90% of cells were detached an equal volume of Trypsin Neutralising Solution (TNS) was added. Cells were then pelleted (5min @ 1000rpm). New flasks were subsequently seeded with the trypsinised cells with a 1:4 to 1:6 ratio.

2.3.3 Cryopreservation

Where cryopreservation was required, trypsinised cells were aliquoted into 1.5ml eppendorfs and centrifuged at 1,000rpm for 1 min. The supernatant was removed and the cells were resuspended in 1ml of freezing medium (DMEM/RPMI 1640 medium containing 20% FCS and 10% dimethylsulphoxide (DMSO)). Freezing medium was transferred to 2ml cryovials and the vials were placed on ice for 10min, then at -20°C for 20min. Vials were stored overnight in an -80°C freezer. Vials were then transferred to a liquid nitrogen storage tank for long-term storage.

2.4 Nucleic acid extraction

Throughout this thesis various analyses were carried out on nucleic acids from a variety of thyroid tissue types stored in different formats (e.g. fresh frozen, FFPE, etc.). The extraction protocol employed was largely dictated by the quantity and quality of nucleic acid required and by the format of the starting tissue.

The extraction of pure, intact RNA is important in a variety of molecular biological techniques, and is essential for gene expression analysis. Ribonucleases however can cause difficulty with RNA isolation because they are very stable, active enzymes that require no cofactors for enzymatic activity. Cell lysis in an environment that causes denaturation of ribonucleases is therefore essential. So too is adequate decontamination of work surface areas, solutions and plastic disposables. DNA extraction need not be as stringent, as simple resuspension with a chelating agent confers nuclease protection to the molecule, however it is wise to be consistent with precaution.

2.4.1 Extraction of RNA from FFPE

This was generally performed on samples following LCM. The PURESCRIPT® total RNA isolation kit (Gentra Systems Inc., MN, USA) was utilised for this function, with slight modifications.

Cell lysis

- Perform microdissection and place cap in a 0.5ml microfuge tube containing 300µl Cell Lysis Solution and 1.5µl Proteinase K solution (20mg/ml).
- Incubate overnight at 55°C with constant agitation (i.e. a rotary oven).

Protein-DNA precipitation

- Transfer solution to a fresh 1.5ml microcentrifuge tube and add 100µl Protein-DNA Precipitation Solution to the cell lysate.
- Invert tube gently 10 times and place tube into an ice bath for 5 minutes.
- Centrifuge at 13,000-16,000 x g for 3 minutes. The precipitated proteins and DNA will form a tight pellet.
- (optional) Transfer the supernatant to a fresh tube and repeat ice incubation and centrifugation steps.

RNA precipitation

- Pipette the supernatant containing the RNA (leaving behind the precipitated protein-DNA pellet) into a clean 1.5ml microcentrifuge tube containing 300µl 100% isopropanol (2-propanol) and 0.5µl glycogen (20mg/ml).
- Mix the sample by inverting gently 50 times and incubate @ -20°C for 1 hour.

- Centrifuge at 13,000-16,000 x g (@ 4°C if possible) for 3min; the RNA will be visible as a small, translucent pellet.
- Pour off supernatant and drain tube on clean absorbent paper. Add 300µl 70% ethanol. Invert the tube several times to wash the RNA pellet.
- Centrifuge at 13,000-16,000 x g for 1min. Carefully pour off the ethanol.
- Invert and drain the tube on clean absorbent paper and allow to air dry for 15 min.

RNA hydration

- Add 25µl RNA Hydration Solution.
- Allow RNA to rehydrate at least 30 minutes on ice. Alternatively, store RNA sample at -70°C to -80°C until use.
- Before use, vortex sample vigorously for 5 seconds and pulse spin. Pipette sample up and down several times to ensure adequate mixing.
- Store RNA sample at -70°C to -80°C.

2.4.2 Extraction of DNA from FFPE

This was generally performed on samples following LCM. The PUREGENE® DNA isolation kit (Gentra Systems Inc., MN, USA) was utilised for this function, with slight modifications.

Cell lysis

- Perform microdissection and place cap in a 0.5ml microcentrifuge tube containing 300µl Cell Lysis Solution and 1.5µl Proteinase K solution (20mg/ml).
- Incubate overnight at 55°C with constant agitation (i.e. a rotary oven).

RNase treatment (optional)

- Add 1.5µl RNase A Solution (4 mg/ml) to the cell lysate.
- Mix the sample by inverting the tube 25 times and incubate at 37°C for 15-60 minutes.

Protein precipitation

- Cool sample to room temperature.
- Transfer solution to a fresh 1.5ml microcentrifuge tube and add 100µl Protein Precipitation Solution to the cell lysate and vortex vigorously for 20s.
- Place tube into an ice bath for 5min.
- Centrifuge at 13,000-16,000 x g for 3min. The precipitated proteins will form a tight pellet.
- (optional) Transfer the supernatant to a fresh tube and repeat ice incubation and centrifugation steps.

DNA precipitation

- Pipette the supernatant containing the DNA (leaving behind the precipitated protein pellet) into a clean 1.5ml microcentrifuge tube containing 300µl 100% isopropanol (2-propanol) and 0.5µl glycogen (20mg/ml).

- Mix the sample by inverting gently 50 times and incubate @ -20°C for 1 hr.
- Centrifuge at 13,000-16,000 x g (@ 4°C if possible) for 5 minutes.
- Pour off supernatant and drain tube on clean absorbent paper. Add 300µl 70% ethanol. Invert the tube several times to wash the DNA pellet.
- Centrifuge at 13,000-16,000 x g for 1 min. Carefully pour off the ethanol.
- Invert and drain the tube on clean absorbent paper and allow to air dry 15min.

DNA hydration

- Add 20µl DNA Hydration Solution.
- Allow DNA to rehydrate for 1 hr @ 65°C and/or overnight at room temperature. If possible, tap tube periodically to aid in dispersing the DNA.
- Store DNA at 4°C. For long-term storage, store at -20°C or -80°C.

2.4.3 RNA extraction from thyroid carcinoma cell lines

When larger quantities of RNA were required, with higher purities, the RNeasy® mini kit (Qiagen Ltd., West Sussex, UK) was used. With some of the more advanced technologies used for gene expression analysis, like expression microarray technology, such requirements are paramount. Microgram quantities are often required for such experiments, as well as high quality poly-A RNA that is completely free of both DNA and protein. The more traditional precipitation methods are insufficient for such a task and a quicker spin column method with on-column DNase digestion is usually employed.

- Following trypsinisation of cultured cells, pellet 3-4 X 10^6 cells by centrifugation and remove supernatant.

- Add 600µl Buffer RLT containing 1% β-mercaptoethanol and homogenise by pipetting the lysate onto a QIAshredder spin column and centrifuging at maximum speed for 2 min.
- Add 1 volume (600µl) of 70% ethanol to the homogenized lysate, and mix well by pipetting. Do not centrifuge.
- Apply up to 700µl of the sample, including any precipitate that may have formed, to an RNeasy mini column placed in a 2 ml collection tube (supplied). Close the tube gently, and centrifuge for 15s at ≥10,000 rpm. Discard the flow through. If the volume exceeds 700µl, load aliquots successively onto the RNeasy column, and centrifuge as above. Discard the flow-through after each centrifugation step.
- Pipette 350µl Buffer RW1 into the RNeasy mini column, and centrifuge for 15s at ≥10,000rpm to wash. Discard the flow-through.
- Add 10µl DNase I stock solution to 70µl Buffer RDD. Mix by gently inverting the tube.
- Pipette the DNase I incubation mix (80µl) directly onto the RNeasy silica-gel membrane, and place on the bench top (20–30°C) for 15min.
- Pipette 350µl Buffer RW1 into the RNeasy mini column, and centrifuge for 15s at ≥10,000rpm. Discard the flow-through.
- Transfer the RNeasy column into a new 2 ml collection tube (supplied). Pipette 500µl Buffer RPE onto the RNeasy column. Close the tube gently, and centrifuge for 15s at ≥10,000rpm to wash the column. Discard the flow-through.

- Add another 500µl Buffer RPE to the RNeasy column. Close the tube gently, and centrifuge for 2 min at ≥10,000rpm to dry the RNeasy silica-gel membrane.
- Place the RNeasy column in a new 2 ml collection tube (not supplied), and discard the old collection tube with the flow-through. Centrifuge in a microcentrifuge at full speed for 1 min.
- To elute, transfer the RNeasy column to a new 1.5 ml collection tube. Pipette 30–50µl RNase-free water directly onto the RNeasy silica-gel membrane. Close the tube gently, and centrifuge for 1 min at ≥10,000rpm to elute.
- If the expected RNA yield is >30µg, repeat the elution step as described with a second volume of RNase-free water. Elute into the same collection tube.
- RNA quantity and quality are assessed by UV spectroscopy and agarose gel electrophoresis respectively.

2.5 Taqman® PCR

A TaqMan® PCR-based system was selected for mRNA quantitation and DNA genotyping in this study. The Taqman® system was chosen for a number reasons. Firstly Taqman® PCR and Reverse-Transcriptase (RT) PCR requires only a few nanograms of target DNA/RNA. This is highly significant since the amount of DNA/RNA extractable from formalin fixed and paraffin embedded archival material is low. Secondly, Taqman PCR and RT-PCR products are small (generally less than 200bp) and thus can be used to amplify partially degraded or fragmented DNA/RNA such as that obtained from FFPE material.

Taqman® PCR exploits the 5′ nuclease activity of AmpliTaq Gold® DNA Polymerase to cleave a TaqMan probe during PCR. The TaqMan probe contains a reporter dye at the 5′ end of the probe and a quencher dye at the 3′ end of the probe. During the reaction, cleavage of the probe separates the reporter dye and the quencher dye, resulting in increased fluorescence of the reporter. Accumulation of PCR products is detected directly by monitoring the increase in fluorescence of the reporter dye, shown in Fig 2.2.

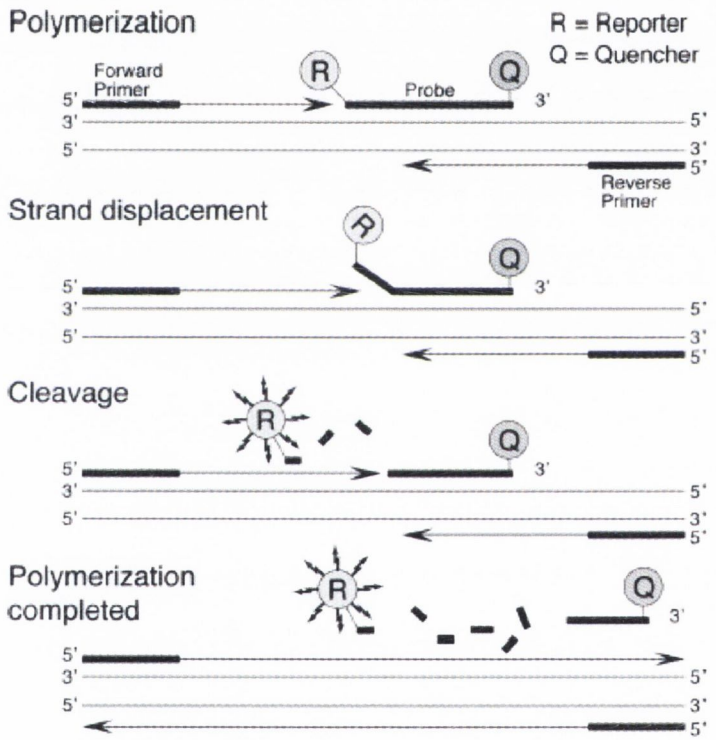

Figure 2.2 The forklike-structure-dependent, polymerisation-associated, 5′–3′ nuclease activity of AmpliTaq Gold DNA Polymerase during PCR

When the probe is intact, the proximity of the reporter dye to the quencher dye results in suppression of the reporter fluorescence primarily by Förster-type energy transfer

(Förster, 1948; Lakowicz, 1983). During PCR, if the target of interest is present, the probe specifically anneals between the forward and reverse primer sites.

The 5´-3´ nucleolytic activity of the AmpliTaq Gold DNA Polymerase cleaves the probe between the reporter and the quencher only if the probe hybridises to the target. The probe fragments are then displaced from the target, and polymerisation of the strand continues. The 3´ end of the probe is blocked to prevent extension of the probe during PCR. This process occurs in every cycle and does not interfere with the exponential accumulation of product.

The probe consists of an oligonucleotide with a 5´-reporter dye and a 3´-quencher dye. A fluorescent reporter dye, such as FAM (6-carboxyfluorescein), is covalently linked to the 5´ end of the oligonucleotide. TET (6-carboxy-4,7,2´,7´-tetrachlorofluorescein), JOE (6-carboxy-4,5-dichloro-2,7-dimethoxyfluorescein), and VIC are also used as reporter dyes. In older Taqman® probes each of the reporters is quenched by TAMRA (6-carboxy-N,N,N´,N´-tetramethylrhodamine) at the 3´ end.

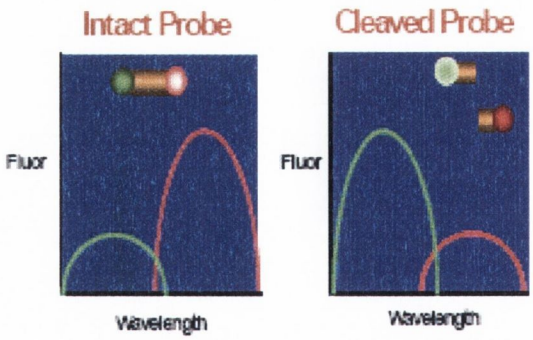

Figure 2.3 Increased fluorescence activity due to cleaved probe

Newer Taqman® MGB probes are recommended for genotyping/allelic discrimination (AD) purposes and when conventional probe exceed 30bp. MGB probes contain:

- A non-fluorescent quencher (NFQ) at the 3´ end - the SDS instruments can measure the reporter dye contributions more precisely because the quencher does not fluoresce.
- A minor groove binder at the 3´ end - The minor groove binder increases the melting temperature (Tm) of probes, allowing the use of shorter probes.

2.5.1 Real-time quantitative Taqman® RT-PCR

Real-time RT-PCR is the ability to monitor the progress of the PCR as it occurs (i.e., in real time). Data is therefore collected throughout the PCR process, rather than at the end of the PCR. This completely revolutionizes the way one approaches PCR-based quantitation of DNA and RNA. In real-time RT-PCR, reactions are characterized by the point in time during cycling when amplification of a target is first detected rather than the amount of target accumulated after a fixed number of cycles. The higher the starting copy number of the nucleic acid target, the sooner a significant increase in fluorescence is observed. In contrast, an endpoint assay (also called a "plate read assay") measures the amount of accumulated PCR product at the end of the PCR cycle. RT-PCR can be one-step or two-step in nature.

In the initial cycles of PCR, there is little change in fluorescence signal. This defines the baseline for the amplification plot. An increase in fluorescence above the baseline indicates the detection of accumulated target. A fixed fluorescence threshold can be

set above the baseline. The parameter C_T (threshold cycle) is defined as the fractional cycle number at which the fluorescence passes the fixed threshold (see Fig 2.4).

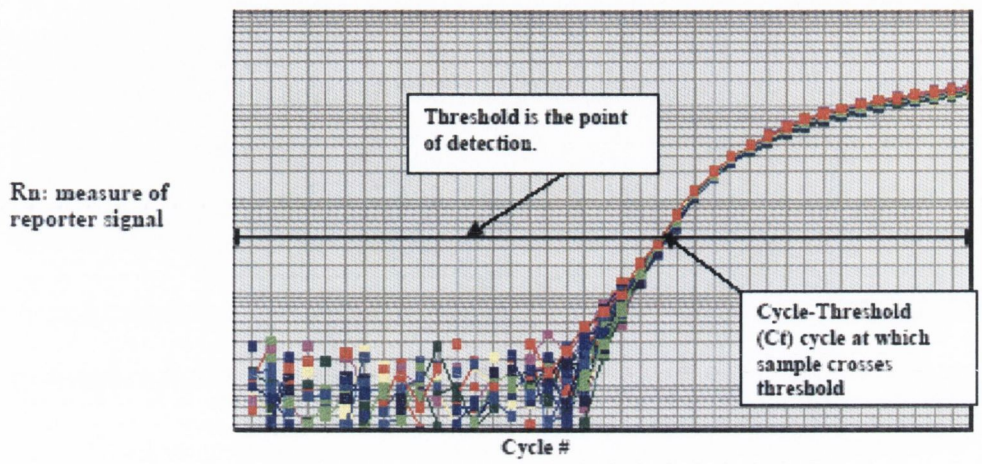

Figure 2.4 Example of an amplification plot

A sample of known concentration used to construct a standard curve. By running standards of varying concentrations, you create a standard curve from which you can extrapolate the quantity of an unknown sample. The standards used depend on whether absolute or relative quantitation is used.

It is easy to prepare standard curves for relative quantitation as quantity is expressed relative to some basis sample, such as the calibrator. For all experimental samples, target quantity is determined from the standard curve and divided by the target quantity of the calibrator. Thus, the calibrator becomes the 1X sample, and all other quantities are expressed as an n-fold difference relative to the calibrator. As an

example, in a study of drug effects on expression, the untreated control would be an appropriate calibrator.

For quantitation normalized to an endogenous control, standard curves are prepared for both the target and the endogenous reference. For each experimental sample, the amount of target and endogenous reference is determined from the appropriate standard curve. Then, the target amount is divided by the endogenous reference amount to obtain a normalized target value. Again, one of the experimental samples is the calibrator, or 1X sample. Each of the normalized target values is divided by the calibrator normalized target value to generate the relative expression levels. For the quantitation of gene expression, researchers have used β-actin, glyceraldehyde-3-phosphate dehydrogenase (GAPDH), ribosomal RNA (rRNA), or other RNAs as an endogenous control.

The standard curve method for absolute quantitation is similar to the standard curve method for relative quantitation, except the absolute quantities of the standards must first be known by some independent means. Plasmid DNA and in vitro transcribed RNA are commonly used to prepare absolute standards. Concentration is measured by UV spectroscopy and converted to the number of copies using the molecular weight of the DNA or RNA.

2.5.2 Taqman® SNP genotyping/allelic discrimination assay

Detection of nucleotide mutations and polymorphisms is central to the modern science of molecular genetics. For example, allelic discrimination detects different forms of the same gene that differ by nucleotide substitution, insertion or deletion. Methods for mutation detection can be divided into two groups: scanning methods that can discover previously unknown nucleotide differences and diagnostic methods designed to detect specific, known mutations and polymorphisms. Large-scale scoring of known SNPs requires techniques with few steps and the ability to automate each of these steps. In this regard, the 5' nuclease assay is ideal because it combines PCR amplification and detection into a single step.

Figure 2.5 demonstrates how fluorogenic probes and the 5' nuclease assay can be used for allelic discrimination. For a bi-allelic system, probes specific for each allele are included in the PCR assay. The probes can be distinguished because they are labelled with different fluorescent reporter dyes (typically FAM and VIC). A fully hybridised probe remains bound during strand displacement, resulting in efficient probe cleavage and release of the reporter dye. A mismatch between probe and target greatly reduces the efficiency of probe hybridisation and cleavage. Therefore, substantial increases in either FAM or VIC fluorescence indicates homozygosity for the FAM- or VIC-specific allele. an increase in both signals indicates heterozygosity. The feasibility of this approach was first demonstrated by Lee et al. (1993) when the used the technology to distinguish between the ΔF508 and normal alleles of the human cystic fibrosis gene.

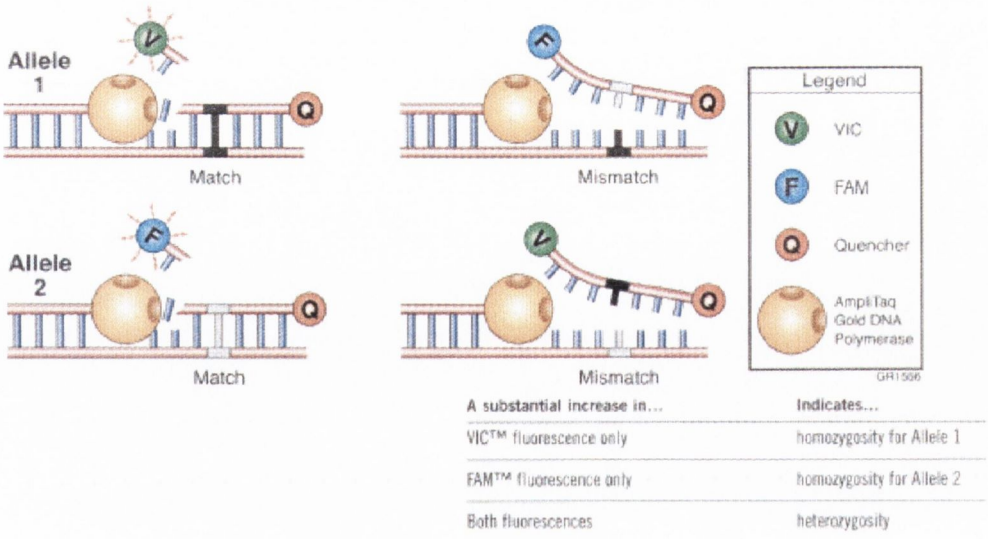

Figure 2.5 Allelic discrimination using the 5' nuclease assay

Three factors contribute to the discrimination based on a single mismatch. First, the mismatch has a disruptive effect on hybridisation. A mismatched probe will have a lower T_m than a perfectly matched probe. Proper choice of annealing/extension temperature during PCR will favour hybridisation of an exact-match probe over a mismatched probe. Second, the assay is performed under competitive conditions with both probes present in the same reaction tube. Therefore, mismatched probes are prevented from binding due to stable binding of exact match probes. Third, the 5' end of the probe must start to be displaced before cleavage occurs. The 5' nuclease activity of Taq polymerase recognises a forked structure with a displaced 5' strand of at least 1 to 3 nucleotides (Lyamichev et al., 1993). Once a probe starts to be displaced, complete dissociation occurs faster with a mismatch than an exact match. This means there is less time for cleavage to occur with a mismatch probe. Thus, the presence of a mismatch promotes dissociation rather than cleavage of the probe.

Unknown samples are typically performed in duplicate. 6 no template controls (NTC) and known samples for all 3 possible outcomes (heterozygote, homozygote allele 1

and 2) are included with each run for allele calling purposes. A generic graphical output from an AD run is shown in Fig 2.6.

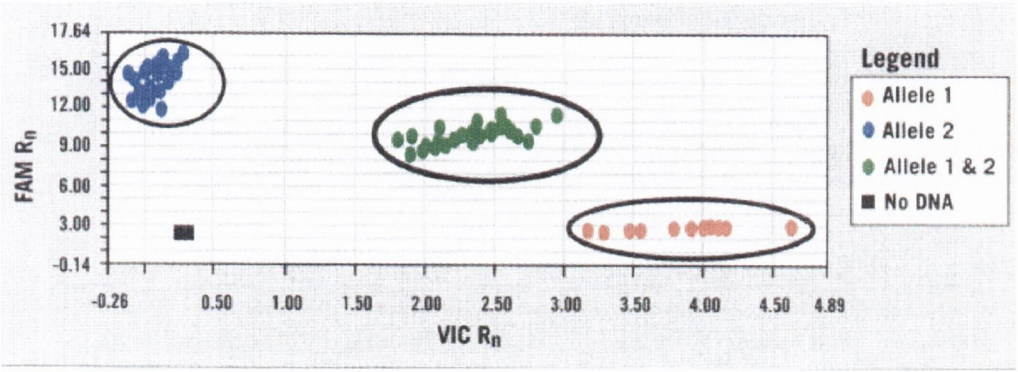

Figure 2.6 Typical allelic discrimination output

2.5.3 Primers and probes

Primers/probes used in expression studies were designed and purchased using Primer Express Software versions 1.5-1.7 (Applied Biosystems, Cheshire, UK) according to the criteria described in the Primer Express manual unless otherwise stated. Specific sequence information is included in the relevant chapters.

Primers/probes used for AD purposes were designed and purchased using the Custom TaqMan® SNP Genotyping Assays service.

2.5.4 Absolute standard generation

2.5.4.1 Amplification of target sequence

RT-PCR was carried out in a two-step manner using TaqMan® Reverse Transcription Reagents and AmpliTaq Gold® DNA Polymerase kit (Applied Biosystems, Cheshire, UK). RNA was extracted from buccal squamous mucosal cells using the PURESCRIPT protocol (see 2.4.1) and reverse transcribed in a 20µl volume using the following reaction conditions: 5mM $MgCl_2$, 1X RT buffer, 0.2mM each dNTP, 1U/µl RNase inhibitor, 2.5U/µl MuLV reverse transcriptase and 2.5µM random hexamers. Reverse transcription was carried out using the PE 9600 Geneamp PCR System (Applied Biosystems, CA, USA) @: 25°C for 10 min, 42°C for 30 min, 99°C for 5min and hold at 4°C. 2µl of the derived cDNA was used in a subsequent PCR reaction to produce an amplicon bigger than that of the TaqMan® amplicon: 1.5mM $MgCl_2$, 1X PCR buffer, 0.2mM each dNTP, 400nM each primer, 1.25U AmpliTaq® Gold DNA Polymerase. PCR was carried out using the PE 9600 Geneamp PCR System @ 95°C for 5min, (95°C 20s, 55°C 30s, 72°C 30s) X 40 cycles, 72°C 7min and hold at 4°C. RT-PCR products were run on a 2% agarose gel containing 0.5µg/ml ethidium bromide at 80 volts.

2.5.4.2 Purification of PCR products

PCR products were purified using the QIAquick® Gel Extraction Kit (Qiagen Ltd., West Sussex, UK). All centrifugation steps are at 13,000rpm in a standard microcentrifuge.

- Excise the gel slice containing the DNA band with a clean, sharp scalpel.
- Weigh the gel slice. Add 1–2 volumes of diffusion buffer to 1 volume of gel (i.e., 100–200µl for each 100 mg of gel).
- Incubate at 50°C for 30 min.
- Centrifuge the sample for 1 min.
- Carefully remove the supernatant using a pipette or a drawn-out Pasteur pipette. Pass the supernatant through a disposable plastic column or a syringe containing either a Whatman GF/C filter or packed, siliconised glass wool to remove any residual polyacrylamide.
- Determine the volume of the recovered supernatant.
- Add 3 volumes of Buffer QG to 1 volume of supernatant and mix. Check that the colour of the mixture is yellow. If the colour of the mixture is orange or violet, add 10µl 3M sodium acetate, pH 5.0. The colour of the mixture will turn yellow.
- Place a QIAquick Spin Column in a provided 2ml collection tube.
- To bind DNA, apply the sample to the QIAquick Spin Column and centrifuge for 30–60s.
- Discard flow-through and place QIAquick Spin Column back into the same collection tube.
- To wash, add 0.75ml Buffer PE to column and centrifuge for 30–60s.

- Discard flow-through and place QIAquick Spin Column back in the same tube. Centrifuge column for an additional minute at maximum speed.
- Place QIAquick Spin Column into a clean 1.5ml microcentrifuge tube.
- To elute DNA, add 50l Buffer EB (10mM Tris·Cl, pH8.5) or water to the center of the QIAquick Spin Column and centrifuge for 1min.

2.5.4.3 Ligation

Cloning was performed using the TOPO TA Cloning® kit (Invitrogen Corp., CA 92008, USA). Taq polymerase has a non-template-dependent terminal transferase activity that adds a single deoxyadenosine (A) to the 3′ ends of PCR products. The linearised vector supplied in this kit has single, overhanging 3′ deoxythymidine (T) residues. This allows PCR inserts to ligate efficiently with the vector.

- Ligation reactions were performed in duplicate with 1µl and 4µl of purified PCR product, 1µl of salt solution, 1µl TOPO vector and sterile water to a volume of 6µl.
- Mix reaction gently and incubate for 5min at room temperature (22-23°C) then place the reaction on ice.

2.5.4.4 Transformation

- Add 2µl of the TOPO® Cloning reaction into a vial of One Shot® Chemically Competent E. coli and mix gently. Do not mix by pipetting up and down.
- Incubate on ice for 5 to 30min.
- Heat-shock the cells for 30s at 42°C without shaking and immediately transfer the tubes to ice.

- Add 250µl of room temperature S.O.C. medium and shake the tube horizontally (200 rpm) at 37°C for 1hr.
- Spread 10µl and 50µl from each transformation on a pre-warmed selective plate (40µl of 100mM IPTG and 40mg/ml X-gal) and incubate overnight at 37°C.
- An efficient TOPO® Cloning reaction should produce several hundred colonies. Pick white or light blue colonies for analysis. Do not pick dark blue colonies.

2.5.4.5 Analysis of positive clones

Four colonies were selected and streaked out on LB plates containing 50µg/ml ampicillin. Single colonies were isolated and grown overnight in 5ml LB broth containing 50µg/ml ampicillin. Plasmid DNA was then extracted using the QIAprep® Miniprep kit (Qiagen Ltd., West Sussex, UK).

- Resuspend pelleted bacterial cells in 250µl Buffer P1 and transfer to a microcentrifuge tube.
- Add 250µl Buffer P2 and gently invert the tube 4–6 times to mix.
- Add 350µl Buffer N3 and invert the tube immediately but gently 4–6 times.
- Centrifuge for 10min at 13,000rpm in a tabletop microcentrifuge.
- Apply the supernatants to the QIAprep spin column by pipetting.
- Centrifuge for 30–60s. Discard the flow-through.
- Wash QIAprep spin column by adding 0.75ml Buffer PE and centrifuging for 30–60s.
- Discard the flow-through, and centrifuge for an additional 1min to remove residual wash buffer.

- Place the QIAprep column in a clean 1.5 ml microcentrifuge tube. To elute DNA, add 50µl Buffer EB (10mM Tris·Cl, pH8.5) or water to the centre of each QIAprep spin column, let stand for 1min, and centrifuge for 1min.

PCR, electrophoresis and gel purification were performed as described earlier (2.5.4.1 and 2.5.4.2). A restriction digest with *Bam* H1 restriction enzyme was preformed to verify that the insert was present. Briefly, 1 unit enzyme/µg of double stranded plasmid DNA was incubated for 30 minutes at 37°C. Agarose gel electrophoresis was performed as previously described.

Plasmids were also sequenced using the ABI 310 Prism Big Dye Terminator Cycle Sequencing Reaction (Applied Biosystems) according to the manufacturers instructions.

2.5.4.6 Preparation of glycerol stocks

Once colonies have been confirmed to contain the appropriate insert, glycerol stocks were prepared.

- Streak the original colony out on LB plates containing 50µg/ml ampicillin.
- Isolate a single colony, inoculate into 1-2ml of LB containing 50µg/ml ampicillin and grow until culture reaches stationary phase.
- Mix 0.85ml of culture with 0.15ml of sterile glycerol and transfer to a cryovial.
- Store at -80°C.

2.5.4.7 cRNA generation

Plasmids found to contain the correct insert were linearised using *HindIII* enzyme. Following restriction digestion, the linearised plasmids were phenol:chloroform:isoamyl alcohol purified. The purified linearised plasmid was then used as template for cRNA synthesis using the Riboprobe® System - SP6/T7 (Promega, Southampton SO16 7NS, UK).

- The following were combined in a 0.2ml MicroAmp reaction tube to a 20µl volume: 4µl Transcription Optimised 5X Buffer, 2µl 100nM DTT, 20U Recombinant RNasin® Ribonuclease Inhibitor, 1µl each 2.5mM rATP, rUTP, rCTP, rGTP, 20U T7 RNA Polymerase and remainder Template DNA.
- Incubate 4hr at 37°C
- Add 2µl (2U) RQ1 RNase-free DNase and incubate at 37°C for an additional 30min
- Perform agarose gel electrophoresis to check for remaining DNA
- Transfer reaction volume to a fresh 1.5ml microcentrifuge tube and increase to 100µl with nuclease-free water.
- Add 1 volume TE-saturated phenol:chloroform:isoamyl alcohol (25:24:1) pH4.5, vortex for 1min and centrifuge at 15,000rpm for 5min.
- Remove upper aqueous layer to a fresh tube and add 1 volume of chloroform:isoamyl alcohol (24:1).
- Vortex for1min and centrifuge at 15,000rpm for 5min.
- Remove upper aqueous layer to a fresh tube and add 0.5 volumes of 7.5M ammonium acetate and 2.5 volumes 100% ethanol.
- Vortex and incubate at -80°C for 30min.

- Centrifuge at 15,000rpm 30min at 4°C.
- Discard supernatant and wash pellet with 500µl 70% ethanol.
- Centrifuge at 15,000rpm 5min, discard supernatant and allow pellet to air dry.
- Resuspend in 20µl nuclease-free water.
- Quantify cRNA by UV spectroscopy.

2.5.4.8 Calculation of cRNA copy number

The following formula was used to calculate the copy number per µl:

Number of base pairs in plasmid plus insert multiplied by the molecular weight of one base pair (330g/L) equals 1M solution of plasmid, which contains Avogadros's constant copies of plasmid (6.02×10^{23} copies per litre). Therefore the number of copies per ng can be calculated; the concentration of plasmid ng/µl multiplied by copies per ng, equals copies per µl.

2.5.5 Microarrays

The Applied Biosystems Expression Array System is based on a microarray design that represents the whole human genome, utilises current transcript data and relies entirely upon gene annotations that have been validated by experts in human curation. Each probe is part of a relational database that includes both Celera Genomics annotations and those in the public domain. Combined with specially developed chemiluminescent chemistries, this complete system delivers greater probe and detection sensitivity than previous generations of microarray systems. In addition annotation information for all of the 31,097 human genes that are represented on the microarray is included in an Oracle® database that is provided with the 1700 system. The manufacturers suggest that the result is a complete system that is capable of rapid and accurate analysis of microarray data for gene expression research. 'Follow on' experiments from microarrays can be achieved by linking to quantitative real time PCR TaqMan® probe based assays that enable microarray data validation, absolute quantitation of transcript production and investigation of alternative splicing events.

The Applied Biosystems Expression Array System consists of an Analyser (Applied Biosystems 1700 Chemiluminescent Analyser) that can image arrays in chemiluminescence, to survey and measure the gene expression at very low levels and in fluorescence, to locate and auto-grid features. The 1700 is equipped with a state-of-the-art high resolution, large format CCD camera. The cooled CCD is back-illuminated for high efficiency and has very low read noise. This, coupled with the low background from chemiluminescence, results in very high sensitivity.

Applied Biosystems microarrays are sealed in a pre-assembled cartridge and contain oligonucleotides with a feature diameter of <180 μm, and a space of >45 μm (edge-to-edge) between each feature. The oligonucleotides target transcripts in each gene of the human genome. Oligonucleotide probes are synthesized at Applied Biosystems and designed to ensure maximal specificity. Prior to microarray manufacture, all probes undergo analysis by mass spectrometry for quality control. All Applied Biosystems microarrays utilize 60-mer oligonucleotides (oligos) as DNA probes. Oligos of this length offer the best combination of sensitivity and specificity when compared to microarrays containing either shorter oligos or cDNA probes. 60-mer oligos offer the good single-base hybridisation specificity that is expected from shorter oligos, and the strong sensitivity of longer fragments expected from cDNA arrays.

Excellent results may be achieved from as little as 500ng of starting total RNA by using the Applied Biosystems Chemiluminescent RT-IVT Labelling Kit. The chemistry of the RT-IVT Kit, which exploits the Eberwine (Eberwine et al., 1992) linear amplification procedure, increases the yield of cRNA from cDNA by >1,000-fold. The reverse transcriptase incorporates deoxynucleotides and digoxigenin-dUTP (DIG-dUTP) in the synthesis of single-stranded cDNA from sample RNA and RT Labelling Control RNA. The reverse transcriptase used in this reaction is a modified version of M-MLV reverse transcriptase. The modified reverse transcriptase has no RNase H activity. It also provides longer cDNA transcripts and higher yields than the wild type enzyme. Multiple transcription rounds result in the production of DIG-labelled cRNA (see Fig 2.7). The resultant digoxigenin-labelled cDNA or cRNA is specifically hybridised to the Applied Biosystems microarray.

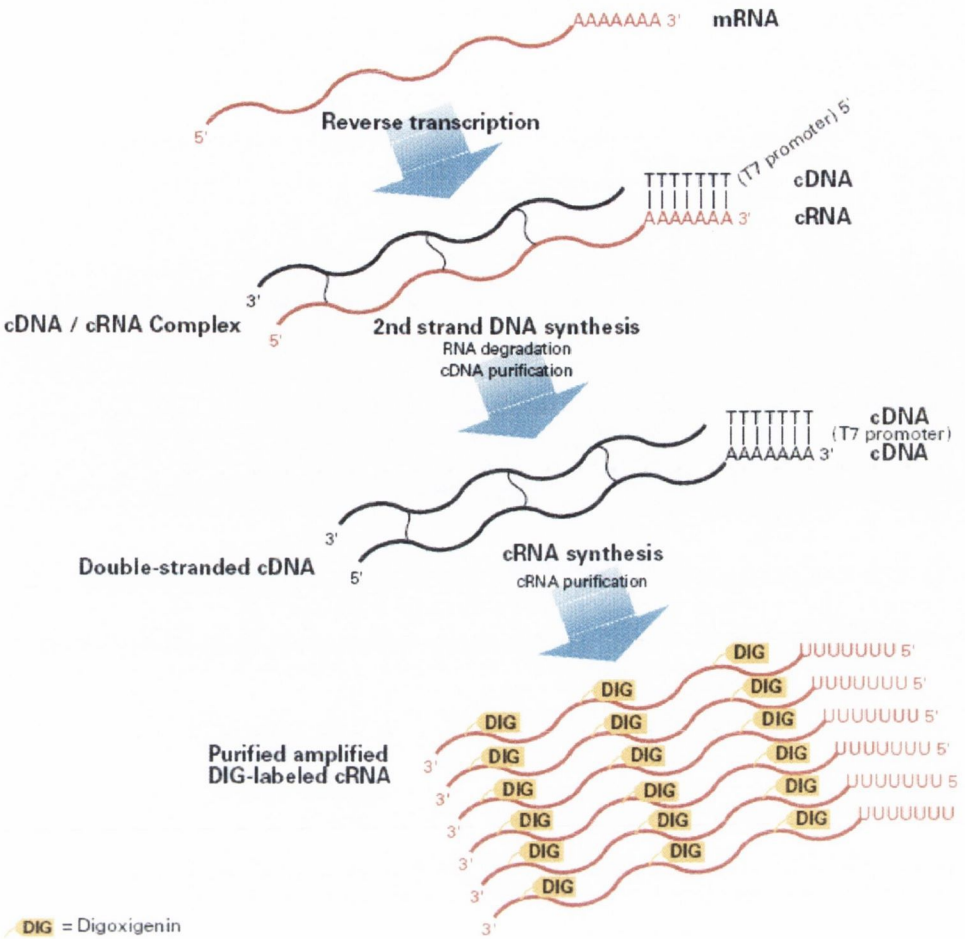

Figure 2.7 RT-IVT DIG-labelling of sample mRNA

When unbound materials have been washed from the microarray, the Applied Biosystems Chemiluminescence Detection Kit is used to visualize features that have digoxigenin-labelled cDNA or cRNA bound to the oligonucleotide probes. Visualization is achieved by incubating the microarray with an anti-digoxigenin alkaline phosphatase conjugate. Alkaline phosphatase hydrolyses a chemiluminescent substrate and emits light at a wavelength of ~458nm. The signal intensity is proportional to the mRNA level expressed in the cells (see Fig 2.8).

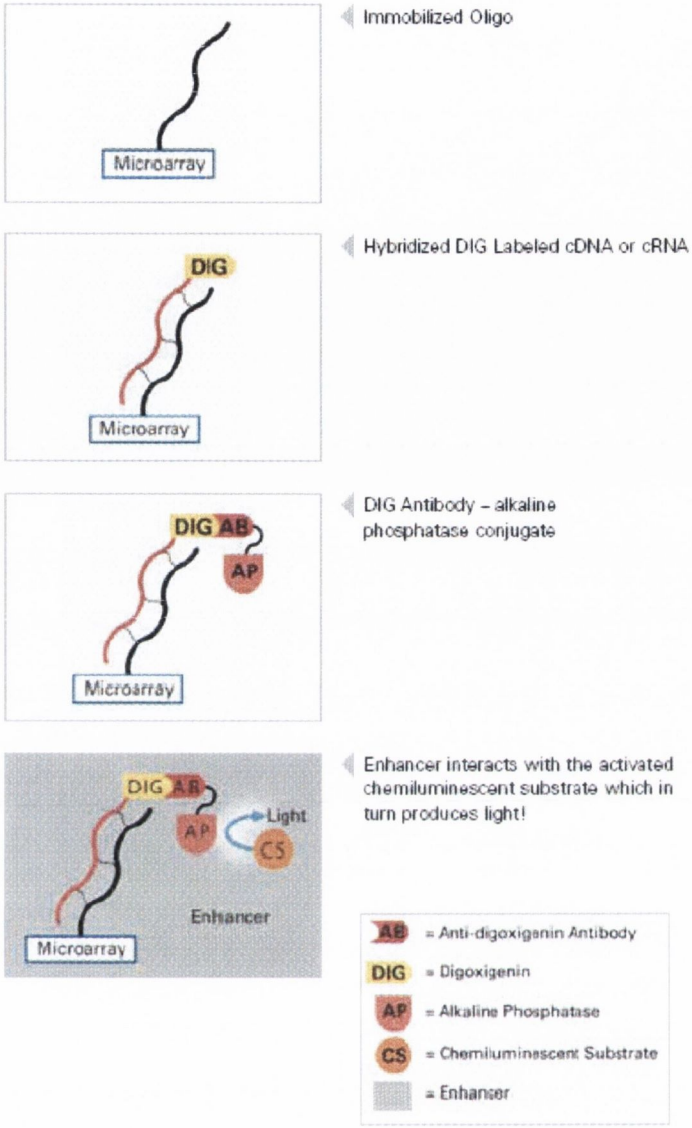

Figure 2.8 Chemiluminescent detection of bound DIG-labelled cRNA

Also present during hybridisation is a 24-mer oligonucleotide labelled with the fluorescent LIZ® dye. This oligonucleotide is complementary to one that is co-deposited at microarray features during manufacture of Applied Biosystems microarrays. The fluorescent signal, which has a close spatial correlation with the

chemiluminescent signal, locates all features on the microarray, even in the absence of gene expression products.

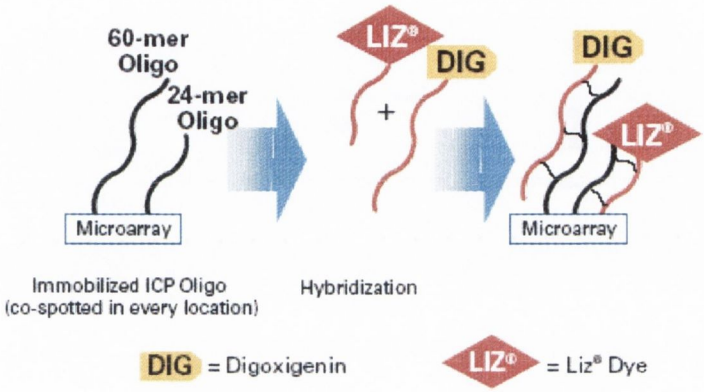

Figure 2.9 Fluorescence oligos used to image microarray features

A motorized chassis moves the microarray into the optical path of the analyser to detect chemiluminescent and fluorescent signals. System software can then relate the resultant intensities to gene expression, accurate feature registration, and data quality control. When the microarray is loaded into the 1700 analyser, the temperature is raised to 35°C in order for the enzymatic reaction to reach a steady state. Multiple images are then taken to bring the microarray into focus and to measure, in turn, the fluorescent and chemiluminescent signals

The microarray is imaged in both short (5 seconds) and long (25 seconds) read times to extend the linear dynamic range of the chemiluminescent signals (>1,000-fold). There are two imaging areas for each microarray. The total time required to image a microarray, including the pre-incubation and focus steps, is approximately 12 minutes. Light production on the microarray reaches a steady state within the first five

minutes, while the microarray is being focused and brought up to 35°C. The chemiluminescent reaction emits light at a steady state for at least 60 minutes thereafter. The absence of an excitation background, together with the highly reproducible photon emissions, makes the signal-to-noise ratio produced from equivalent hybridisations superior to that found in alternative array systems.

Chemiluminescent and fluorescent fiducials are features that monitor data quality and analysis, and are built into every Applied Biosystems microarray. Labelled oligonucleotides (DIG and LIZ® dye-labelled oligos) in concentration ladders ranging over 500-fold are deposited on the microarray during manufacture. The resident software is able to recognize these features and uses them to monitor the efficacy of the chemiluminescent chemistries and the efficiency of fluorescent detection (see Fig 2.10).

Labelled oligonucleotides are included with the hybridisation controls in the Applied Biosystems Chemiluminescence Detection Kit. These oligonucleotides are complementary to those deposited on the microarray during manufacture. They monitor hybridisation conditions, such as sample mixing and washing stringency, providing protocol diagnostics and ensuring signal uniformity (see Fig 2.10).

Finally, labelling kit controls are included with both the Applied Biosystems Chemiluminescent RT Labelling Kit and the RT-IVT Labelling Kit. They are synthetic bacterial control genes (Dap, Lys, Phe, BioB, BioC, and BioD). These controls provide quality information on RT and RT-IVT Kit enzyme activity and DIG-label incorporation efficiency for each experiment (see Fig 2.10).

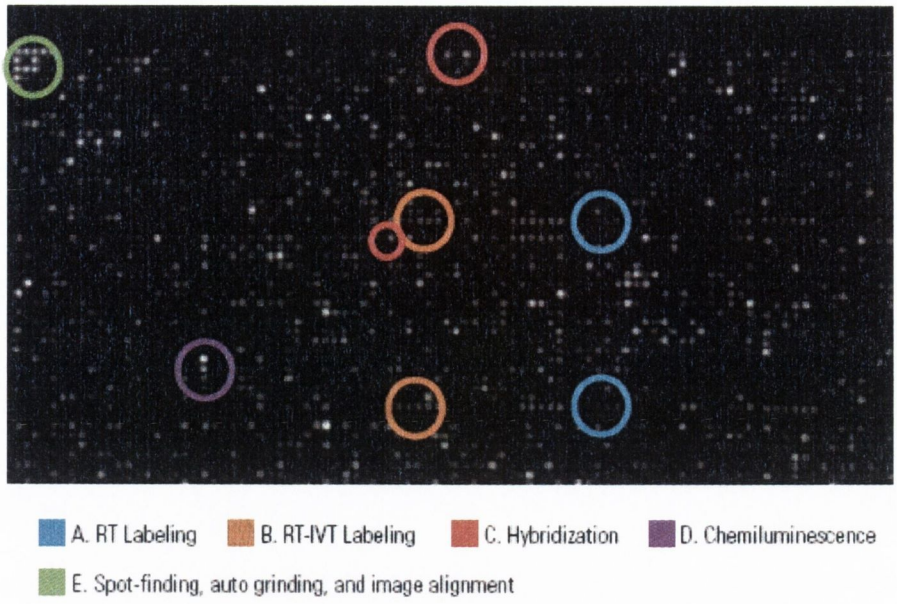

Figure 2.10 Examples of controls used in Applied Biosystems microarrays

2.5.5.1 RT-IVT labelling

RT

- Pipette the following components into 0.2ml MicroAmp reaction tube on ice: 2µl T7-Oligo (dT) primer, 4µl Control RNA, RNA sample (1-10µg) and nuclease-free water to 15µl.
- Heat the RNA and primer mixture in a thermal cycler to 70°C for 5min followed by a 4°C hold.
- After the run, place the tube on ice.
- Add the following components to the reaction tube on ice and mix thoroughly by pipetting: 2µl 10X 1st Strand Buffer Mix and 3µl RT Enzyme Mix.

- Perform reverse transcription in a thermal cycler: 25°C 10min, 42°C 2hr, 70°C 15min and 4°C hold.
- After the run, place the tube on ice and add the following components to the cDNA mixture: 30µl 5X 2nd Strand Buffer Mix, 5µl 2nd Strand Enzyme Mix and 95µl nuclease-free water.
- Perform second strand synthesis in a thermal cycler: 16°C 2hr, 70°C 15min and 4°C hold.

Purifying cDNA

- In a 1.5ml nuclease-free microcentrifuge tube, combine: 150µl DNA Binding Buffer and 150µl 2nd strand synthesis reaction mix.
- Insert a DNA purification column into a 2.0-ml receptacle tube.
- Transfer the reaction-DNA Binding Buffer mixture (300µl) to the column and centrifuge at 10,000rpm for 1min.
- Remove the column from the tube, discard the liquid, and then reinsert the column into the tube.
- Add 700µl of DNA Wash Buffer to the column and centrifuge at 10,000rpm for 1min.
- Remove the column from the tube, discard the liquid, and then reinsert the column into the tube.
- Add 700µl of DNA Wash Buffer to the column and centrifuge at 10,000rpm for 1min.
- Remove the column from the tube, discard the liquid, and then reinsert the column into the tube.

- Close the tube, then centrifuge the empty column and tube at 10,000rpm for 1 minute.
- Transfer the column to a new 1.5ml elution tube.
- Pipette 30µl of DNA Elution Buffer onto the fibre matrix at the bottom of the column and allow to stand at room temperature for 1min.
- Centrifuge the column and tube at 10,000rpm for 1min.
- Repeat elution step twice more for a final elution volume of 90µl.

IVT labelling

- Calculate the volume of cDNA output required, based on the amount of RNA input:

Amount of RNA input	**Volume of cDNA output required**
≤2µg	90µl
>2µg	150 ÷ (µg of total RNA input)

- If the volume of cDNA output required is:
    - Greater than 24 µl: Use a vacuum concentrator to concentrate the required volume of cDNA output to 24 µl.
    - Less than 24µL: Add nuclease-free water to the required volume of cDNA output until the total volume is 24 µL.
- Add the following IVT components to the 24 µl cDNA output at room temperature: 8µl 5X IVT Buffer Mix, 4µl DIG-UTP (approximately 14 nmol) and 4µl IVT Enzyme Mix.
- Perform IVT in the thermal cycler: 37°C 9hr followed by a 4°C hold.

Purifying cRNA

- In a new 1.5ml nuclease-free microcentrifuge tube, combine and then vortex briefly to mix: 20µl nuclease-free water and 40µl IVT reaction.
- Add and mix by pipetting: 200µl RNA Binding Buffer and 140µl 100% ethanol.
- Insert an RNA purification column into a 2ml receptacle tube, add the IVT reaction-RNA Binding Buffer-ethanol mixture (400µl) to the column, and centrifuge at 10,000rpm for 1min.
- Discard the flow-through.
- Add 500µl of RNA Wash Buffer to the column and centrifuge at 10,000rpm for 1min.
- Discard the flow-through.
- Add 500µl of RNA Wash Buffer to the column and centrifuge at 10,000rpm for 1min.
- Discard the flow-through.
- Close the tube, then centrifuge the column and tube at 10,000rpm for an additional minute.
- Transfer the column to a new 1.5ml elution tube.
- Pipette 50µl of RNA Elution Buffer onto the fibre matrix at the bottom of the column and incubate at room temperature for 2min.
- Centrifuge at 10,000rpm for 1min for an elution volume of 50µl.
- Pipette 50µl of RNA Elution Buffer onto the fibre matrix at the bottom of the column and incubate at room temperature for 2min.
- Centrifuge at 10,000rpm for 1min for a final elution volume of 100µl.

- Resulting labelled cRNA should be stored on ice while quantity and quality are assessed using UV spectroscopy and agarose gel electrophoresis respectively.
- cRNA can be stored at -20°C for up to months or -80°C for long term storage.

2.5.5.2 Chemiluminescence detection

Pre-hybridisation

- Prepare pre-hybridisation mixture in a nuclease-free tube and vortex to mix: 150µl nuclease-free water, 330µl Hybridisation Buffer, 100µl Hybridisation Denaturant and 420µl Blocking Reagent.
- Transfer pre-hybridisation mixture into each microarray cartridge and incubate in a 55°C oven at 100prm for 1hr.

Fragmenting cRNA

- Combine components into a 0.2mL MicroAmp® reaction tube on ice, then mix by pipetting: 10µl cRNA Fragmentation Buffer and 90µl 10µg DIG-labelled cRNA and nuclease-free water.
- Heat the tube in a thermal cycler at 60°C for 30min.
- Add 50µL of cRNA Fragmentation Stop Buffer, mix by pipetting and place on ice.

Hybridisation

- For each microarray, prepare hybridisation mixture in a nuclease-free microcentrifuge tube: 100µl nuclease-free water, 170µl Hybridisation Buffer, 30µl Hybridisation Controls, 50µl Hybridisation Denaturant and 150µl fragmented cRNA targets.
- Vortex the hybridisation mixture, then centrifuge the tube briefly.

- Quickly transfer hybridisation mixture into each microarray cartridge, drying the port with lint-free tissue prior to sealing.
- Return cartridges to the oven and incubate at 55°C at 100rpm for 16hr.

Hybridisation washes

- Add 600ml hybridisation wash buffer 1 to a clean wash tray.
- Remove microarrays from their cartridges, decant liquid and submerge in wash buffer.
- Agitate on the rocking platform shaker (tilt angle 10°; tilt speed 30 tilts back and forward per min) for 5min.
- Add 600ml hybridisation wash buffer 2 to a clean wash tray. Transfer microarray to new tray, draining them in the process.
- Agitate on the rocking platform shaker for 5min.
- Drain the buffer from the wash tray.
- Add 400ml CL rinse buffer to the wash tray, making sure that all microarrays are submerged in buffer.
- Agitate on the rocking platform shaker for 5min.
- Drain the buffer from the wash tray.
- Add 400ml CL rinse buffer to the wash tray, making sure that all microarrays are submerged in buffer.
- Agitate on the rocking platform shaker for 5min.
- Remove wash tray from the rocking platform shaker.
- Microarrays may be left in CL rinse buffer at room temperature for up to 1hr.

Antibody binding

- Combine components for the CL blocking buffer/antibody mixture in a nuclease-free tube and mix well by inversion. Do not vortex (N.B. per microarray): 2.8ml nuclease free water, 200µl Chemiluminescence Rinse Buffer Concentrate, 1ml Blocking Reagent and 15µl Anti-digoxigenin-AP.
- Remove one microarray from the wash tray, shake and tap it gently, then place it vertically on the rocking platform shaker.
- Immediately add 4ml CL blocking buffer/antibody mixture to the microarray.
- Cover the arrays with the wash tray cover and agitate on the rocking platform shaker for 20min at room temperature.

Antibody washes

- Add 500ml CL rinse buffer to a clean wash tray.
- Decant CL blocking buffer/antibody mixture, shake and tap the microarray gently, then place it in the wash tray.
- Cover the wash tray and agitate on the rocking platform shaker for 10min.
- Drain the buffer from the wash tray.
- Add 500ml CL rinse buffer to the wash tray and agitate on the rocking platform shaker for 10min.
- Drain the buffer from the wash tray.
- Add 500ml CL rinse buffer to the wash tray and agitate on the rocking platform shaker for 10min.
- Remove wash tray from the rocking platform shaker. Microarrays may be left in the CL rinse buffer at room temperature for up to 3hr.

Chemiluminescent reaction

- The chemiluminescent reaction is time-dependent. Perform this procedure with only one microarray at a time.
- Place 100ml CL enhancing rinse buffer in a 10.2 X 12.7cm (4 X 5inch) tray.
- Remove one microarray from the wash tray, decant the CL rinse buffer, shake and tap the microarray gently and place it in the CL enhancing rinse buffer.
- Agitate on the rocking platform shaker for 10 min.
- Remove the microarray from the small tray, decant CL enhancing rinse buffer, shake and tap the microarray gently, then place it vertically on the rocking platform shaker.
- Quickly add 4ml of Chemiluminescence Enhancing Solution to the microarray.
- Agitate on the rocking platform shaker for 20 min.
- Place 100ml CL enhancing rinse buffer in a second small tray.
- Decant the enhancing solution from the microarray, then shake and tap the microarray gently.
- Place the microarray in the second small tray and agitate on the rocking platform shaker for 5min.
- Remove the microarray from the small tray, decant the CL enhancing rinse buffer, then shake and tap the microarray gently.
- Wipe the bottom of the microarray with lint-free tissue.
- Add 3.5ml of Chemiluminescence Substrate to the microarray.
- The chemiluminescent reaction is time dependent. After you perform this step, proceed with performing CL detection immediately on the ABI 1700 Chemiluminescent Analyser.

2.6 References

Eberwine J, Yeh H, Miyashiro K, Cao Y, Nair S, Finnell R, Zettel M, Coleman P. Analysis of gene expression in single live neurons. Proc Natl Acad Sci U S A 1992; 89:3010-4.

Förster VT. Zwischenmolekulare Energiewanderung und Fluoreszenz. Annals of Physics (Leipzig) 1948; 2: 55–75.

Lakowicz JR. Principles of Fluorescence Spectroscopy. New York: Plenum Press 1983; xiv, 496 pp.

Lyamichev V, Brow MAD, Dahlberg JE. Structure-specific endonucleolytic cleavage of nucleic acids by eubacterial DNA polymerases. Science 1993; 260: 778-83.

Chapter 3

E-cadherin expression in ret/PTC-1 activated thyroid neoplasms

3.1 Summary

Papillary thyroid carcinoma (PTC), the commonest variety of thyroid cancer is found in a variety of morphological variants, usually grows slowly and is clinically indolent, although rare, aggressive forms, with local invasion or distant metastases occur. Our group has previously demonstrated an association between Hashimoto thyroiditis and ret/PTC-1 activation, and have hypothesised that c-*ret* activation might be implicated in immune reaction to thyroid epithelium.

The objective of this study was to examine expression of the cellular adhesion molecule, E-cadherin, in various thyroid tumour types and Hashimoto thyroiditis in the context of ret/PTC-1 positivity using laser capture microdissection and TaqMan™ RT-PCR.

Variable down-regulation of E-cadherin among carcinomas was demonstrated, with anaplastic carcinomas showing little or no expression. Follicular thyroid carcinomas consistently had significantly decreased E-cadherin expression compared with papillary thyroid carcinomas. The ret/PTC-1 positive papillary thyroid carcinoma and Hashimoto thyroiditis cases had consistently lower E-cadherin expression levels than the corresponding ret/PTC-1 negative papillary carcinomas, suggesting not only an association between ret activation and the loss of cellular adhesion but, more significantly an association between papillary thyroid carcinoma and Hashimoto thyroiditis.

3.2 Introduction

Epithelial tissues typically have complex architecture and undergo continuous turnover within an organism. The maintenance of artefacts such as glandular or villous structures requires complex control mechanisms to ensure correct cellular spatial arrangement and the balance of cell proliferation and death. Damaged tissue must also be allowed to regenerate until normal architecture is restored and equilibrium restored. Failure of the above mentioned control mechanisms can therefore result in tissue disorganisation, abnormal growth and neoplasia. Key to these control mechanisms are the cellular adhesion molecules (CAMS): the integrins, the immunoglobulin superfamily, the selectins and the cadherins.

The family of molecules known as the cadherins are considered one of the most important CAMS, and are key to intercellular cell junctions. Cadherins are single transmembrane proteins that mediate cell–cell adhesion and cell motility in a strictly Ca^{2+}-dependent, homophilic manner, and have been divided up into more than 10 subgroups, depending on their tissue distribution. These groups include E- (epithelial), N- (neuronal), and P- (placental) cadherins.

3.2.1 E-cadherin

Although members of the family are expressed differentially across all tissue types, the predominant member in epithelium is E-cadherin (CDH1). E-cadherin (16q22.1) is a 120kDa protein that was first isolated from embryonal carcinoma cell membranes (Hyafil et al., 1980). In embryogenesis, it is expressed in the fertilised egg and is necessary for blastocyst development, the earliest embryonic epithelium (Ekblom et al., 1986).

The protein is comprised of an intracellular domain for cytoskeletal anchoring, a single-span transmembrane domain and an extracellular cadherin repeats domain with requires the presence of extracellular calcium for functionality. The extracellular domain of E-cadherin has five cadherin repeats, each of which containing a histidine-arginine-valine (HAV) motif (Overduin et al., 1995). These repeats allow E-cadherin molecules on adjacent cells to form the homotypic interactions, thereby strongly bonding two cells together. It is normally located on the lateral surfaces of epithelial cells in a region of cell-cell contact known as the adherens junction. In most epithelial tissues, adherens junctions form a type of belt around each cell, creating a continuous zipper of cell adhesion (Shapiro et al., 1995). This is facilitated by bundles of actin filaments which run parallel to the adhesion belt on the cytoplasmic side of the membrane (see Fig 3.1).

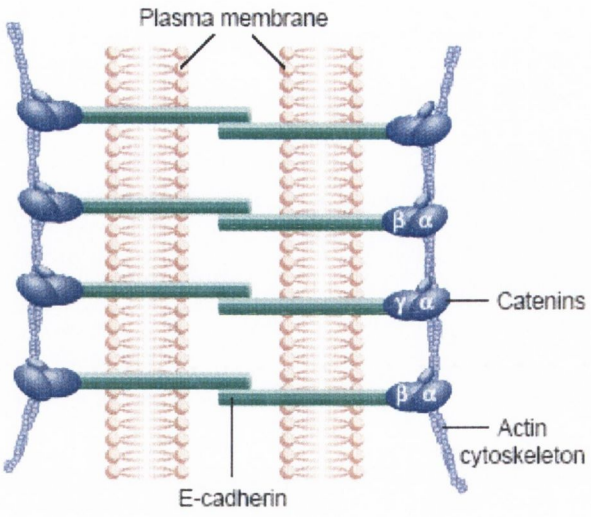

Figure 3.1 A typical adherens junction in epithelial tissue showing the "zipper-like" formations caused by E-cadherin interactions

(adapted from Guilford. E-cadherin downregulation in cancer: fuel on the fire? Mol Med Today 1999; 5: 172-7)

E-cadherin associates with a group of cytoplasmic proteins known as the catenins (e.g. α-, β- and γ-catenin) (Ozawa et al., 1989). Its cytoplasmic tail is linked via the catenins (with which the tumour suppressor gene product APC also interacts) to the actin cytoskeleton (see Fig 3.2). Thus, catenins are cytoplasmic proteins that interact with the intracellular domain of E-cadherin to provide anchorage to the microfilament cytoskeleton.

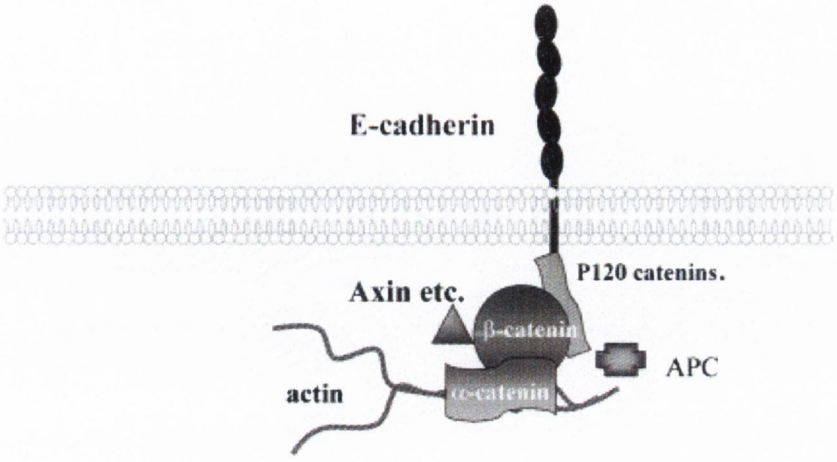

Figure 3.2 Structure and functionality of E-cadherin

(adapted from Jiang et al., E-cadherin complex and its abnormalities in human breast cancer. Surg Oncol 2000; 9: 151-71)

3.2.2 E-cadherin and cancer

Given the roles played by cadherins in development and homeostasis, disruption of their normal function would be expected to result in diseases characterised by abnormal tissue morphology and aggressive cell migration. Cadherins are therefore, by their very nature, regarded as tumour suppressor genes and defects in their expression or function have been associated with tumour progression (Hedrich et al., 1993).

Abnormal E-cadherin function has been shown to be caused by several factors, including: reduction in the level of E-cadherin, abnormal localisation, mutation, shedding or enzymatic degradation, changes in phosphorylation status and abnormalities in binding partners such as the catenins. Any of the above may contribute to an overall decreased level of E-cadherin protein, which has been described in many human tumours such as colon (Pignatelli et al., 1992), squamous cell carcinoma of the head and neck (Schipper et al., 1991; Sorscher et al., 1995), pancreas (Pignatelli et al., 1994), bladder (Umbas et al., 1994) and prostate (Umbas et al., 1992). Its downregulation has also been shown to correlate with increased tumour invasion, metastasis and poor prognosis (Mareel et al., 1995).

3.2.3 E-cadherin in thyroid carcinoma

Studies of E-cadherin expression in thyroid tissue, at both the mRNA and protein levels, have produced conflicting results. Brabant et al. (Brabant et al., 1993) demonstrated minimal or absent E-cadherin expression in undifferentiated/anaplastic thyroid carcinomas, and variably reduced levels of expression in differentiated phenotypes when

compared with normal thyroid. These results have been supported by other workers, some of whom have also proposed E-cadherin expression as a prognostic indicator (Sheumman et al., 1995; Soares et al., 1997; Von Wasielewski et al., 1997; Cerrato et al., 1998; Naito et al., 2001). Additional studies suggest that while both differentiated (Huang et al., 1998, 1999; Celetti et al., 2000) and poorly differentiated thyroid carcinomas (Graff et al., 1998) do express E-cadherin, it is relocated from the cell surface to the cytoplasm in both entities.

3.2.4 ret/PTC-1

c-*ret* is one of many proto-oncogenes whose activation in thyroid disease has been investigated to assess its prognostic significance. ret/PTC is the activated form of c-ret, which until recently (Sheils et al., 2000), was thought to be exclusive to PTC (Grieco et al., 1990; Santoro et al., 1993). To date, nine genes have been shown to be involved in ret/PTC rearrangements (Klugbauer et al., 2000) (see Table 1.1). ret/PTC-1 is the variant most commonly detected (≈70%). All rearrangements result in an mRNA chimera in which the tyrosine kinase domain of ret is fused with a donor sequence (Williams et al., 1995). The membrane-anchoring and ligand-binding domains of ret are lost as a result of this fusion, while the 5' sequences that donate their promoters become juxtaposed to the ret tyrosine kinase domain. In their native form, each protein acting as a donor in the generation of a ret chimera, is ubiquitously expressed.

ret/PTC-1 has been characterised and shown to be generated by fusion of the tyrosine kinase encoding region of c-*ret* to the 5' terminal sequences of a gene termed H4 (Grieco

et al., 1994; Pasini et al., 1995). It has been hypothesised that ret/PTC fusion proteins may effect cellular transformation via reactivation of the foetal c-*ret* tyrosine kinase domain which is found in all chimeric RET proteins (Tong et al., 1995). From previous experiments, our group has suggested that activation of chimeric c-*ret* transcripts may cause not only the structural and nuclear peculiarities of PTC, but also an immune reaction to thyroid epithelium due to alteration of the cellular antigenic profile. This alteration of cellular antigenicity could be caused by the loss of adhesive junctions or ligand binding and transmembrane domains.

3.2.5 Aims

Although several studies have shown reduced E-cadherin expression levels in thyroid carcinomas, its association with ret/PTC oncogenes has not previously been investigated. This study was undertaken to further elucidate the expression profile of E-cadherin in thyroid in association with ret/PTC-1 activation in thyroid tissue and to determine if a link exists between expression of the chimeric transcript and cellular adhesion.

3.3 Materials & methods

3.3.1 Specimens

Samples (n=78) of papillary thyroid carcinoma (PTC) (n=31), Hashimoto thyroiditis (HT) (n=14), follicular carcinoma (FTC) (n=12), anaplastic carcinoma (ATC) (n=5) or follicular adenoma/normal thyroid tissue (FA/NORM) (n=16) accessioned between 1982 and 2001 in St. James's Hospital, Dublin were analysed. All material was fixed in 10% buffered formal saline and embedded in paraffin wax. Stained sections were reviewed blind by two histopathologists and classified according to a recognised system (Rosai et al., 1992).

3.3.2 Microdissection and RNA extraction

In order to correctly measure E-cadherin expression, it was necessary to acquire homogeneous cell populations of thyrocytes. 2 consecutive 7μm sections were cut from each block, dewaxed and stained with haematoxylin and eosin (H&E). Thyrocytes from one section in each case were laser capture microdissected using the PixCell®II System (Arcturus Engineering, Inc., CA, USA) for subsequent expression analysis (see chapter 2.2). Following microdissection the Capsures® were placed in sterile Eppendorf tubes and RNA extraction was performed using the PURESCRIPT® RNA Isolation Kit (Gentra Systems Inc., MN, USA) using the protocol described in chapter 2.4.1.

3.3.3 Standard preparation

To demonstrate the linearity and efficiency of the reverse transcription and TaqMan® reactions and for the purpose of absolute quantitation, standard curves were required. A GAPDH RNA standard curve was generated by performing a serial dilution on control human RNA (supplied by Applied Biosystems, CA, USA) and analysing as per the test samples.

E-cadherin standards were produced as follows. E-cadherin cDNA was obtained by extracting RNA from buccal squamous mucosal cells and reverse transcribing. External primers (see Table 3.1 for sequences) were used in a solution phase PCR to amplify an amplicon larger than the TaqMan® product from the resultant cDNA. The product was isolated by electrophoresis in a 1% agarose gel, cutting the bands from the gel, and recovery with a QIAamp Spin Column (QIAGEN Inc., CA, USA). The purified product was cloned into a plasmid using the TOPO™ TA Cloning® Kit (Invitrogen™, CA, USA) and the recombinant plasmid was recovered using QIAprep® Miniprep System (QIAGEN Inc., CA, USA). Recombinant plasmid sequences were verified by solution phase PCR using the external primers, restriction analysis using BamHI and finally by direct M13 sequencing using ABI Prism® BigDye™ Terminator Cycle Sequencing Kit and the ABI Prism® 310 Genetic Analyser (Applied Biosystems, CA, USA). The appropriate plasmid was then linearised and extracted with phenol:chloroform:isoamyl alcohol. cRNA was then generated from linearised template DNA by using the Riboprobe® Combination System - SP6/T7 RNA Polymerase (Promega Corporation, WI, USA). This cRNA was

then quantified by UV spectroscopy and serial dilutions performed as appropriate (see Fig 3.6 for GAPDH/E-cadherin standard curves).

Reaction		Sequence
ret/PTC-1 Taqman®	F	CGC GAC CTG CGC AAA
	P (FAM labelled)	TTA CCA TCG AGG ATC CAA
	R	ACC AAG TTC TTC CGA GGG AAT T
GAPDH TaqMan®	F	CAT CCA TGA CAA CTT TGG TAT CGT
	P (VIC labelled)	ACT CAT GAC CAC AGT CC
	R	GGG TGG CAG TGA TGG CAT
E-cadherin TaqMan®	F	AGG TGA CAG AGC CTC TGG ATA GA
	P (VIC labelled)	TGC CAC ATA CAC TCT C
	R	TGG ATG ACA CAG CGT GAG AGA
E-cadherin (cloning) external primers	F	ACA CCC CCT GTT GGT GTC T
	R	CGG TTA CCG TGA TCA AAA TC

Table 3.1 Primers/probes sequences

3.3.4 Reverse transcription and TaqMan® PCR analysis

TaqMan® RT-PCR was carried out in a two-step manner with an initial randomly primed RT reaction followed by a separate PCR reaction. Extracted RNA was reverse-transcribed using TaqMan® Reverse Transcription Reagents kit (Applied Biosystems, CA, USA) under the following reaction conditions: 5mM $MgCl_2$, 1X PCR buffer, 0.2mM

each dNTP, 1U/µl RNase inhibitor, 2.5U/µl MuLV reverse transcriptase and 2.5µM random hexamers. Reverse transcription was carried out using the PE 9600 Geneamp PCR System (Applied Biosystems, CA, USA) @: 25°C for 10 min, 42°C for 30 min, 99°C for 5min and hold at 4°C. Derived cDNA was used as a template in the TaqMan® reactions. TaqMan® reactions were carried out using the TaqMan® PCR Universal Master Mix kit (Applied Biosystems, CA, USA) in a 25µl reaction volume. Reactions were performed using an Applied Biosystems 7700 Sequence Detection System (Applied Biosystems, CA, USA) with the following thermocycling parameters: 50°C 2min, 95°C 10mins and 40 cycles of [95°C 15s, 60°C 1min].

The principle of the TaqMan®/5' nuclease assay was discussed in detail in chapter 2.5. Real time analysis was used for quantitation of expression. In order to compensate for degradation of target RNA and differences in the amount of starting material, TaqMan® PCR was contemporaneously performed on cDNA from each sample in a separate reaction using glyceraldehyde phosphate dehydrogenase (GAPDH) as an endogenous control. The copy numbers obtained for E-cadherin were divided by the corresponding copy numbers for GAPDH to yield an expression index, $E\text{-}cad_i$. In the case of ret/PTC-1 detection, end-point detection was used to confirm the presence/absence of the ret/PTC-1 chimeric transcript. All PCR reactions and sequence detection were performed using the ABI Prism 7700 Sequence Detector. All primers/probes (see Table 3.1 for sequences) were designed using ABI Prism Primer Express 1.5 software (Applied Biosystems, Cheshire, UK) with the probes spanning exon-exon junctions to eliminate the possibility of residual genomic DNA detection. All probes used in the TaqMan® reactions were

designed to have non-fluorescent quenchers (NFQ) and minor groove binding (MGB) modifications (see chapter 2.5 for descriptions).

At least six negatives were included in each TaqMan® run. For ret/PTC-1 detection, cDNA from the cell line TPC-1 was included as a positive control. In the case of GAPDH and E-cadherin, the standards functioned as positive controls. All samples were run in duplicate and the standards were run in triplicate.

3.3.5 Statistical analysis

All statistical analyses were performed using Analyse-it™, version 1.62 (Analyse-it Software, Ltd.). As the data were non-parametric, the Kruskal-Wallis ANOVA and Mann-Whitney U tests were used to determine statistical significance between groups.

3.4 Results

3.4.1 Synthesis of cRNA standards for E-cadherin

RNA extracted from buccal squamous mucosal cells was used as template for the amplification of E-cadherin mRNA using flanking primers. The resulting RT-PCR products as illustrated in Figure 3.3 were gel purified and subsequently ligated into the plasmid vector (pCR 2.1-TOPO).

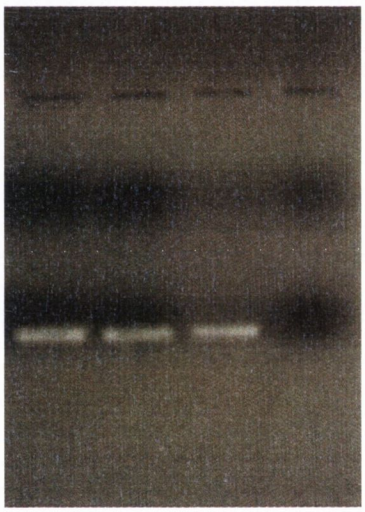

Figure 3.3 E-cadherin amplification using flanking primers

Solution phase RT-PCR products electrophoresed on a 2% agarose gel containing ethidium bromide. Lane 1-3: E-cadherin RT-PCR products from buccal squamous mucosal cells (166 bp amplicon), lane 4: negative RT-PCR control.

E-cadherin ligations in pCR 2.1-TOPO were transformed into *E.coli* (TOPO Top 10F') and cultured overnight. Single colonies were chosen, grown in broth, minipreped, and

the presence of E-cadherin inserts in the plasmids was checked using PCR with specific E-cadherin primers (Fig 3.4) and by restriction analysis using *BamH1* (Fig 3.5).

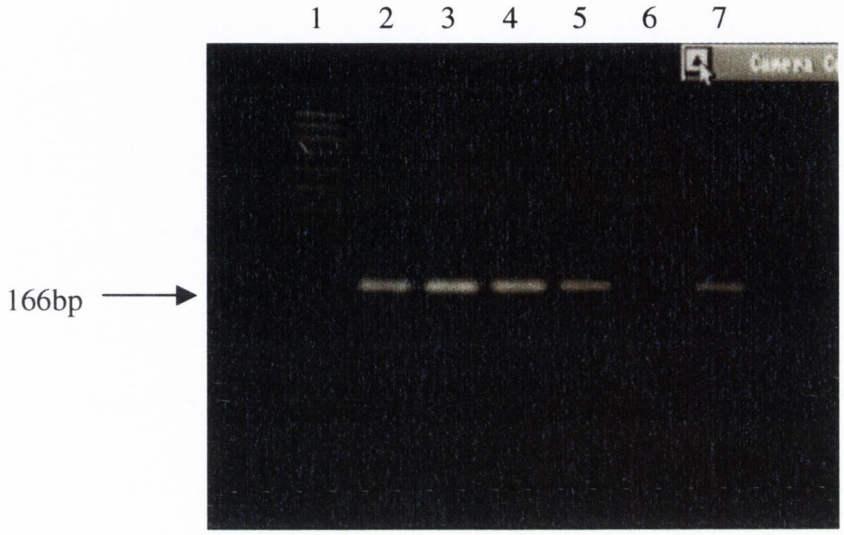

Figure 3.4 PCR check of selected clones

Solution phase PCR products electrophoresed on a 2% agarose gel containing ethidium bromide. Lane 1: DNA ladder, lanes 2-5: E-cadherin PCR products from plasmids from selected clones (166 bp amplicon), lane 6: negative PCR control, lane 7 positive PCR control (normal total human cDNA).

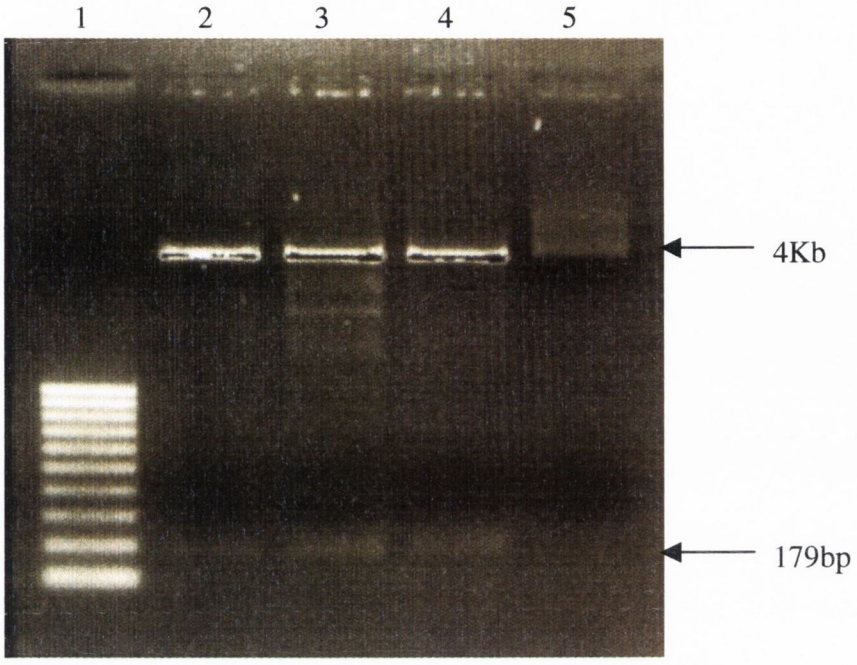

Figure 3.5 Endonuclease restriction analysis of selected clones

Restriction digested plasmids electrophoresed on a 2% agarose gel containing ethidium bromide. Lane 1: DNA ladder, lanes 2-4: *BamH1* digested plasmids from selected clones, lane 5: uncut pCR 2.1-TOPO.

Standard curves for E-cadherin and GAPDH were generated as outlined in chapter 2.5.4 and are illustrated in figure 3.6.

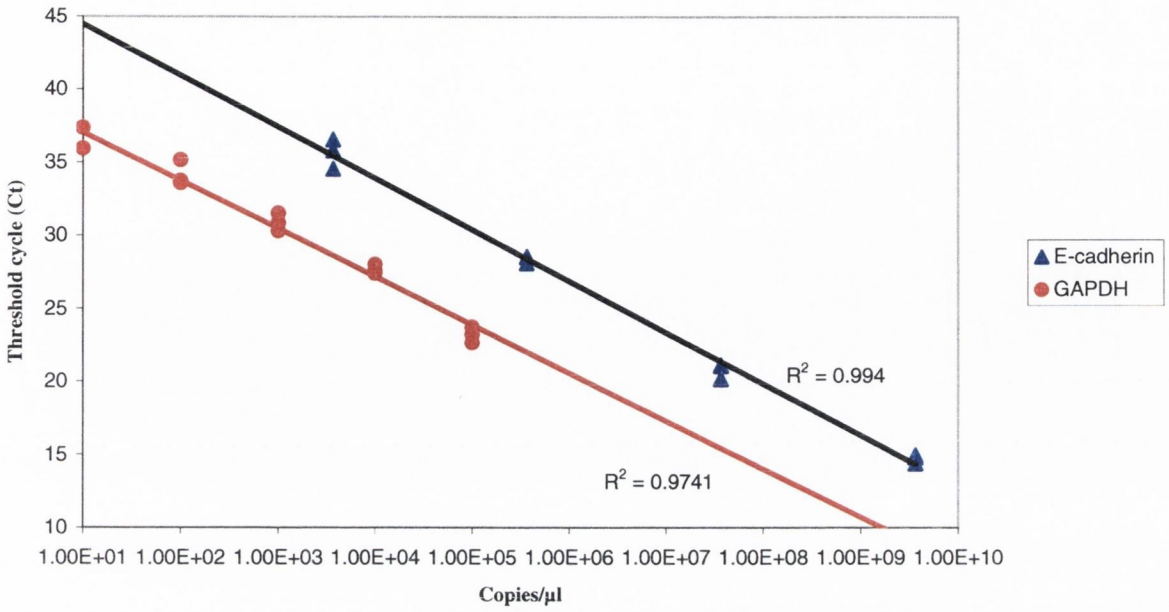

Figure 3.6 TaqMan® standard curves for E-cadherin and GAPDH

3.4.2 E-cadherin TaqMan® Quantitative RT-PCR

All samples included in the study tested positive for GAPDH. The results are summarized in table 3.2. A scatter plot of the individual E-cad$_i$ values for each sample within each category of tumour is displayed in Fig 3.7. The square roots of the corresponding E-cad$_i$ values were plotted in order to facilitate visualisation of the points on the graph. An example of the differential expression levels of E-cadherin are illustrated in a TaqMan® amplification plot in Fig 3.8.

Tumour type	ret/PTC-1 positive	E-cad$_i$ range	Median
PTC (total)	14/31	0 – 579	10
PTC $^{ret-}$	0/17	0 – 579	16
PTC $^{ret+}$	14/14	0 – 36	3
HT	11/14	0 – 277	4
FTC	0/12	0 – 11	3
ATC	5/5	0 – 2	0
FA/Normal	0/16	4 – 57	6.5

Table 3.2 E-cadherin expression in thyroid tissues

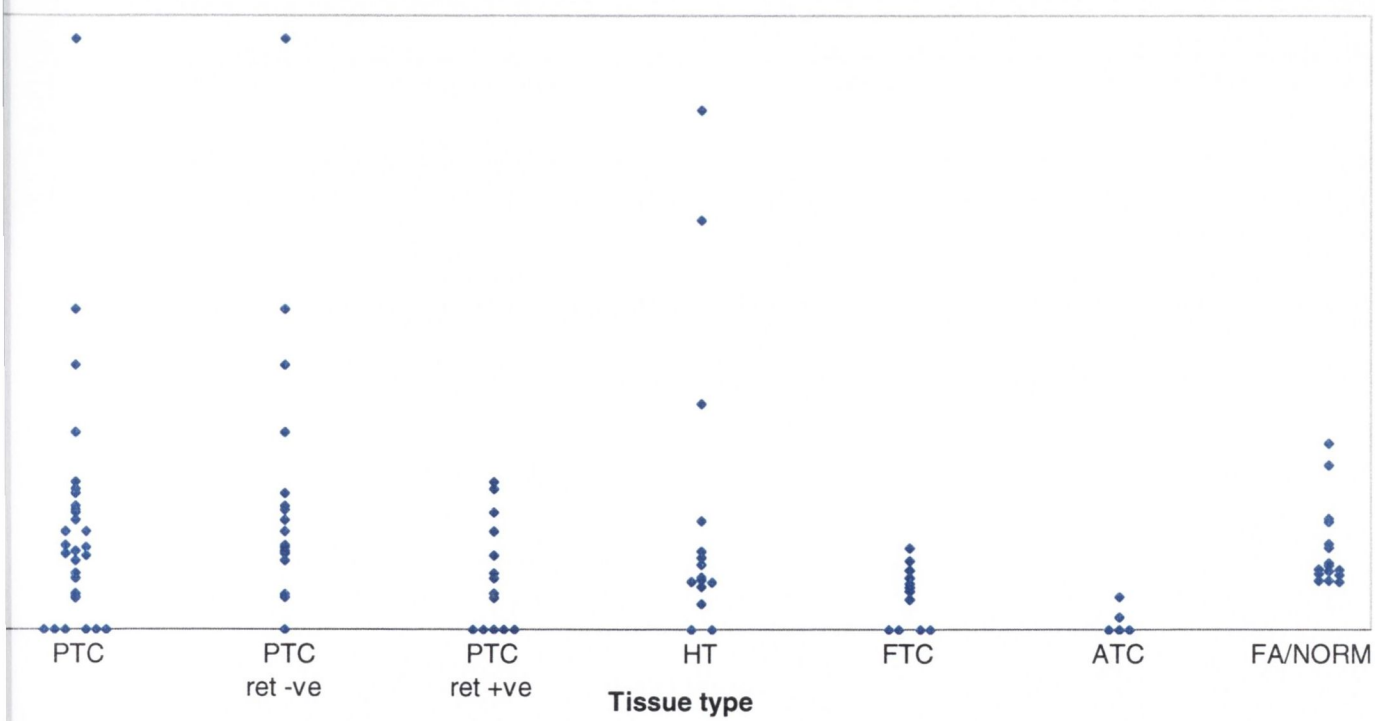

Figure 3.7 Normalised E-cadherin expression vs. tissue type

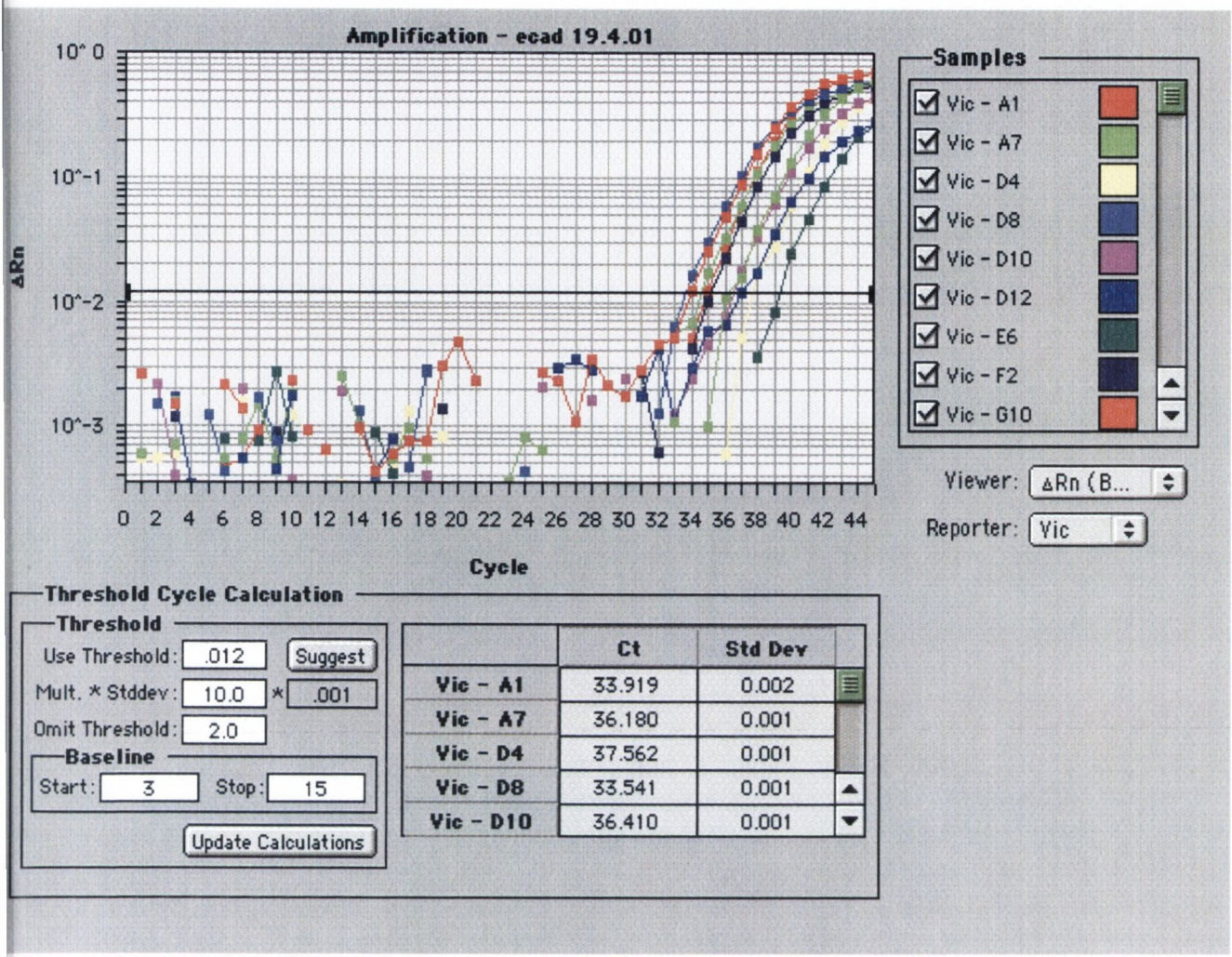

Figure 3.8 Sample computer generated E-cadherin TaqMan® amplification plots

E-cadherin expression was detected in all 16 cases of follicular adenoma/non-malignant thyroid. Among the 5 anaplastic tumours, 3 showed no expression of E-cadherin and the remainder had very low expression levels. Similarly, among the follicular thyroid carcinomas 4 displayed an absence of E-cadherin with the rest having varying levels of expression though never as low as the anaplastic lesions. The papillary thyroid

carcinomas displayed a wide range of expression levels (with 6 having no expression), as did the Hashimoto thyroiditis cases (see Fig 3.7).

3.4.3 Statistical analysis

The Kruskal-Wallis ANOVA test showed there to be a significant effect of group (p= 0.0009) across the specified disease cohorts. Pairwise comparisons using the Mann-Whitney U test are displayed in Table 3.3.

Test	p value
FA/Normal vs ATC	0.0009
FA/Normal vs. FTC	0.0025
FA/Normal vs. PTC	0.8927
FA/Normal vs. HT	0.1975
PTC vs FTC	0.0206
FA/Normal vs PTC $^{ret+}$	0.08
PTC $^{ret-}$ vs HT	0.0428
PTC $^{ret-}$ vs PTC $^{ret+}$	0.0244

Table 3.3 Statistical analysis of results using Mann-Whitney U test
Significant result at $p<0.05$

3.5 Discussion

It is well recognised that progressive loss of E-cadherin expression accompanies increasing dedifferentiation of thyroid (Brabant et al., 1993; Scheumman et al., 1995; Soares et al., 1997; Von Wasielewski et al., 1997; Cerrato et al., 1998; Naito et al., 2001) and other neoplasms (Shimoyama et al., 1991; Shiozaki et al., 1991; Inoue et al., 1992; umbas et al., 1992; Sorscher et al., 1995), with anaplastic carcinomas having minimal or undetectable levels of the adhesion molecule.

Of the differentiated thyroid carcinomas studied here, true follicular neoplasms (FTC) demonstrated a significant reduction in E-cadherin expression when compared to normal thyroid or follicular adenoma. In contrast, papillary carcinomas (PTC) overall showed no significant diminution in expression. This striking difference between FTC and PTC (Fig 3.7, Table 3.3) has not been reported previously and although the data are at variance with previously published work (Brabant et al., 1993; Graff et al., 1998), they support the suggestion (Pierotti et al., 1996) that the mechanism of oncogenesis in the two subtypes is as different as their morphology and biological behaviour.

When the PTCs in this study were stratified according to whether they did or did not exhibit the ret/PTC-1 chimera it was found that there was a statistically significant deviation from normal E-cadherin expression amongst the ret/PTC-1 positive (PTC $^{ret+}$) cohort. Five of a total of six PTC, which were devoid of E-cadherin expression were PTC $^{ret+}$ (the sixth being a highly aggressive tall-cell variant) suggesting that ret/PTC-1 activation is implicated in E-cadherin down-regulation. This hypothesis is supported by

the view that epigenetic or transcriptional factors, rather than gross genetic changes, are responsible for adhesion molecule loss in thyroid tumours (Shiozaki et al., 1991) and also by the work of Graff et al. (1998) on methylation silencing of E-cadherin. Furthermore, ret/PTC-1has commonality with other receptor tyrosine kinases such as c-ErbB2 and EGF, which have been shown to reduce E-cadherin expression in human mammary cell lines (D'Souza et al., 1994), and thyroid follicular cells of dogs and humans (Brabant et al., 1995) respectively *in vitro*.

There is strong evidence to suggest that down-regulation of E-cadherin expression is associated with greater tumour aggressiveness and metastatic potential and it is possible that the differences shown here between PTC $^{ret+}$ and PTC $^{ret-}$ cohorts may, at least in part, account for the known variability in behaviour of ostensibly similarly differentiated PTCs. The fact that one PTC $^{ret-}$ tumour in this series showed a total loss of E-cadherin expression is difficult to rationalise but highlights the problem of placing so-called tall-cell variants of PTC correctly within the spectrum of thyroid neoplasms.

The distinctive histological and nuclear morphology of PTC are mainstays in the diagnosis of the tumour and studies have previously postulated a causal role for ret/PTC-1 in the development of these features (Fischer et al., 1998; Sheils et al., 2000). Diminished E-cadherin expression has been proposed as a factor dictating the characteristic growth-pattern of diffuse gastric carcinoma (Machado et al., 1999) on the basis of aberrant tyrosine kinase activity and resultant alteration in cell adhesion properties (Yap et al., 1997). In the case of PTC $^{ret+}$ it is possible that both these factors

act synergistically, though this begs the question of why PTC $^{ret-}$ tumours should be morphologically indistinguishable. One explanation (Brabant et al., 1995) may be aberrant tyrosine activity *per se* may phosphorylate the E-cadherin/β-catenin complex resulting in ineffective function while maintaining normal E-cadherin mRNA levels (Behrens et al., 1993).

We included cases of Hashimoto thyroiditis in this study because of previous identification of ret/PTC-1 expression therein (Wirtschafter et al., 1997; Sheils et al., 2000). The demonstration of significant reduction of E-cadherin expression in follicular cells of HT has not been demonstrated hitherto. It is of interest that the 11 HT $^{ret+}$ tissues had E-cadherin levels significantly lower than PTC $^{ret-}$ tumours (and FA/normal tissue) whereas the 3 HT $^{ret-}$ tissue samples displayed near normal E-cadherin expression. This finding not only supports the hypothesis that ret/PTC-1 activation is instrumental in E-cadherin down-regulation but also lends further weight to the argument that HT may represent a pre-neoplastic phase of PTC. In addition, it is interesting to speculate that activation of ret/PTC-1, with its associated down-regulation of E-cadherin, may be responsible for alteration in the antigenic profile of follicular cell membranes sufficient to incite the cytotoxic lymphocytic response characteristic of the disease.

3.6 References

Behrens J, Vakaet L, Friis R, Winterhager E, Van Roy F, Mareel MM, Birchmeier W. Loss of epithelial differentiation and gain of invasiveness correlates with tyrosine phosphorylation of the E-cadherin/β-catenin complex in cells transformed with a temperature-sensitive v-SRC gene. J Cell Biol 1993; 120: 757-66.

Brabant G, Hoang-Vu C, Behrends J, Cetin Y, Potter E, Dumont JE, Maenhaut C. Regulation of the cell-cell adhesion protein, E-cadherin, in dog and human thyrocytes *in vitro*. Endocrinology 1995; 36: 3113-9.

Brabant G, Hoang-Vu C, Cetin Y, Dralle H, Scheumann G, Molne J, Hansson G, Jansson S, Ericson LE, Nilsson M. E-cadherin: a differentiation marker in thyroid malignancies. Cancer Res 1993; 53: 4987-93.

Celetti A, Garbi C, Consales C, Cerrato A, Greco D, Mele E, Nitsch L, Grieco M. Analysis of cadherin/catenin complexes in transformed thyroid epithelial cells: modulation by beta 1 integrin subunit. Eur J Cell Biol 2000; 79: 583-93.

Cerrato A, Fulciniti F, Avallone A, Benincasa G, Palombini L, Grieco M. Beta- and gamma-catenin expression in thyroid carcinomas. J Pathol 1998; 185: 267-72.

D'Souza B, Taylor-Papadimitriou J. Over-expression of ERBB2 in human mammary epithelial cells signals inhibition of transcription of the E-cadherin gene. Proc Natl Acad Sci USA 1994; 91: 7202-6.

Ekblom P, Vestweber D, Kemler R. Cell-matrix interactions and cell adhesion during development. Annu Rev Cell Biol 1986; 2: 27-47.

Fischer AH, Bond JA, Taysavang P, Battles OE, Wynford-Thomas D. Papillary thyroid carcinoma oncogene (RET/PTC) alters the nuclear envelope and chromatin structure. Am J Pathol 1998; 153: 1443-1450.

Graff J, Greenberg VE, Herman JG, Westra WH, Boghaert ER, Ain KB, Saji M, Zeiger MA, Zimmer SG, Baylin SB. Distinct patterns of E-cadherin CpG island methylation in papillary, follicular, Hurthle's cell and poorly differentiated human thyroid carcinoma. Cancer Res 1998; 58: 2063-66.

Grieco M, Cerrato A, Santoro M, Fusco A, Melillo RM, Vecchio G. Cloning and characterisation of H4 (D10S170), a gene involved in RET rearrangement *in vivo*. Oncogene 1994; 9: 2531-5.

Grieco M, Santoro M, Berlingieri M, Melillo RM, Donghi R, Bongarzone I, Pierotti MA, Della Porta G, Fusco A, Vecchio G. PTC is a novel rearranged form of the ret proto-

oncogene and is frequently detected *in vivo* in human thyroid papillary carcinomas. Cell 1990; 60: 557-63.

Guilford P. E-cadherin downregulation in cancer: fuel on the fire? Mol Med Today 1999; 5: 172-7.

Hedrick L, Cho KR, Vogelstein B. Cell adhesion molecules as tumour suppressors. Trends Cell Biol 1993; 3: 36-9.

Huang S, Wu J, Chang K, Liaw KY, Wang SM. Distribution of the cadherin-catenin complex in normal human thyroid epithelium and a thyroid carcinoma cell line. J Cell Biochem 1998; 70: 330-37.

Huang S, Wu J, Chang K, Liaw KY, Wang SM. Expression of the cadherin-catenin complex in well-differentiated human thyroid neoplastic tissue. Thyroid 1999; 9: 1095-1103.

Hyafil F, Morello D, Babinet C, Jacob F. A cell surface glycoprotein involved in the compaction of embryonal carcinoma cells and cleavage stage embryos. Cell 1980; 21: 927-34.

Jiang WG, Mansel RE. E-cadherin complex and its abnormalities in human breast cancer. Surg Oncol 2000; 9: 151-71.

Klugbauer S, Jauch A, Lengfelder E, Demidchik E, Rabes HM. A novel type of RET rearrangement (PTC8) in childhood papillary thyroid carcinomas and characterization of the involved gene (RFG8). Cancer Res 2000; 60: 7028-32.

Machado JC, Soares P, Carneiro F, Rocha A, Beck S, Blin N, Berx G, Sobrinho-Simoes M. E-cadherin gene mutations provide a genetic basis for the phenotypic divergence of mixed gastric carcinomas. Lab Invest 1999; 79: 459-65.

Mareel M, Bracke M, Van Roy F. Cancer metastasis: negative regulation by an invasion-suppressor complex. Cancer Detect Prev 1995; 19: 451-64.

Naito A, Iwase I, Kuzushima T, Nakamura T, Kobayashi S. Clinical significance of E-cadherin expression in thyroid neoplasms. J Surg Oncol 2001; 76: 176-80.

Overduin M, Harvey TS, Bagby S, Tong KI, Yau P, Takeichi M, Ikura M. Solution structure of the epithelial cadherin domain responsible for selective cell adhesion. Science 1995; 267: 386-9.

Ozawa M, Baribault H, Kemler R. The cytoplasmic domain of the cell adhesion molecule uvomorulin associates with three independent proteins structurally related in different species. EMBO J 1989; 8: 1711-17.

Pasini B, Hofstra R, Yin L, Bocciardi R, Santamaria G, Grootscholten PM, Ceccherini I, Patrone G, Priolo M, Buys CH, et al. The physical map of the human RET proto-oncogene. Oncogene 1995; 11: 1737-43.

Pierotti MA, Bongarzone I, Borello MG, Greco A, Pilotti S, Sozzi G. Cytogenetics and molecular genetics of carcinomas arising from thyroid epithelial follicular cells. Genes, Chromosomes & Cancer 1996; 16: 1-14.

Pignatelli M, Ansari TW, Gunter P, Liu D, Hirano S, Takeichi M, Kloppel G, Lemoine NR. Loss of membranous E-cadherin expression in pancreatic cancer: correlation with lymph node metastasis, high grade, and advanced stage. J Pathol 1994; 174: 243-8.

Pignatelli M, Liu D, Nasim MM, Stamp GW, Hirano S, Takeichi M. Morphoregulatory activities of E-cadherin and beta-1 integrins in colorectal tumour cells. Br J Cancer 1992; 66: 629-34.

Rosai J, Carcangiu M, DeLellis R. Atlas of Tumour Pathology – Tumours of the Thyroid Gland. 3rd Series. Fascicle 5. Washington DC: AFIP 1992.

Santoro M, Sabino N, Ishizaka Y, Ushijima T, Carlomagno F, Cerrato A, Grieco M, Battaglia C, Martelli ML, Paulin C, et al. Involvement of RET oncogene in human tumours: specificity of RET activation to thyroid tumours. Br J Cancer 1993; 68: 460-4.

Scheumman G, Houng-Vu C, Cetin Y, Gimm O, Behrends J, von Wasielewski R, Georgii A, Birchmeier W, von Zur Muhlen A, Dralle H, et al. Clinical significance of E-cadherin as a prognostic marker in thyroid carcinomas. J Clin Endocrinol Metab 1995; 80: 2168-72.

Schipper JH, Frixen UH, Behrens J, Unger A, Jahnke K, Birchmeier W. E-cadherin expression in squamous cell carcinomas of head and neck: inverse correlation with tumor dedifferentiation and lymph node metastasis. Cancer Res 1991; 51(23 Pt 1): 6328-37.

Shapiro L, Fannon AM, Kwong PD, Thompson A, Lehmann MS, Grubel G, Legrand JF, Als-Nielsen J, Colman DR, Hendrickson WA. Structural basis of cell-cell adhesion by cadherins. Nature 1995; 374: 327-37.

Sheils OM, O'Leary JJ, Uhlmann V, Lattich K, Sweeney EC. ret/PTC-1 activation in Hashimoto's thyroiditis. Int J Surg Pathol 2000; 8: 185-9.

Sheils OM, O'Leary JJ, Sweeney EC. Assessment of ret/PTC-1 rearrangements in neoplastic thyroid tissue using TaqMan RT-PCR. J Pathol 2000; 192: 32-6.

Soares P, Berx G, Van Roy F, Sobrinho-Simoes M. E-cadherin gene alterations are rare events in thyroid tumours. Int J Cancer 1997; 70: 32-38.

Sorscher SM, Russack V, Cagle M, Feramisco JR, Green MR. Immunolocalization of E-cadherin in human head and neck cancer. Arch Pathol Lab Med 1995; 119: 82-84.

Tong Q, Li Y, Smanik PA, Fithian LJ, Xing S, Mazzaferri EL, Jhiang SM. Characterisation of the promoter region and oligomerisation domain of H4 (D10S170), a gene frequently rearranged with the ret proto-oncogene. Oncogene 1995; 10: 1781-7.

Umbas R, Isaacs WB, Bringuier PP, Schaafsma HE, Karthaus HF, Oosterhof GO, Debruyne FM, Schalken JA. Decreased E-cadherin expression is associated with poor prognosis in patients with prostate cancer. Cancer Res 1994; 54: 3929-33.

Umbas R, Schalken JA, Aalders TW, Carter BS, Karthaus HF, Schaafsma HE, Debruyne FM, Isaacs WB. Expression of the cellular adhesion molecule E-cadherin is reduced or absent in high-grade prostate cancer. Cancer Res 1992; 52: 5104-9.

Von Wasielewski R, Rhein A, Werner M, Scheumann GF, Dralle H, Potter E, Brabant G, Georgii A. Immunohistochemical detection of E-cadherin in differentiated thyroid carcinoma correlates with clinical outcome. Cancer Res 1997; 57: 2501-7.

Williams G, Williams E. Identification of tumour specific translocations in archival material. J Pathol 1995; 175: 279-81.

Wirtschafter A, Schmidt R, Rosen D, Kundu N, Santoro M, Fusco A, Multhaupt H, Atkins JP, Rosen MR, Keane WM, Rothstein JL. Expression of the RET/PTC fusion gene as a marker for papillary carcinoma in Hashimoto's thyroiditis. Laryngoscope 1997; 107: 95-100.

Yap AS, Stevenson BR, Cooper V, Manley SW. Protein tyrosine phosphorylation influences adhesive junction assembly and follicular organisation of cultured thyroid epithelial cells. Endocrinology 1997; 138: 2315-24.

Chapter 4

β- and γ-catenin mRNA expression levels in ret/PTC-1 activated thyroid neoplasms

4.1 Summary

In the previous chapter an association between ret/PTC-1 activation and decreased E-cadherin mRNA levels in papillary thyroid carcinoma was demonstrated. We also observed similarities in the E-cadherin expression profiles of Hashimoto thyroiditis and ret/PTC-1 positive papillary thyroid carcinomas and have hypothesised that ret/PTC-1 activation might cause, not only the structural and nuclear peculiarities of PTC, but also an immune reaction to thyroid epithelium.

The objective of this study was to examine the expression of E-cadherin's ligands, β- and γ-catenin, in various thyroid tissue types in the context of ret/PTC-1 positivity using laser capture microdissection and TaqMan® One-Step RT-PCR.

β-catenin mRNA levels were found to be consistently decreased in both papillary and anaplastic carcinomas when compared with a normal/follicular adenoma group. A significant difference in expression levels was observed between papillary and follicular thyroid carcinomas with the latter having elevated mRNA levels of β-catenin. γ-catenin mRNA was decreased in anaplastic carcinomas compared with normal/follicular adenoma groups. A similar expression profile of γ-catenin as β-catenin was observed in papillary and follicular carcinomas with the latter once again having higher mRNA levels. These results therefore suggest that although β- and γ-catenin may play a role in the progression of thyroid cancer in general, they do not appear to be associated with ret/PTC-1 modulated pathways.

4.2 Introduction

Adherens junctions (AJs; also called the zonula adherens) are critical for the establishment and maintenance of epithelial layers, such as those lining organ surfaces. AJs mediate adhesion between cells, communicate a signal that neighbouring cells are present, and anchor the actin cytoskeleton. In serving these roles, AJs regulate normal cell growth and behaviour. At several stages of embryogenesis, wound healing, and tumour cell metastasis, cells form and leave epithelia. This process, which involves the disruption and reestablishment of epithelial cell-cell contacts, may be regulated by the disassembly and assembly of AJs. AJs may also function in the transmission of the 'contact inhibition' signal, which instructs cells to stop dividing once an epithelial sheet is complete.

4.2.1 β-catenin

As discussed in the previous chapter, the AJ is a multi-protein complex assembled around calcium-regulated cell adhesion molecules called cadherins. Cadherins are transmembrane proteins: the extracellular domain mediates homotypic adhesion with cadherins on neighbouring cells, and the intracellular domain interacts with cytoplasmic proteins that transmit the adhesion signal and anchor the AJ to the actin cytoskeleton. These cytoplasmic proteins include p120 and the alpha-, beta-, and gamma-catenins. The β-catenin gene (3p22-p21.3; 85 kDa), which was cloned by McCrea et al. (1991), shows no similarity in sequence to α-catenin. The β-catenin protein shares 70% amino acid identity with both γ-catenin (plakoglobin), which is found in desmosomes (another type of intracellular junction), and the product of the Drosophila segment polarity gene

'armadillo.' Armadillo is part of a multi-protein AJ complex in Drosophila that also includes some homologs of α-catenin and cadherin, and genetic studies indicate that it is required for cell adhesion and cytoskeletal integrity. The armadillo gene was originally identified as one of a group of segment polarity genes that regulate pattern formation of the Drosophila embryonic cuticle.

4.2.2 γ-catenin

γ-catenin (17q21; 82 kDa) is a major cytoplasmic protein that occurs in a soluble and a membrane-associated form and is the only known constituent common to the sub-membranous plaques of both kinds of adhering junctions, the desmosomes and the intermediate junctions. It is a desmoplakin and is referred to as DP III. DP I and DP II are splice variants of the same gene. γ-catenin associates with the cytoplasmic region of desmoglein I, one of the transmembrane desmosomal proteins (Mathur et al., 1994). It is also a component of the cadherin-catenin complex, which is predominantly localised where actin filaments anchor in adherens junction of epithelial cells.

4.2.3 Function

In normal tissues both proteins are engaged in the cadherin/catenin complex, where membranous E-cadherin is anchored to the actin cytoskeleton by either β- or γ-catenin. β-/γ-catenin bind to the cytoplasmic domain of E-cadherin and simultaneously to α-catenin. α-catenin then anchors the entire complex to the cytoskeleton via α-actinin (Knudsen et al., 1995) or vinculin (Hazan et al., 1997).

The cadherin-catenin complex can interact with epidermal growth factor receptor (EGFR) and β- and γ-catenin are substrates for tyrosine phosphorylation following EGF stimulation of cells. These findings coupled with the fact that catenins are associated with the tumour suppressor protein APC, opened the possibility that catenins were involved in signalling pathways and tumorigenesis. The most extensively studied of these pathways is the Wnt-signalling pathway.

In the absence of an external mitotic signal, excess β-/γ-catenin is sequestered into a complex with the adenomatous polyposis coli (APC) gene product, a serine threonine glycogen synthetase kinase (GSK-3β), protein phosphatase 2A and either of the scaffolding proteins axin or conductin/axil. This results in the phosphorylation of the catenins by GSK-3β. Phosphorylated catenins are then able to bind an F-box protein, slimb/βTrCP. As a consequence of this interaction, they are ubiquitinated by the E3/SCF-ubiquitin ligase complex and are degraded by processing through the 26S proteosome (Aberle et al., 1997; Sadot et al., 2000). In certain cancers, particularly colon cancer, APC is frequently mutated at the binding regions for catenins and GSK3β. These mutations lead to damage of the catenin complex and prevent effective phosphorylation of the catenins. The consequence of such mutations would be a build-up of cytoplasmic catenin levels.

Wnts constitute a family of cysteine-rich, secreted glycoproteins with distinct expression patterns in the embryo and adult organism. Wnts are involved in differentiation processes by controlling embryonic induction, polarity of cell division, cell fate and growth. The

molecules act on target cells in a paracrine fashion through members of the frizzled receptor family of seven transmembrane proteins (Bhanot et al., 1996). Activated frizzled receptors in turn phosphorylate the cytoplasmic phosphoprotein dishevelled (dsh) (Noordermeer et al., 1994), which can interfere with the catenin destruction complex described above. In this situation, GSK-3β activity is inhibited and the phosphorylation of the catenins is therefore blocked.

When this happens, the hypophosphorylated catenins are not degraded resulting in a build-up of extra-junctional catenins in the cytoplasm and their subsequent translocation to the nucleus. The build-up of catenin levels in the nucleus leads to their association with member of the LEF/TCF family of transcription factors, such as LEF-1, TCF-1 and TCF-3 (Behrens et al., 1996; Simcha et al., 1998; Zhurinsky et al., 2000). TCF/LEFs are quite different from the classic transcription factors as they have no classical transactivation domain and are therefore unable to activate transcription by themselves. The TCF/catenin complexes however, act as transcriptional activators of Wnt target genes and transmit the Wnt signal into the nucleus. C-myc (He et al., 1998), cyclin D1 (Shtutman et al., 1999), fibronectin (Gradl et al., 1999), multidrug resistance 1 (MDR 1) (Yamada et al., 2000) and matrilysin (Crawford et al., 1999) are among the genes thought to be affected.

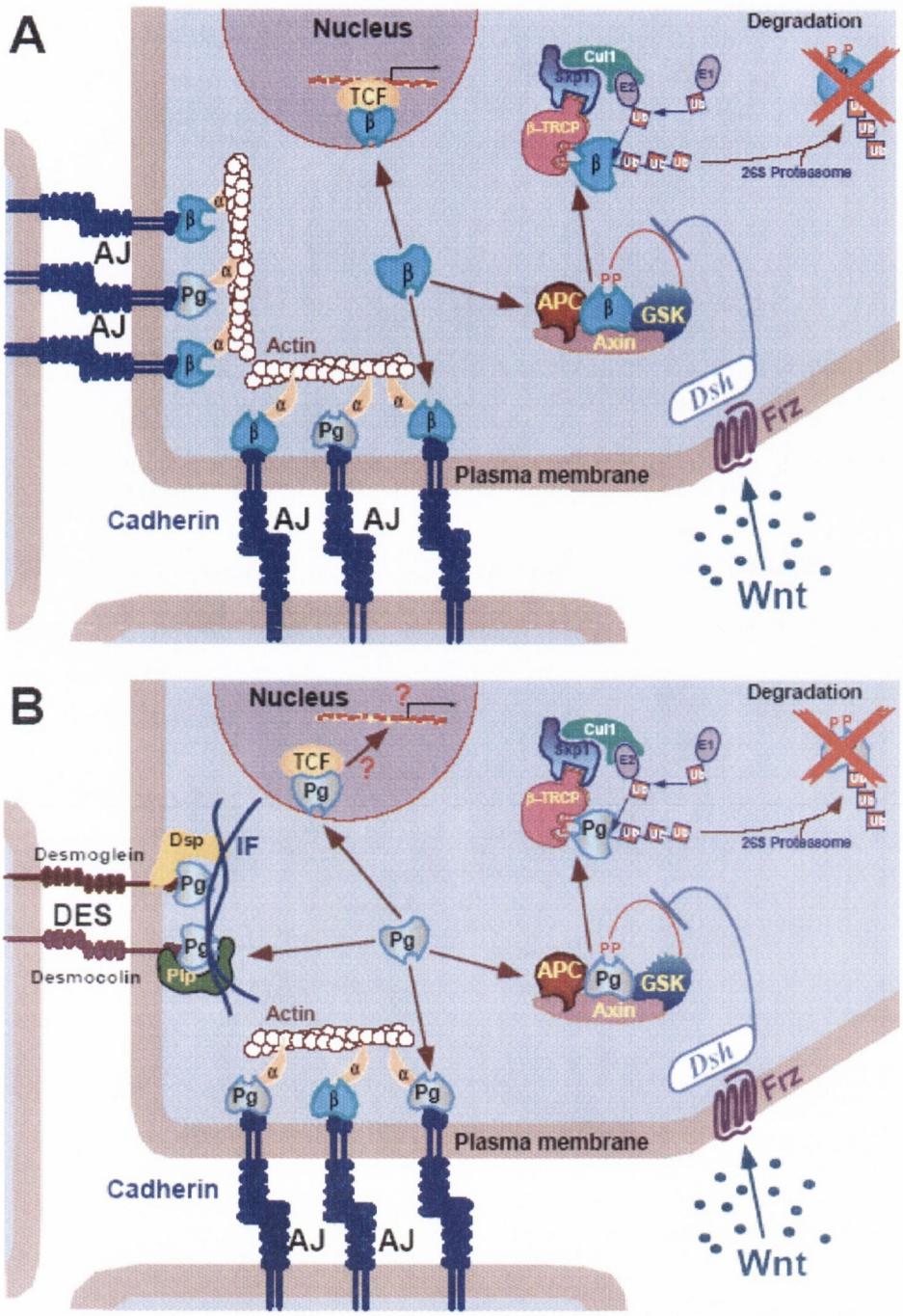

Figure 4.1 The various interactions involving (A) β-catenin and (B) γ-catenin

See text for description. Abbreviations used: β – β-catenin; Pg – plakoglobin; α – α-catenin; Ub – ubiquitination; DES – desmosomes; Dsp – desmoplakin; Plp – plakophilin; IF – inutermediate filaments; Frz – Frizzled. (adapted from Zhurinsky et al., Plakoglobin and beta-catenin: protein interactions, regulation and biological roles. J Cell Sci 2000; 113: 3127-39)

In chapter 3 it was suggested that ret/PTC-1 may be involved in the down-regulation of the cellular adhesion molecule E-cadherin in both papillary thyroid carcinoma and Hashimoto thyroiditis, providing further evidence that this autoimmune disease may represent a pre-neoplastic lesion of papillary thyroid carcinoma. ret/PTC oncogenes and their role in thyroid pathology are discussed in detail in chapters 1.5.1 and 3.2.4.

The purpose of this study was to investigate the mRNA levels of β- and γ-catenin in conjunction with ret/PTC-1 activation in the thyroid, to establish if any further link exists between expression of the chimeric transcript and cellular adhesion in thyroid autoimmune disease and thyroid neoplasia.

4.3 Materials & methods

4.3.1 Specimens

Samples (n=80) of papillary thyroid carcinoma (PTC) (n=31), Hashimoto thyroiditis (HT) (n=14), anaplastic thyroid carcinoma (ATC) (n=5), follicular thyroid carcinoma (FTC) (n=12), follicular adenoma (FA) (n=11) and non-malignant thyroid tissue (NORM) (n=7) accessioned between 1982 and 2001 in St. James's Hospital, Dublin were analysed. All material was fixed in 10% buffered formal saline and embedded in paraffin wax. Stained sections were reviewed blind by a histopathologist and classified according to a recognised system (Rosai et al., 1992).

4.3.2 Microdissection and RNA extraction

Laser capture microdissection was performed for the same reasons and in the same manner as described in chapter 3.3.2. Following microdissection the Capsures® were placed in sterile Eppendorf® tubes and RNA extraction was performed using the PURESCRIPT® RNA Isolation Kit (Gentra Systems Inc., MN, USA) with modification of the protocol as previously described (chapter 2.4.1).

4.3.3 Standard preparation

To demonstrate the linearity and efficiency of the One-Step TaqMan® RT-PCR reactions and for the purpose of quantitation, standard curves were required. A GAPDH RNA standard curve was generated by performing a serial dilution on control human RNA (supplied by Applied Biosystems, CA, USA) and analysing as per the test samples.

For the purposes of this study, it was decided that relative quantitation would be used to generate ratios of catenin expression to the housekeeping gene GAPDH for each sample. To this end, total RNA was extracted from human buccal squamous mucosal cells using the PURESCRIPT® RNA Isolation Kit and serial 10-fold dilutions were performed of the resulting purified RNA. Each dilution was assigned an arbitrary copy value from 10^6 down to 10^1 copies/µl. The same serial dilutions were used for both catenin assays and were analysed in parallel with test samples to demonstrate the linearity of the reactions (see Fig 4.4 for standard curves).

4.3.4 TaqMan® One-Step RT-PCR analysis

Extracted RNA was analysed using TaqMan® One-Step RT-PCR. One-step RT-PCR performs RT as well as PCR in a single buffer system. The reaction proceeds without the addition of reagents between the RT and PCR steps, offering the convenience of a single tube preparation for RT and PCR amplification and reducing the risks of contamination.

The principle of the TaqMan™/5' nuclease assay is discussed in detail in chapter 2.5. Real time analysis was used to quantitate expression. To compensate for potential degradation

of target RNA and differences in the amount of starting material, TaqMan® One-Step RT-PCR was performed in parallel on RNA from each sample using glyceraldehyde phosphate dehydrogenase (GAPDH) as an endogenous control. The copy numbers obtained for β- and γ-catenin were divided by the corresponding copy numbers for GAPDH to yield an expression index. In the case of ret/PTC-1 detection, an end-point detection was used to confirm the presence/absence of the ret/PTC-1 chimeric transcript.

One-Step RT-PCR was carried out according to the manufacturers instructions under the following conditions: 1X One-Step Master Mix, 1X MultiScribe and RNase Inhibitor Mix (0.25U/μl MultiScribe and 0.4U/μl RNase Inhibitor), 300nM forward and reverse primers, 100nM probe, RNA template (10pg-100ng) and nuclease-free water to 25μl. One-Step RT-PCR was performed using an Applied Biosystems 7000 Sequence Detection System (Applied Biosystems, CA, USA) with the following thermocycling parameters: 48°C 30min, 95°C 10mins and 40 cycles of [95°C 15s, 60°C 1min].

All primers/probes (see Table 4.1 for sequences) were designed using ABI Prism Primer Express 1.5 software (Applied Biosystems, Cheshire, UK) with the probes spanning exon-exon junctions to eliminate the possibility of residual genomic DNA detection. All probes used in the TaqMan® reactions were designed to have non-fluorescent quenchers (NFQ) and minor groove binding (MGB) modifications.

Reaction		Sequence
GAPDH TaqMan®	F	CAT CCA TGA CAA CTT TGG TAT CGT
	P (5' VIC labelled)	ACT CAT GAC CAC AGT CC
	R	GGG TGG CAG TGA TGG CAT
ret/PTC-1 TaqMan®	F	CGC GAC CTG CGC AAA
	P (5' FAM labelled)	TTA CCA TCG AGG ATC CAA
	R	ACC AAG TTC TTC CGA GGG AAT T
β-catenin TaqMan®	F	GGG ATG TTC ACA ACC GAA TTG T
	P (5' VIC labelled)	TGT GCA GCT GCT TTA T
	R	GCT ACT CTT TGG ATG TTT TCA ATG G
γ-catenin TaqMan®	F	GCG CCA GTA CAC GCT CAA
	P (5' VIC labelled)	CCA GCC AAG GTG ACC TG
	R	CCC TGG CTG TTG TGG ACA TC

Table 4.1 Primer/probe sequences

At least six negatives were included in each TaqMan® run. For ret/PTC-1 detection, cDNA from the cell line TPC-1 was included as a positive control. In the case of GAPDH and β-/γ-catenin, the standards functioned as positive controls. All samples were run in duplicate and standards were run in triplicate.

4.3.5 Statistical analysis

All statistical analyses were performed using Analyse-it™, version 1.62 (Analyse-it Software, Ltd.). As the data were non-parametric, the Kruskal-Wallis ANOVA and Mann-Whitney U tests were used to determine statistical significance between groups.

4.4 Results

4.4.1 β- and γ-catenin TaqMan® Quantitative RT-PCR

All samples used in the study tested positive for GAPDH. Catenin expression indices for each sample were obtained by expressing catenin levels as ratios to their respective GAPDH levels. A scatter plot of the individual β- and γ-catenin values for each sample within each category of thyroid tissue type is displayed in Figs 4.2 and 4.3.

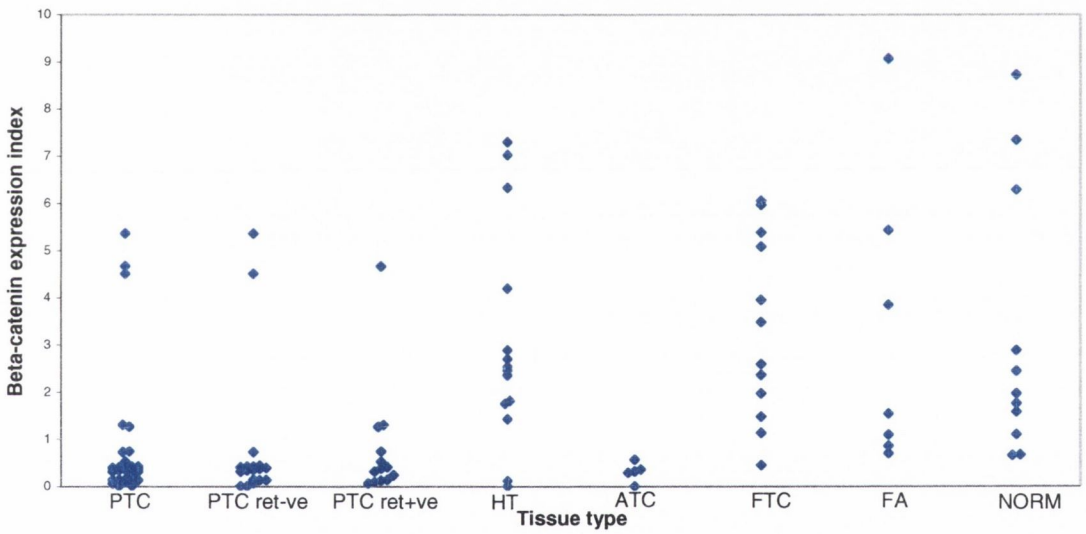

Figure 4.2 β-catenin expression in thyroid tissues

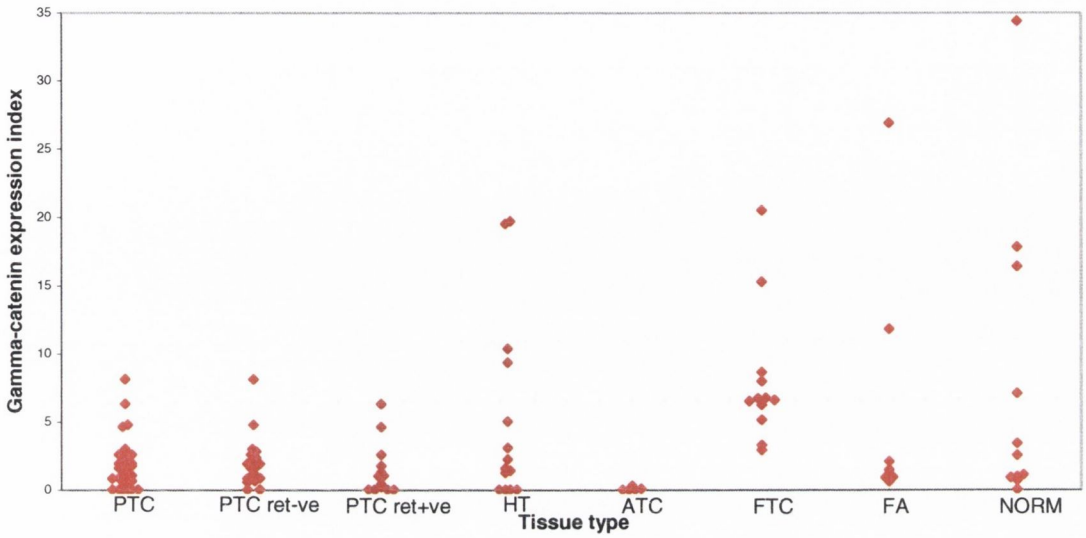

Figure 4.3 γ-catenin expression in thyroid tissues

It should be noted that although the follicular adenoma (FA) and normal thyroid tissue (NORM) groups are graphed separately in figures 4.2 and 4.3, they were combined to generate statistical data with respect to the other cohorts because both groups had statistically similar expression profiles.

The PTC group was further sub-divided into ret/PTC-1 positive (n=13) and negative (n=18) cohorts. All 5 ATCs and 11 of the 14 Hashimoto thyroiditis cases were found to be ret/PTC-1 positive. No other samples displayed ret/PTC-1 positivity. TaqMan® One-Step RT-PCR standard curves for GAPDH, β- and γ-catenin are represented in figure 4.4.

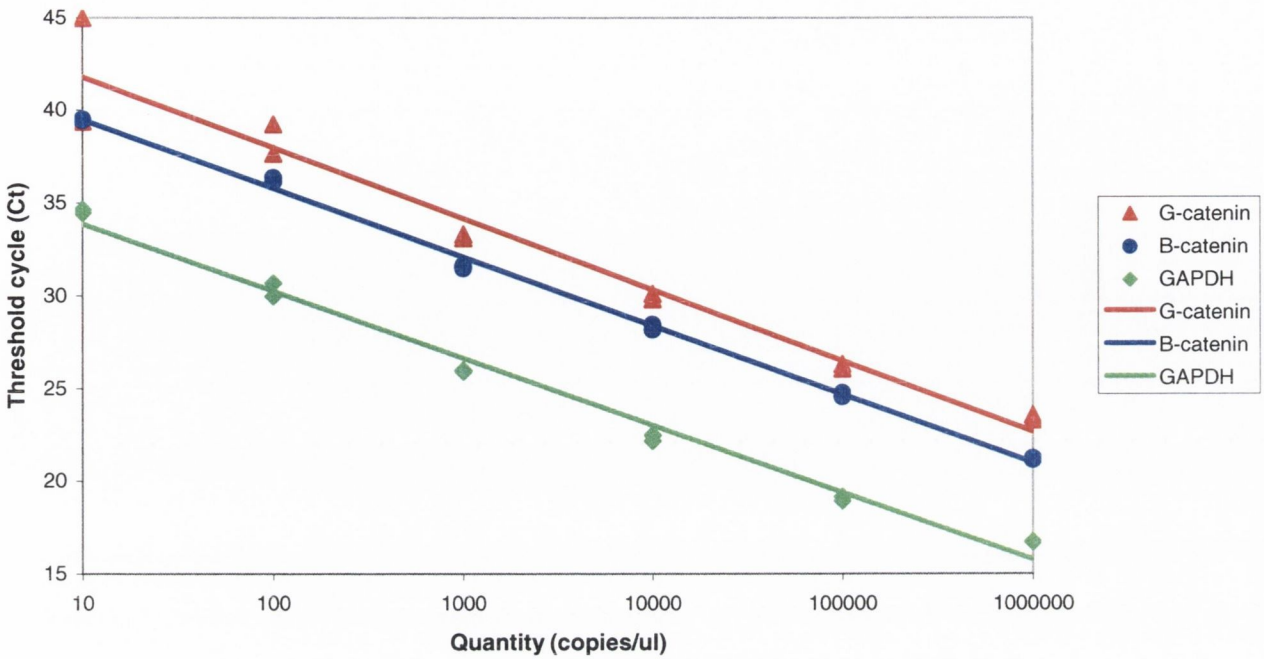

Figure 4.4 TaqMan® One-Step RT-PCR standard curves for GAPDH, β- and γ-catenin

β-catenin expression was detected in all cases of follicular adenoma/non-malignant thyroid tissue and in all cases of follicular thyroid carcinoma. Of the five anaplastic thyroid carcinomas, one displayed no expression of β-catenin while the rest showed significantly reduced levels compared with the normal controls. The Hashimoto thyroiditis and papillary carcinomas displayed varying expression levels of β-catenin with the latter having significantly reduced values compared to the controls.

A similar pattern was observed for γ-catenin expression. FTCs and the FA/NORM group displayed varied but substantial expression levels, whereas ATCs had little or no

expression of γ-catenin, and the HT and PTC groups showed diverse expression levels with generally reduced expression in the PTC group.

4.4.2 Statistical analysis

The Kruskal-Wallis ANOVA test showed there to be a significant effect of group across the specified disease cohorts for both β- and γ-catenin expression ($p<0.0001$ for both analyses). Individual pair wise comparisons were performed using the Mann-Whitney U test and selected results are displayed in Table 4.2.

Test	p value
β-catenin - PTC ≠ FA/NORM	<0.0001
β-catenin - ATC ≠ FA/NORM	0.0008
β-catenin - PTC ≠ FTC	<0.0001
γ-catenin - ATC ≠ FA/NORM	0.0019
γ-catenin - FTC ≠ FA/NORM	0.0754
γ-catenin - PTC ≠ FTC	<0.0001

Table 4.2 Statistical analysis of results using Mann-Whitney U test

4.5 Discussion

Although β- and γ-catenin are molecules that have been extensively studied in a diverse range of human malignancies, there are relatively few studies of their expression in thyroid tissue. In the previous chapter (data from which was published in Smyth et al., 2001) levels of E-cadherin mRNA were examined in various thyroid disease states. Our results demonstrated that E-cadherin expression was decreased in ret/PTC-1 positive papillary thyroid carcinomas and that levels were comparable to that in ret/PTC-1 positive Hashimoto thyroiditis samples. Therefore, to further investigate the hypothesis that ret/PTC-1 may be implicated in cellular adhesion, we examined thyroid samples for the expression of E-cadherin's natural ligands, β- and γ-catenin, to see if ret/PTC-1 correlated with their expression.

The anaplastic thyroid carcinoma group, which is known to be highly aggressive and have a poor prognosis, displayed very low levels of β- and γ-catenin mRNA. Both catenin levels were very significantly decreased when compared to the normal/follicular adenoma group (NORM/FA). These results mirror those in the catenin protein study carried out by Cerrato et al. (Cerrato et al., 1998), where they showed β- and γ-catenin levels to be reduced or absent in 5 of 5 samples by immunohistochemistry (IHC). Garcia-Rostan et al. (Garcia-Rostan et al., 1999) also showed that the majority of anaplastic thyroid tumours had absent or reduced levels of β-catenin using IHC. However, other studies vary in their results for catenin expression in ATC. Husmark et al. (Husmark et al., 1999) found γ-catenin to be reduced in an anaplastic carcinoma cell line but not β-catenin. However this may be accounted for by differences between *in vitro* and *in vivo*

experiments. While the finding of ret/PTC-1 activation among ATC is surprising, it has been described by our group previously (Sheils et al., 2000). We postulated the reasons for positivity included the increased sensitivity of TaqMan analysis vs. solution phase RT-PCR, and that many ATC originate in or at least co-exist with PTC moieties.

The well-differentiated thyroid carcinomas showed varying levels of catenin expression. β-catenin expression was significantly decreased in papillary thyroid carcinomas compared with the control group, while follicular thyroid carcinomas had β-catenin expression levels similar to the control group. The PTC group had significantly decreased β-catenin expression compared with the FTC cohort ($p<0.0001$). Likewise, γ-catenin expression was significantly reduced in the PTC group compared with FTC. The level of γ-catenin expression in the FTC group was moderately higher than the control group. This expression pattern in the FTC cohort may be due to a mixture of well- and poorly-differentiated tumours within the overall group.

The overall results obtained in this study somewhat contradict those of previous immunohistochemistry analyses (Cerrato et al., 1998; Bohm et al., 2000). These analyses have shown there to be varying levels of β- and γ-catenin in differentiated thyroid carcinomas. Although they have shown β-catenin levels to be consistently decreased in PTC, FTCs frequently displayed lower levels of β- and γ-catenin protein than PTCs. An *in vitro* experiment conducted by Huang et al. (1998) using a cell line of follicular thyroid carcinoma origin showed absence of γ-catenin protein in these cells. Another study by the same group (Huang et al., 1999) using follicular carcinomas showed both β- and γ-

catenin proteins to be reduced/absent with β-catenin proving to be the most affected. All of the above experiments would seem to contradict our current study, which suggests that the expression of the catenins is more adversely affected in PTCs than FTCs.

The highlighted differences in the described studies may be accounted for by the different technologies involved. The above studies used IHC and/or Western blotting in their experiments to measure expression levels and localisation of the proteins while we used Taqman® RT-PCR, to quantitate mRNA levels of the catenins. However, as highlighted by some of the above authors, their detection methods are prone to genetic changes in the catenins, which are quite common. An epitope change in either catenin could lead to false negatives using immunohistochemical detection methods. The assay system in this study is not so prone to false reductions in expression due both to the small amplicon sizes involved in Taqman® technology and the fact that the amplicons for each catenin are located at the junctions of exons 11 and 12, and 1 and 2 for β-catenin and γ-catenin respectively, some distance removed from the known mutation "hot spots". Other possibilities for high mRNA levels coupled with low protein levels include perturbations in post-translational modification and possibly introduction of destabilising mutations that may result in a labile protein more prone to degradation.

Division of the papillary carcinoma group into ret/PTC-1 positive and negative groups did not generate significant statistical differences in β- and γ-catenin expression unlike the difference observed with E-cadherin expression previously (Smyth et al., 2001).

Similar examination of catenin expression levels in the Hashimoto thyroiditis cohort revealed no detectable trends.

Therefore, it seems that while β- and γ-catenin may have roles to play in the development and progression of thyroid cancer in general, they appear to operate in a manner independent of ret/PTC-1 activation and unlike E-cadherin do not appear to involved in the pathobiology of Hashimoto thyroiditis.

4.6 References

Aberle H, Bauer A, Stappert J, Kispert A, Kemler R. β-catenin is a target for the ubiquitin-proteasome pathway. EMBO J 1997; 16: 3797-804.

Behrens J, von Kries JP, Kuhl M, Bruhn L, Wedlich D, Grosschedl R, Birchmeier W. Functional interaction of β-catenin with the transcription factor LEF-1. Nature 1996; 382: 638-42.

Bhanot P, Brink M, Samos CH, Hsieh JC, Wang Y, Macke JP, Andrew D, Nathans J, Nusse R. A new member of the frizzled family from Drosophila functions as a Wingless receptor. Nature 1996; 382: 225-30.

Bohm J, Niskanen L, Kiraly K, Kellokoski J, Eskelinen M, Hollmen S, Alhava E, Kosma VM. Expression and prognostic value of alpha-, beta-, and gamma-catenins in differentiated thyroid carcinoma. J Clin Endocrinol Metab 2000; 85: 4806-11.

Cerrato A, Fulciniti F, Avallone A, Benincasa G, Palombini L, Grieco M. Beta- and gamma-catenin expression in thyroid carcinomas. J Pathol 1998; 185: 267-72.

Crawford HC, Fingleton BM, Rudolph-Owen LA, Goss KJ, Rubinfeld B, Polakis P, Matrisian LM. The metalloproteinase matrilysin is a target of beta-catenin transactivation in intestinal tumors. Oncogene 1999; 18: 2883-91.

Garcia-Rostan G, Tallini G, Herrero A, D'Aquila TG, Carcangiu ML, Rimm DL. Frequent mutation and nuclear localization of beta-catenin in anaplastic thyroid carcinoma. Cancer Res 1999; 59: 1811-5.

Gradl D, Kuhl M, Wedlich D. The Wnt/Wg signal transducer β-catenin controls fibronectin expression. Mol Cell Biol 1999; 19: 5576-87.

Hazan RB, Kang L, Roe S, Borgen PI, Rimm DL. Vinculin is associated with the E-cadherin adhesion complex. J Biol Chem 1997; 372: 32448-53.

He TC, Sparks AB, Rago C, Hermeking H, Zawel L, da Costa LT, Morin PJ, Vogelstein B, Kinzler KW. Identification of c-myc as a target of the APC pathway. Science 1998; 281: 1509-12.

Huang SH, Wu JC, Chang KJ, Liaw KY, Wang SM. Distribution of the cadherin-catenin complex in normal human thyroid epithelium and a thyroid carcinoma cell line. J Cell Biochem 1998; 70: 330-7.

Huang SH, Wu JC, Chang KJ, Liaw KY, Wang SM. Expression of the cadherin-catenin complex in well-differentiated human thyroid neoplastic tissue. Thyroid 1999; 9: 1095-103.

Husmark J, Heldin NE, Nilsson M. N-cadherin-mediated adhesion and aberrant catenin expression in anaplastic thyroid-carcinoma cell lines. Int J Cancer 1999; 83: 692-9.

Knudsen KA, Soler AP, Johnson KR, Wheelock MJ. Interaction of α-actinin with the cadherin-catenin cell-cell adhesion complex via α-catenin. J Cell Biol 1995; 130: 67-77.

Mathur M, Goodwin L, Cowin P. Interactions of the cytoplasmic domain of the desmosomal cadherin Dsg1 with plakoglobin. J Biol Chem 1994; 269: 14075-14080.

McCrea PD, Turck CW, Gumbiner B. A homolog of the armadillo protein in Drosophila (plakoglobin) associated with E-cadherin. Science 1991; 254: 1359-1361.

Noordermeer J, Klingensmith J, Perrimon N, Nusse R. dishevelled and armadillo act in the wingless signalling pathway in Drosophila. Nature 1994; 367: 80-3.

Rosai J, Carcangiu M, DeLellis R. Atlas of Tumour Pathology – Tumours of the Thyroid Gland. 3rd Series. Fascicle 5. Washington DC: AFIP 1992.

Sadot E, Simcha I, Iwai K, Ciechanover A, Geiger B, Ben-Ze'ev A. Differential interaction of plakoglobin and beta-catenin with the ubiquitin-proteasome system. Oncogene 2000; 19: 1992-2001.

Sheils OM, O'Leary JJ, Sweeney EC. Assessment of ret/PTC-1 rearrangements in neoplastic thyroid tissue using TaqMan RT-PCR. J Pathol 2000; 192: 32-6.

Shtutman M, Zhurinsky J, Simcha I, Albanese C, D'Amico M, Pestell R, Ben-Ze'ev A. The cyclin D1 gene is a target of the beta-catenin/LEF-1 pathway. Proc Natl Acad Sci USA 1999; 96: 5522-7.

Simcha I, Shtutman M, Salomon D, Zhurinsky J, Sadot E, Geiger B, Ben-Ze'ev A. Differential nuclear translocation and transactivation potential of beta-catenin and plakoglobin. J Cell Biol 1998; 141: 1433-48.

Smyth P, Sheils O, Finn S, Martin C, O'Leary JJ, Sweeney EC. Real-time quantitative analysis of E-cadherin expression in ret/PTC-1-activated thyroid neoplasms. Int J Surg Pathol 2001; 9: 265-72.

Yamada T, Takaoka AS, Naishiro Y, Hayashi R, Maruyama K, Maesawa C, Ochiai A, Hirohashi S. Transactivation of the multidrug resistance 1 gene by T-cell factor 4/beta-catenin complex in early colorectal carcinogenesis. Cancer Res 2000; 60: 4761-6.

Zhurinsky J, Shtutman M, Ben-Ze'ev A. Differential mechanisms of LEF/TCF family-dependent transcriptional activation by beta-catenin and plakoglobin. Mol Cell Biol 2000; 20: 4238-52.

Zhurinsky J, Shtutman M, Ben-Ze'ev A. Plakoglobin and beta-catenin: protein interactions, regulation and biological roles. J Cell Sci 2000; 113: 3127-39.

Chapter 5

Trends in ret/PTC oncogene and T1799A BRAF mutation detection in Irish thyroid neoplasms.

5.1 Summary

The Ras/Raf/MEK/ERK pathway has been implicated in a variety of human neoplasms. BRAF, a serine/threonine kinase is an integral part of this signalling pathway. Mutation rates of 90% have been described in some cancers, with 80% of these mutations being a V600E amino acid substitution caused by a missense mutation (T1799A). Its mutation rate in thyroid carcinomas is second only to that observed in melanomas/nevi.

ret/PTC oncogene activation was the most common genetic change detected among papillary thyroid carcinomas (PTCs) prior to the discovery of BRAF mutation in this disease cohort. The purpose of this study was to assess BRAF mutation rates in various thyroid tissues and to investigate if concomitant mutations with ret/PTC activation occurred in inflammatory and neoplastic lesions.

Heterozygous T1799A mutations were detected in 15 of 34 (44%) PTCs tested. No such mutations were detected in the other tissue types tested. Their absence in Hashimoto's thyroiditis further supports the notion that this type of thyroiditis may be a pre-neoplastic lesion of PTC or that it belongs to a different progression pathway. Concomitant presence of both oncogenes was reported in 5 of the 34 PTCs. A significant temporal trend was observed, with ret/PTC chimera detected for the most part pre-1997 and BRAF mutations being more prevalent post-1997. Our results suggest that some environmental/etiological agent(s) may have influenced the pathobiology of thyroid tumour development, among the population examined, over time.

5.2 Introduction

5.2.1 Raf kinases

Raf kinases are proto-oncogenes that function in the mitogen-activated protein kinase/extracellular-signal-regulated kinase (MAPK/ERK) pathway, an important membrane to nucleus signalling module. The pathway is involved in all of the characteristics that define cancer cells: immortalisation, mitogen-independent growth, insensitivity to inhibitory signals, invasion and metastasis, angiogenesis, evasion of apoptosis and even resistance to therapy. The pathway is thought to be implicated in up to 30% of all human neoplasms.

The v-*raf* oncogene was originally discovered in the efforts to find an oncogene that induced carcinomas in mice (Rapp *et al.*, 1980). It was the first serine/threonine kinase oncogene to be discovered, as all other oncogenes at the time were tyrosine kinases, transcription factors or Ras-family members. Soon thereafter the human cellular homologue, c-*raf*-1, was cloned. This was soon followed by two other family members: A-*raf* (Huebner et al., 1986) and B-*raf* (Ikawa et al., 1988). RAF-1 or C-RAF has been the most extensively studied although BRAF has been more implicated in human neoplasia.

5.2.2 Expression

The three Raf isoforms differ in their tissue-specific expression and subcellular location. RAF-1 is ubiquitously expressed in human tissues whereas BRAF expression is generally restricted to neuronal tissue (Barnier et al., 1995), testis and spleen. Although BRAF and RAF-1 are co-expressed in neurons, BRAF is localised to cell bodies and neurite processes whereas RAF-1 is perinuclear (Morice et al., 1999). Both A-RAF and RAF-1 have been shown to be localised to the mitochondria (Wang et al., 1996; Yuryev et al., 2000). A-RAF is predominantly expressed in urogenital tissue.

5.2.3 Structure

Raf kinases are all composed of three evolutionary conserved regions: CR1, CR2 and CR3 (see Fig 5.1 for detailed Raf structure). CR1 can be further divided into a Ras binding domain (RBD) and a cysteine rich domain (CRD) and also possesses a putative zinc-binding domain. CR1 is primarily involved in the interaction of Raf with active GTP-bound Ras. The role of the serine/threonine rich CR2 is relatively unknown but phosphorylation and other protein-protein interactions via CR2 are thought to affect Raf localisation and activation. CR3 comprises the catalytic kinase domain of the protein and can also be phosphorylated for regulatory purposes. CR3 is the most homologous domain between the Raf kinase isoforms.

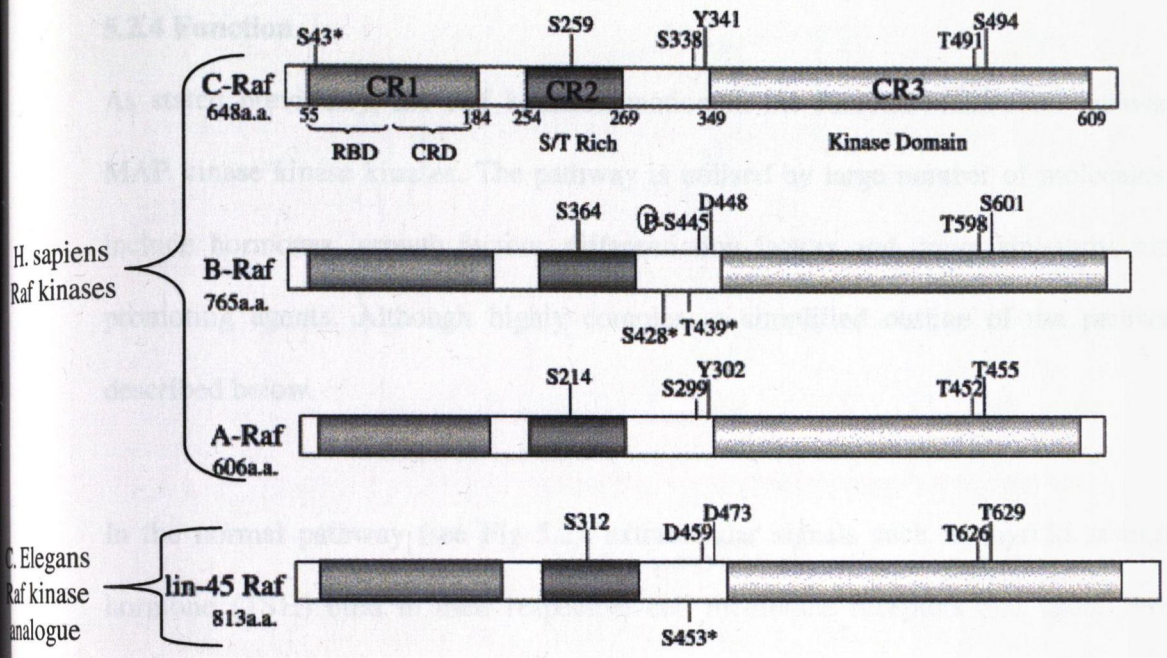

Figure 5.1 Basic structure of the Raf kinase family

The three conserved regions of Raf are conserved across isoforms and species. CR1 has two sub-domains for Ras binding: RBD and CRD. CR2 is a serine/threonine rich region and is involved in Raf regulation. CR3 is the catalytic kinase domain. Conserved regulatory phosphorylation amino acids are shown. Sites not conserved are marked with an asterisk (*). (adapted from Chong et al.. Cell Signal. 2003 May;15(5):463-9.)

Further complexity in Raf kinase structure becomes apparent upon closer examination of BRAF. In mice, this Raf gene has been shown to have in excess of 10 isoforms through alternative splicing mechanisms. These are produced by the differential splicing of exons 8b and 10a, and also by the presence of two alternate N-termini. The alternatively spliced variants of BRAF still possess the essential CRD domains but display tissue-specific expression profiles and differ in their affinity for MEKs and their activation efficiencies (Barnier et al., 1995; Papin el al., 1998).

5.2.4 Function

As stated previously, the Raf kinases function in the Ras/Raf/MEK/ERK pathway as MAP kinase kinase kinases. The pathway is utilised by large number of molecules that include hormones, growth factors, differentiation factors and, more sinisterly, tumour promoting agents. Although highly complex, a simplified outline of the pathway is described below.

In the normal pathway (see Fig 5.2), extracellular signals such as thyroid stimulating hormone (TSH) bind to their respective cell membrane receptors and cause receptor dimerisation and autophosphorylation on tyrosine residues. The typical G-protein exchange factor, SOS (son of sevenless), is then towed to the cell membrane by growth-factor-receptor-binding protein 2 (Grb2) which recognises the phosphotyrosines on the cell membrane receptors as docking sites. Once these molecules have been recruited to the cell membrane where Ras is localised, they can then activate Ras. This is accomplished by inducing the exchange of GDP with GTP, which elicits a conformational change in Ras to its active form.

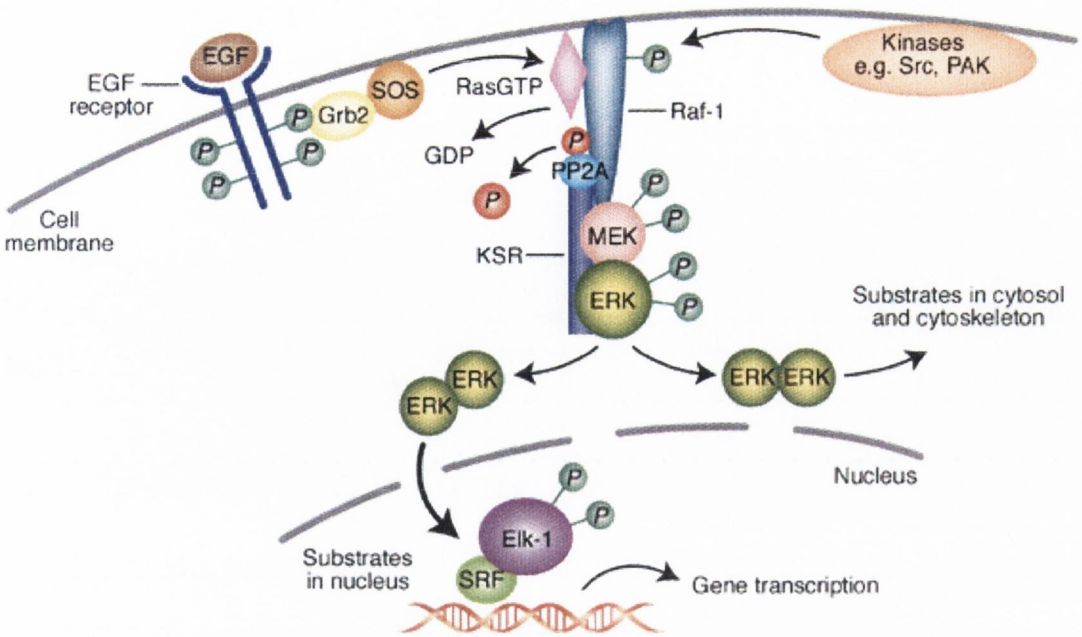

Figure 5.2 Organisation and structure of the Ras/Raf/MEK/ERK pathway

General representation of the pathway. See text for details (adapted from Kolch et al.. The role of Raf kinases in malignant transformation. Expert Rev Mol Med. 2002 Apr 25;2002:1-18).

Following activation, Ras acts as an adapter molecule that can bind Raf kinases with high affinity (via the RBD motif) and recruit them from the cytosol to the cell membrane where Raf activation occurs (via the CRD motif). Although all Ras isoforms bind Raf kinases with comparable affinity, their activation efficiencies vary. K-Ras is known to activate RAF-1 more efficiently than H-Ras (Yan et al., 1998). Raf activation is a complex process that includes dephosphorylation of inhibitory sites by protein phosphatase 2A (PP2A) and phosphorylation of activating sites by $p21^{rac/cdc42}$-activated kinases (PAKs), Src-family and other kinases.

This rings true for both A-RAF and RAF-1. BRAF however, does not require this so-called "activation by compartmentalisation". In its case, the binding of activated Ras to BRAF is sufficient to activate it directly. This has been attributed to a change of amino acid in one of the four phosphorylation activation sites in the wild-type BRAF that can mimic phosphorylation, leading to a "pre-activated" Raf kinase, which merely requires RBD engagement by Ras for functionality (Mason et al., 1999).

Another important difference in Raf activation is the involvement of another, related G-protein; Rap1. Rap1 has an identical effector domain to Ras and although it possesses the ability to bind all Raf isoforms, it selectively activates BRAF (Vossler et al., 1997) and has even been shown to inhibit RAF-1 activation by displacing Ras from the CRD of Raf-1 (Okada et al., 1999). However, Rap1 activation of BRAF often predominates over the inhibition of RAF-1, resulting in a net effect of ERK activation. Rap1 is activated by messengers such as calcium, diacylglycerol and cyclic adenosine monophosphate (cAMP). cAMP signalling is mediated via cAMP-dependant exchange factors such as Epac (de Rooij et al., 1998) or cAMP-activated protein kinase (PKA) (Vossler et al., 1997). cAMP can therefore mediate stimulation of ERKs via BRAF (see Fig 5.3).

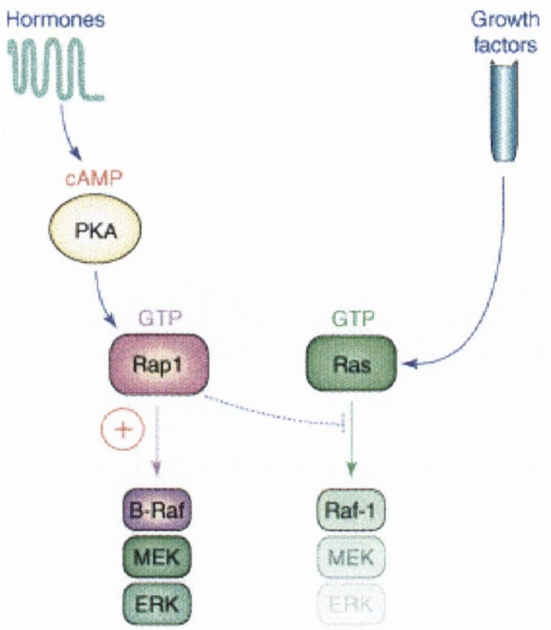

Figure 5.3 The effects of Rap1 on the Ras/Raf/MEK/ERK pathway

An illustration of how the Rap1 G-protein regulates ERK signalling in cells. See text for details (adapted from Stork et al.. Crosstalk between cAMP and MAP kinase signaling in the regulation of cell proliferation. Trends Cell Biol. 2002 Jun;12(6):258-66).

Activated Raf kinases are then free to phosphorylate and activate MEKs, which in turn, can do likewise to ERKs. The entire kinase complex is supported by a scaffolding protein known as KSR (kinase suppressor of Ras) which is also important in the regulation of the pathway.

The three protein isoforms differ in their ability to activate MEK. Studies have shown A-RAF to be a much weaker MEK activator than BRAF or RAF-1 (Pritchard et al., 1995). Although BRAF expression has been shown to be more prevalent in certain tissue types,

it has been identified as the major MEK activator even in tissues where its expression is barely detectable (Huser et al., 2001; Mikula et al., 2001). BRAF shows higher affinity for MEK-1 and -2 than Raf-1 (Papin et al., 1996; Papin et al., 1998) and is better at phosphorylating MEKs than Raf-1 (Pritchard et al., 1995; Papin et al., 1998). This has been attributed to the afore mentioned alternate splicing variants of the BRAF protein.

Activated ERK molecules have a plethora of molecular targets in both the cytosol and nucleus. Substrates within the cytosol include cytoskeletal proteins, ribosomal proteins, tyrosine kinase receptors, SOS and signal transducer and activator of transcription proteins (STATs) among others. Within the nucleus it can further exert its effects by phosphorylating transcription factors such as Elk-1, which promotes expression of genes such as fos, and other members of the Ets-family of proteins.

Studies with Raf knockout mice have yielded interesting results. A-RAF knockout mice are born alive but have intestinal and neurological defects depending on the genetic background (Pritchard et al., 1996). Mice with targeted disruption of the BRAF gene have defects in neuroepithelial differentiation and in the maturation and maintenance of endothelial cells and die during midgestation (Wojnowski et al., 1997). The fate of RAF-1 knockout mice is highly dependent on genetic background (Mikula et al., 2001; Huser et al., 2001). RAF-1 knockout in inbred strains results in death during midgestation. In outbred strains, RAF-1 knockout mice die shortly after birth showing general growth retardation and developmental defects.

These knockout studies and others are beginning to suggest that Raf kinases may have additional targets to MEK that are independent to the Ras/Raf/MEK/ERK pathway and that they may be involved in other cell activities such as apoptosis.

5.2.5 Aim

Previous chapters have investigated the possible effects of ret/PTC oncogene activation on members of the adherens junctions, namely E-cadherin and the catenins. Originally thought to be exclusively present in PTCs, our group demonstrated that Hashimoto thyroiditis cases could also harbour ret/PTC oncogene activation (Sheils et al., 2000).

While ret/PTC oncogenes are accountable for genetic aberrations leading to some PTCs, the purpose of this study was to assess the frequency of the T1799A BRAF mutation in a panel of thyroid tissues derived from the archives of St James's Hospital, Dublin and to determine what, if any overlap existed between ret/PTC and T1799A BRAF mutation.

5.3 Materials & methods

5.3.1 Specimens

Samples (n=66) of papillary thyroid carcinoma (PTC) (n=34), Hashimoto thyroiditis (HT) (n=15), anaplastic carcinoma (ATC) (n=5) and follicular adenoma/non-malignant thyroid tissue (FA/NORM) (n=12) accessioned between 1982 and 2003 in St. James's Hospital, Dublin were analysed. All material was fixed in 10% buffered formal saline and embedded in paraffin wax. Stained sections were reviewed blind by a histopathologist and classified according to a recognised system (Rosai et al., 1992). The PTC cohort consisted of several morphological variants of PTC and are listed in Table 5.1.

Year of diagnosis	Age	Sex	Variant of PTC	Tumour size (cm)	ret/PTC oncogene activation	BRAF allele (T1799A) status
1982	55	F	encaps fv	3	ret/PTC-3	wt
1983	33	M	fv	0.6	none	wt
1984	44	M	tcv	5.5	ret/PTC-1	wt
1986	60	M	fv	ukn	none	het
1989	35	F	classic	4	none	wt
1991	61	F	classic	2	ret/PTC-1	wt
1991	51	M	fv	3.5	none	wt
1991	58	F	fv	3.5	ret/PTC-1	wt
1992	40	M	fv	1.5	ret/PTC-1	het
1992	33	F	classic	4	ret/PTC-1	wt
1992	35	F	fv	2	none	wt
1992	41	F	fv	0.1	none	wt
1992	56	M	tcv	5	both	wt
1993	79	F	fv	9	ret/PTC-3	wt
1994	24	F	classic	7.8	ret/PTC-1	wt

1996	56	M	tcv	5	ret/PTC-3	wt
1997	71	M	classic & solid	4	ret/PTC-1	het
1997	41	F	classic	2.2	none	wt
1998	64	F	classic	5	none	het
1998	39	M	classic	2	ret/PTC-1	het
1998	39	F	classic	5	none	het
1998	86	F	classic	7	none	wt
1999	45	F	classic	1.3	ret/PTC-1	het
2000	50	F	classic	1	none	het
2001	19	M	classic	13	none	het
2001	52	F	classic	5	none	het
2001	71	F	classic	1.5	none	het
2001	25	M	classic	6	none	het
2001	44	F	insular	5	none	het
2002	78	M	classic	7	ret/PTC-1	het
2002	67	F	classic	3	none	het
2002	22	F	fv	3	both	het
2002	29	F	classic	1.5	none	wt
2002	73	M	mixed fv & columnar	2	none	wt

Table 5.1 Clinicopathological features with T1799A BRAF mutation and ret/PTC occurrence in the PTC cohort

Abbreviations – encaps - encapsulated variant, fv - follicular variant, tcv - tall cell variant, ukn - unknown, het – heterozygous, wt – wild-type.

5.3.2 Microdissection and DNA extraction

In order to accurately detect the BRAF mutant/wild type status of cases, it was necessary to acquire homogeneous cell populations of thyrocytes. 7μm sections were cut from each block, de-waxed and lightly stained with haematoxylin and eosin (H&E). Thyrocytes in each case were laser capture microdissected using the PixCell II™ System (Arcturus Engineering, Inc., CA, USA) for subsequent mutation analysis (see chapter 2.2).

Following microdissection the Capsures™ were placed in sterile Eppendorf tubes and DNA extraction was performed using the PUREGENE® DNA Isolation Kit (Gentra Systems Inc., MN, USA) with modification of the protocol as previously described (chapter 2.4.2).

5.3.3 BRAF mutation (T1799A) detection

Taqman® SNP detection was used for mutation detection. The principle of the Taqman®/5' nuclease assay and its use in SNP detection is described in chapter 2.5.2. Briefly, for allelic discrimination, two differentially labelled fluorescent (FAM and VIC) MGB-NFQ probes, differing by the one base pair T or A at the mutation site, competitively bind to target sequence between the forward and reverse primers. Mismatches between probe and target reduce hybridisation efficiency and DNA polymerase is more likely to displace mismatched probe than cleave it. The appropriate probe(s) are cleaved by 5' nuclease activity on a perfectly matched probe/target duplex thereby generating fluorescence depending on the presence and abundance of target sequence(s). In this regard the assay functions as its own endogenous control as the wild-type allele would be detected even in the absence of mutant allele(s).

Following thermal cycling, the fluorescence generated during PCR amplification can be read. By quantifying and comparing the fluorescent signals, it is then possible to determine the allelic content of each sample by comparison to known control samples.

Primers and probes used in this experiment were designed and used according to the Applied Biosystems (Foster City, CA, USA) Assays-by-Design^{SM} service. The primers/probes used were as follows: 5' CAT GAA GAC CTC ACA GTA AAA ATA GGT GAT 3' [BRAF-F], 5' GGA TCC AGA CAA CTG TTC AAA CTG A 3' [BRAF-R], VIC-5' CCA TCG AGA TTT CAC TGT AG 3' [BRAF-P^{WT}], and FAM-5' CCA TCG AGA TTT CTC TGT AG 3' [BRAF-P^{MUT}]. Amplification and analysis was performed on an ABI Prism 7000 Sequence Detection System (Applied Biosystems, CA, USA) for 40 cycles (92°C for 15sec, 60°C for 1min).

DNA from cell lines was used for control purposes. The cell lines used as controls are described briefly in Table 2. Detailed descriptions of the cell lines and their culture and passage can be found in chapter 2.3.1. The assay was validated using several operator samples and the following additional thyroid cell lines: 8505C, Nthy-ori, HTH74, KAT4 and KAT10.

Cell line	Derived from	ret/PTC oncogene activation	BRAF allele status (HOM/HET/WT)
B-CPAP	PTC	none	HOM
K-2	PTC	none	HET
TPC-1	PTC	ret/PTC-1	WT
HTH74	ATC	none	WT
Nthy-ori	Normal thyroid	none	WT
KAT4	ATC	none	HET
KAT10	PTC	none	HET
8505C	ATC	none	HOM

Table 5.2 Cell lines used as controls throughout the experiment

Abbreviations: HOM – homozygous, HET – heterozygous, WT – wild-type

Six of each; no template controls (NTC), homozygous controls and heterozygous mutation controls were included in each run for control and allele calling purposes. All unknown samples were analysed in duplicate. Allele calls were defined using the 7000 SDS software and the relative distances between unknowns and controls. Fluorescent signals from controls fell into clusters (see Fig 5.4), which were used to form sectors, i.e. mutant, wild-type or heterozygous. Signals from NTCs (no template controls) formed the origin from which the sectors emanated. Signals greater than 0.5 fluorescent units from the NTCs were called according to the sector in which they were located (see Fig 5.4).

Samples that did not reliably fall into a defined allele "sector" and those that displayed no amplification were subsequently re-extracted and/or reanalysed.

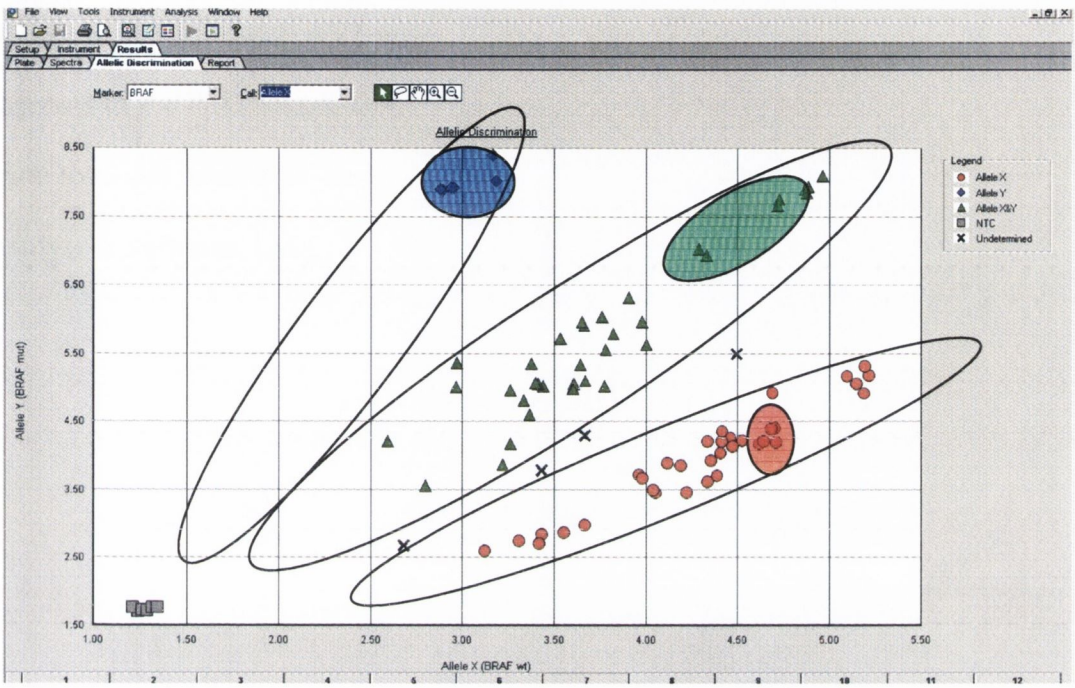

Figure 5.4 Example of the output from an AD (allelic discrimination) assay

Figure shows clustering of the samples into 3 distinct groups depending on their respective levels of VIC/FAM fluorescence: homozygous T1799A mutation (◆), homozygous wild-type/normal (●) and heterozygous T1799 mutation (▲). Negative controls (■) and undetermined samples are also displayed (×). The locations of cell line controls are indicated by appropriate coloured shading.

5.3.4 ret/PTC rearrangement detection

ret/PTC rearrangements were evaluated as described in the previous two chapters.

5.3.5 Statistical analysis

Association between BRAF mutant and ret/PTC activated samples was examined. Dividing the respective cohorts into pre- and post-1997 diagnosis enabled a temporal analysis to be performed. 1997 was chosen arbitrarily as it represented the median year of diagnosis in the PTC cohort. Comparison between groups was performed using Fisher's exact test. All statistical analyses were performed using Analyse-it™, version 1.71 (Analyse-it Software, Ltd.).

5.4 Results

An example of the graphical output of a typical allelic discrimination run is displayed in Fig 5.4. Using the allelic discrimination technique, the BRAF T1799A mutation was detected in 15 of the 34 (44%) PTCs. No mutations were detected among HT, ATC or FA/NORM samples. All BRAF mutations detected were heterozygous. In all samples that did not harbour the BRAF mutation, homozygous wild-type BRAF was detected. Mutations were detected in 11/18 (61%) classic PTCs, 3/11 (27%) of follicular variants of PTC and 1/1 (100%) insular PTC.

Statistical analysis of $BRAF^{mut}$ samples and ret/PTC positive samples showed no association between the two variables (p=0.64). Segregation of the PTC cohort into pre- and post-1997 groups exposed an interesting temporal pattern (Table 5.1, Fig 5.5). Analysis of both $BRAF^{mut}$ and ret/PTC detection in their pre- and post-1997 groups, shows significant association (p=0.0012 and 0.04 respectively) between the variables with a "molecular shift" from ret/PTC in the samples pre-1997, to $BRAF^{mut}$ in the samples post-1997. A similar temporal analysis of PTC variant revealed a shift from follicular variant pre-1997 to classic PTC post-1997 (p=0.0213).

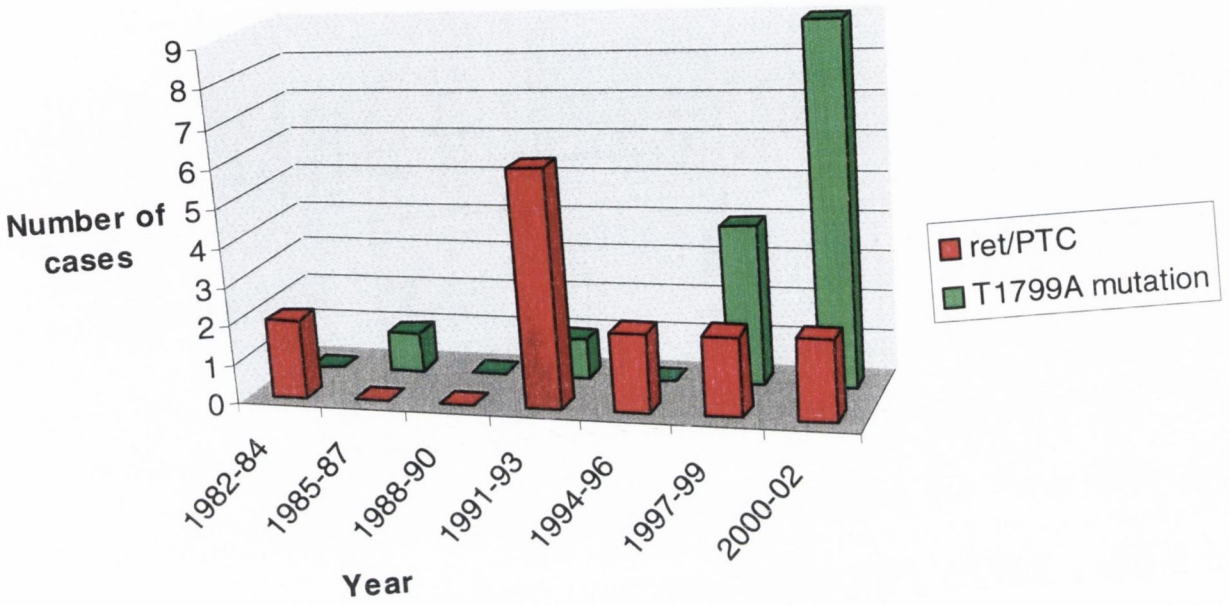

Figure 5.5 Temporal trends in ret/PTC oncogene and T1799A BRAF mutation occurrence

5.5 Discussion

This study examines the prevalence of the BRAF T1799A mutation in thyroid tissues in the context of ret/PTC positivity. The study utilized the Assay-by-Design^{SM} service to produce a novel allelic discrimination assay for segregation of cases into wild-type and mutant BRAF. The technique was effective and reproducible in analysing both paraffin-embedded samples and control material validated by sequencing. The exon 15, T1799A mutation was selected because it is the most commonly occurring BRAF mutation, being responsible for greater than 80% of all BRAF mutations in several types of cancer (Davies et al., 2002).

The T1799A mutation was detected in 15 of 34 (44%) PTC samples. It was not detected in other thyroid tissue types (ATC, HT and FA/NORM) examined. This detection rate in PTC is comparable with the results of other studies - albeit in a smaller study group - whose detection rates were 29% (Namba et al., 2003), 35.8% (Kimura et al., 2003), 38% (Nikiforova et al., 2003; Xu et al., 2003), 45% (Xing et al., 2004b), 46% (Soares et al., 2003), 53% (Fukushima et al., 2003) and 69% (Cohen et al., 2003). Trovisco et al. (2004) reported a detection rate of 75% in Warthin-like PTCs, 53% in conventional PTCs and an absence of mutations in follicular variant of PTC. Their overall detection rate in PTCs was 36% demonstrating that the prevalence of the mutation varies substantially depending on the prevalence of PTC histotypes which are known to be more associated with BRAF T1799A. This study shows a similar mutation rate in conventional PTC and although mutations were detected in follicular variant, their rate is much lower compared

to the former. This data supports the theory that BRAF mutations are more often associated with classic PTC.

T1799A mutation was also examined in context to ret/PTC-1 and -3 positivity. Although 5 of the 34 (15%) PTCs examined had concomitant presence of a ret/PTC rearrangement and T1799A mutation (Table 1), there was no significant statistical association between the two. Data on Ras aberrations and ret/PTC prevalence is abundant (Zhu et al., 2003; Xing et al., 2004a), but there is relatively little information on the co-existence of BRAF and ret/PTC. Xu et al. (2003) found both aberrations within the same tumour, detecting ret/PTC oncogene in 8 of 21 BRAF mutated PTCs. Another study (Nikiforova et al., 2004) found ret/PTC in 3 of 32 BRAF mutated PTCs. Others found the two genetic events to be mutually exclusive (Kimura et al., 2003; Soares et al., 2003). With regard to the current study, there was no consistent histological subtype or background of thyroiditis observed among those tumours with both mutations. The data in this and the above mentioned studies suggest that a double hit on the RET/Ras/Raf/MEK/ERK pathway is a relatively rare occurrence and may not result in an enhanced significant biological effect compared to a single aberration of either oncogene.

Our group has previously demonstrated pathobiological links between PTC and HT (Sheils et al., 2000; Smyth et al., 2001). In this study no T1799A mutations were detected in HT lesions. This observation suggests that the acquisition of a BRAF mutation may be a later or alternative event in thyroid cancer progression than that engendered by ret/PTC rearrangement.

T1799A was not detected in the ATC cohort. An absence or low incidence of BRAF mutation in ATC has been observed in other studies (Fukushima et al., 2003; Namba et al., 2003; Nikiforova et al., 2003; Xing et al., 2004b), although a recent report found a mutation in 35% of undifferentiated thyroid carcinomas (Soares et al., 2004). It is interesting to speculate that T1799A-negative ATCs originate from FTC as opposed to pre-existing PTC, given that BRAF mutations have not previously been reported in FTC. Additionally, the fact that a high percentage of BRAF mutated, poorly differentiated/undifferentiated carcinomas often have a papillary carcinoma component (Nikiforova et al., 2003) supports the concept of alternative origins in poorly differentiated/undifferentiated thyroid carcinoma.

It is widely acknowledged that exposure to ionising radiation, such as that occurred in Belarus and the Ukraine following the Chernobyl nuclear accident, results in a sharp increase in the incidence of PTC and detection rates of ret/PTC oncogenes 4 to 7 years post-exposure. It is apparent from the data in Fig 2 that there was a spike in ret/PTC activation among PTCs in the 1991-93 period. This coincides with a 4 to 7 year latency period following the Chernobyl disaster in 1986. Studies have shown increased thyroid cancer cases in areas as far away as Utah and Connecticut in the US in the same time period (Mango, 1996). It is therefore feasible that fallout from the Chernobyl accident may have influenced thyroid cancer rates in a geographical region as distant as Ireland.

Surprisingly, the results generated reveal a significant temporal trend in oncogene detection. 1997 was chosen as the median year of diagnosis. There were significant

increases and decreases in T1799A mutation and ret/PTC activation respectively, among the PTC cohort, pre- and post-1997. The finding that classic PTC is more prevalent post-1997 further supports such a theory as BRAF mutations have been shown to associate with this particular morphological variant (Trovisco et al., 2004). Interestingly, Burgess et al. (2003) examined ret/PTC activation in a Tasmanian series of thyroid tumours and found no temporal phenomenon in their PTC cohort, using 1994 as the median year.

The temporal switch in T1799A detection in PTC is striking. 2 cases were detected pre-1997 (n=16) and 13 cases post-1997 (n=18). It is reasonable to assume that ret/PTC activation is an early event capable of securing progression to PTC without the intervention of BRAF mutation. This concept is supported by Suchy et al. (1998) who concluded that ret/PTC rearrangements are the prevalent molecular aberration in radiation-induced thyroid tumours in the absence of Ras mutations (another downstream RET signal transducer), in a series of children exposed to post-Chernobyl radioactive fallout.

Another study by Xing et al. (2004b), found T1799A mutation rates to be comparable in a North American and Ukrainian series. However, the radiation-exposed subgroup of the Ukrainian series had reduced mutation rates when compared to the corresponding non-exposed subgroup. The ret/PTC oncogene frequency among these samples however was not assessed.

Notwithstanding this, it is interesting to speculate that our results may indicate a form of evolution from the potentially radiation-induced ret/PTC positive papillary carcinomas in the period 1991-96 to a more normally distributed, spontaneously BRAF mutated variety from 1996 to date. The PTC cohort in this study however, had only 5 samples diagnosed prior to 1991 and in that context is of limited value. Further work in the pre-1991 PTC cohort is warranted to investigate this hypothesis fully.

5.6 References

Barnier JV, Papin C, Eychene A, Lecoq O, Calothy G. The mouse B-raf gene encodes multiple protein isoforms with tissue-specific expression. J Biol Chem. 1995 Oct 6;270(40):23381-9.

Burgess JR, Skabo S, McArdle K, Tucker P. Temporal trends and clinical correlates for the ret/PTC1 mutation in papillary thyroid carcinoma. ANZ J Surg 2003; 73: 31-5.

Cohen Y, Xing M, Mambo E, Guo Z, Wu G, Trink B, Beller U, Westra WH, Ladenson PW, Sidransky D. BRAF mutation in papillary thyroid carcinoma. J Natl Cancer Inst 2003; 95: 625-7.

Davies H, Bignell GR, Cox C, Stephens P, Edkins S, Clegg S, Teague J, Woffendin H, Garnett MJ, Bottomley W, Davis N, Dicks E, Ewing R, Floyd Y, Gray K, Hall S, Hawes R, Hughes J, Kosmidou V, Menzies A, Mould C, Parker A, Stevens C, Watt S, Hooper S, Wilson R, Jayatilake H, Gusterson BA, Cooper C, Shipley J, Hargrave D, Pritchard-Jones K, Maitland N, Chenevix-Trench G, Riggins GJ, Bigner DD, Palmieri G, Cossu A, Flanagan A, Nicholson A, Ho JW, Leung SY, Yuen ST, Weber BL, Seigler HF, Darrow TL, Paterson H, Marais R, Marshall CJ, Wooster R, Stratton MR, Futreal PA. Mutations of the BRAF gene in human cancer. Nature 2002; 417: 949-54.

de Rooij J, Zwartkruis FJ, Verheijen MH, Cool RH, Nijman SM, Wittinghofer A, Bos JL. Epac is a Rap1 guanine-nucleotide-exchange factor directly activated by cyclic AMP. Nature. 1998 Dec 3;396(6710):474-7.

Fukushima T, Suzuki S, Mashiko M, Ohtake T, Endo Y, Takebayashi Y, Sekikawa K, Hagiwara K, Takenoshita S. BRAF mutations in papillary carcinomas of the thyroid. Oncogene 2003; 22: 6455-7.

Huebner K, ar-Rushdi A, Griffin CA, Isobe M, Kozak C, Emanuel BS, Nagarajan L, Cleveland JL, Bonner TI, Goldsborough MD, et al. Actively transcribed genes in the raf oncogene group, located on the X chromosome in mouse and human. Proc Natl Acad Sci U S A. 1986 Jun;83(11):3934-8.

Huser M, Luckett J, Chiloeches A, Mercer K, Iwobi M, Giblett S, Sun XM, Brown J, Marais R, Pritchard C. MEK kinase activity is not necessary for Raf-1 function. EMBO J. 2001 Apr 17;20(8):1940-51.

Ikawa S, Fukui M, Ueyama Y, Tamaoki N, Yamamoto T, Toyoshima K. B-raf, a new member of the raf family, is activated by DNA rearrangement. Mol Cell Biol. 1988 Jun;8(6):2651-4.

Kimura ET, Nikiforova MN, Zhu Z, Knauf JA, Nikiforov YE, Fagin JA. High prevalence of BRAF mutations in thyroid cancer: genetic evidence for constitutive activation of the

RET/PTC-RAS-BRAF signaling pathway in papillary thyroid carcinoma. Cancer Res 2003; 63: 1454-7.

Kolch W, Kotwaliwale A, Vass K, Janosch P. The role of Raf kinases in malignant transformation. Expert Rev Mol Med. 2002 Apr 25;2002:1-18.

Mangano JJ. A post-Chernobyl rise in thyroid cancer in Connecticut, USA. Eur J Cancer Prev 1996; 5: 75-81.

Mason CS, Springer CJ, Cooper RG, Superti-Furga G, Marshall CJ, Marais R. Serine and tyrosine phosphorylations cooperate in Raf-1, but not B-Raf activation. EMBO J. 1999 Apr 15;18(8):2137-48.

Mikula M, Schreiber M, Husak Z, Kucerova L, Ruth J, Wieser R, Zatloukal K, Beug H, Wagner EF, Baccarini M. Embryonic lethality and fetal liver apoptosis in mice lacking the c-raf-1 gene. EMBO J. 2001 Apr 17;20(8):1952-62.

Morice C, Nothias F, Konig S, Vernier P, Baccarini M, Vincent JD, Barnier JV. Raf-1 and B-Raf proteins have similar regional distributions but differential subcellular localization in adult rat brain. Eur J Neurosci. 1999 Jun;11(6):1995-2006.

Namba H, Nakashima M, Hayashi T, Hayashida N, Maeda S, Rogounovitch TI, Ohtsuru A, Saenko VA, Kanematsu T, Yamashita S. Clinical implication of hot spot BRAF

mutation, V599E, in papillary thyroid cancers. J Clin Endocrinol Metab 2003; 88: 4393-7.

Nikiforova M, Ciampi R, Salvatore G, Santoro M, Gandhi M, Knauf J, Thomas G, Jeremiah S, Bogdanova T, Tronko M, Fagin J, Nikiforov Y. Low prevalence of BRAF mutations in radiation-induced thyroid tumors in contrast to sporadic papillary carcinomas. Cancer Lett 2004; 209: 1-6.

Nikiforova MN, Kimura ET, Gandhi M, Biddinger PW, Knauf JA, Basolo F, Zhu Z, Giannini R, Salvatore G, Fusco A, Santoro M, Fagin JA, Nikiforov YE. BRAF mutations in thyroid tumors are restricted to papillary carcinomas and anaplastic or poorly differentiated carcinomas arising from papillary carcinomas. J Clin Endocrinol Metab 2003; 88: 5399-404.

Okada T, Hu CD, Jin TG, Kariya K, Yamawaki-Kataoka Y, Kataoka T. The strength of interaction at the Raf cysteine-rich domain is a critical determinant of response of Raf to Ras family small GTPases. Mol Cell Biol. 1999 Sep;19(9):6057-64.

Papin C, Denouel A, Calothy G, Eychene A. Identification of signalling proteins interacting with B-Raf in the yeast two-hybrid system. Oncogene. 1996 May 16;12(10):2213-21.

Papin C, Denouel-Galy A, Laugier D, Calothy G, Eychene A. Modulation of kinase activity and oncogenic properties by alternative splicing reveals a novel regulatory mechanism for B-Raf. J Biol Chem. 1998 Sep 18;273(38):24939-47.

Pritchard CA, Bolin L, Slattery R, Murray R, McMahon M. Post-natal lethality and neurological and gastrointestinal defects in mice with targeted disruption of the A-Raf protein kinase gene. Curr Biol. 1996 May 1;6(5):614-7.

Pritchard CA, Samuels ML, Bosch E, McMahon M. Conditionally oncogenic forms of the A-Raf and B-Raf protein kinases display different biological and biochemical properties in NIH 3T3 cells. Mol Cell Biol. 1995 Nov;15(11):6430-42.

Rapp UR, Todaro GJ. Generation of oncogenic mouse type C viruses: in vitro selection of carcinoma-inducing variants. Proc Natl Acad Sci U S A. 1980 Jan;77(1):624-8.

Rosai J, Carcangiu M, DeLellis R. Atlas of Tumour Pathology – Tumours of the Thyroid Gland. 3rd Series. Fascicle 5. Washington DC: AFIP, 1992.

Sheils OM, O'Leary JJ, Sweeney EC. Assessment of ret/PTC-1 rearrangements in neoplastic thyroid tissue using TaqMan RT-PCR. J Pathol 2000; 192: 32-6.

Smyth P, Sheils O, Finn S, Martin C, O'Leary JJ, Sweeney EC. Real-time quantitative analysis of E-cadherin expression in ret/PTC-1-activated thyroid neoplasms. Int J Surg Pathol 2001; 9: 265-72.

Soares P, Trovisco V, Rocha AS, Feijao T, Rebocho AP, Fonseca E, Vieira de Castro I, Cameselle-Teijeiro J, Cardoso-Oliveira M, Sobrinho-Simoes M. BRAF mutations typical of papillary thyroid carcinoma are more frequently detected in undifferentiated than in insular and insular-like poorly differentiated carcinomas. Virchows Arch 2004; 444: 572-6.

Soares P, Trovisco V, Rocha AS, Lima J, Castro P, Preto A, Maximo V, Botelho T, Seruca R, Sobrinho-Simoes M. BRAF mutations and RET/PTC rearrangements are alternative events in the etiopathogenesis of PTC. Oncogene 2003; 22: 4578-80.

Stork PJ, Schmitt JM. Crosstalk between cAMP and MAP kinase signaling in the regulation of cell proliferation. Trends Cell Biol. 2002 Jun;12(6):258-66.

Suchy B, Waldmann V, Klugbauer S, Rabes HM. Absence of RAS and p53 mutations in thyroid carcinomas of children after Chernobyl in contrast to adult thyroid tumours. Br J Cancer 1998; 77: 952-5.

Vossler MR, Yao H, York RD, Pan MG, Rim CS, Stork PJ. cAMP activates MAP kinase and Elk-1 through a B-Raf- and Rap1-dependent pathway. Cell. 1997 Apr 4;89(1):73-82.

Wang HG, Rapp UR, Reed JC. Bcl-2 targets the protein kinase Raf-1 to mitochondria. Cell. 1996 Nov 15;87(4):629-38.

Wojnowski L, Zimmer AM, Beck TW, Hahn H, Bernal R, Rapp UR, Zimmer A. Endothelial apoptosis in Braf-deficient mice. Nat Genet. 1997 Jul;16(3):293-7.

Xing M, Cohen Y, Mambo E, Tallini G, Udelsman R, Ladenson PW, Sidransky D. Early occurrence of RASSF1A hypermethylation and its mutual exclusion with BRAF mutation in thyroid tumorigenesis. Cancer Res 2004a; 64: 1664-8.

Xing M, Vasko V, Tallini G, Larin A, Wu G, Udelsman R, Ringel MD, Ladenson PW, Sidransky D. BRAF T1796A transversion mutation in various thyroid neoplasms. J Clin Endocrinol Metab 2004b; 89: 1365-8.

Xu X, Quiros RM, Gattuso P, Ain KB, Prinz RA. High prevalence of BRAF gene mutation in papillary thyroid carcinomas and thyroid tumor cell lines. Cancer Res 2003; 63: 4561-7.

Yan J, Roy S, Apolloni A, Lane A, Hancock JF. Ras isoforms vary in their ability to activate Raf-1 and phosphoinositide 3-kinase. J Biol Chem. 1998 Sep 11;273(37):24052-6.

Yuryev A, Ono M, Goff SA, Macaluso F, Wennogle LP. Isoform-specific localization of A-RAF in mitochondria. Mol Cell Biol. 2000 Jul;20(13):4870-8.

Zhu Z, Gandhi M, Nikiforova MN, Fischer AH, Nikiforov YE. Molecular profile and clinical-pathologic features of the follicular variant of papillary thyroid carcinoma. An unusually high prevalence of ras mutations. Am J Clin Pathol 2003; 120: 71-7.

Chapter 6

Microarray analysis of thyroid cell lines.

6.1 Summary

The use of cDNA microarrays is a powerful method for the quantitative analysis of disease-specific gene expression that can detect altered gene expression associated with the pathology or the altered biology of a disease entity. This study was undertaken as a step toward identifying previously uncharacterised molecular genetic mechanisms in thyroid carcinoma and to further understand the roles played by ret/PTC oncogenes and BRAF V600E mutation in said disease.

Gene expression profiles for several thyroid cell lines were compared using a whole genome microarray system from Applied Biosystems. A variety of cell lines were analysed which were characteristic of various papillary and anaplastic thyroid carcinomas harbouring genetic abnormalities consistent with those found *in vivo* such as ret/PTC and BRAF mutations, in addition to an SV40 transformed normal thyroid cell line.

Genes involved in cell structure and motility and the extracellular matrix were consistently found to be differentially expressed between compared groups. This, coupled with the discovery of over-expressed histones in some groups, led to speculation that these genes may be responsible for the structural peculiarities of certain types of PTC. Escape of apoptosis was also a consistent theme with its inducers and inhibitors frequently found to be down- and up-regulated respectively. Individual genes from inter-group comparisons were also evaluated.

6.2 Introduction

Fifty years after the discovery of the DNA double helix, the reference sequence for *Homo sapiens* was explicated (Lander et al.; McPherson et al.; Venter et al., 2001). The international effort to sequence the 3 billion DNA letters in the human genome has ushered in an exciting new genomic era. DNA microarrays provide an important adjunct in the exploitation of uncharted genomic territory particularly in the area of gene expression.

It is widely believed that thousands of genes and their products (i.e., RNA and proteins) in a given living organism function in a complicated and orchestrated way, insight into which houses potential for a variety of diagnostic and therapeutic modalities. Traditional methods in molecular biology generally work on a "one gene in one experiment" basis, which means that the throughput is very limited and the "whole picture" of gene function is hard to obtain.

In the past several years, a new technology, called DNA microarray, has attracted increasing interest among biologists. This technology comprises assays that simultaneously generate data pertaining to the expression levels of many thousands of genes. This facility represents a dramatic increase in throughput (Schena et al., 1995; Elkins et al., 1999; Lockhart et al., 2000).

6.2.1 Microarrays

The birth of microarrays can be credited to Mark Schena and his co-workers at Stanford University in the early 1990s. The group were studying plant transcription factors and spent considerable time isolating and characterising transcription factors in a very slow and arduous manner. They conceived a strategy to manufacture microscopic arrays (microarrays) containing plant gene sequences attached to a glass substrate and use these microarrays to quantify plant gene expression in hybridisation experiments with fluorescently labelled plant mRNA samples.

A microarray is an ordered array of microscopic elements on a planar substrate that allows the specific binding of genes or gene products. It provides a medium for matching known and unknown DNA samples based on base-pairing rules and automating the process of identifying the unknowns. DNA microarray, or DNA chips are fabricated by high-speed robotics, on a solid matrix/substrate, for which probes with known identity are used to determine complementary binding, thus allowing massively parallel gene expression and gene discovery studies. The sample spot sizes in the original microarrays were typically less than 200μm in diameter and these arrays usually contain thousands of spots. Current diameters can be as small as 4μm.

Initial microarray experiments were performed using cDNA microarrays. The lengths of the spotted cDNAs were typically 500-2500 base pairs. Microarrays that contain such molecules provide very intense hybridisation signals due their extensive complimentarity to fluorescent probes in solution. Unfortunately, due to the length of the cDNA

molecules, they can be quite susceptible to unspecific hybridisation and cross-talk between similar genes. It is for these reasons that there is a trend towards oligonucleotide microarrays in a variety of applications. Oligonucleotides are single-stranded 15- to 70-nucleotide molecules and are produced by chemical synthesis. These synthetic targets provide for high levels of specificity during hybridisation reactions without overtly decreasing signal strength.

The microarray market has grown with alarming rapidity over the last number of years. As the price of this technology has fallen, there has been a tendency to shift from homemade DIY options towards the expanding range of commercial devices currently available. For expression analysis, the field has been dominated in the past by two major technologies: pre-fabricated oligonucleotide arrays and spotted oligonucleotide arrays.

6.2.2 Pre-fabricated arrays (Affymetrix GeneChips)

This sector of the market is exclusive to Affymetrix Inc. GeneChip technology. Affymetrix uses similar equipment to that used for making computer silicon chips in order to permit mass production of very large, low cost chips. This process combines photolithography and combinatorial chemistry (Fig 6.1). For expression analysis, up to 40 separate oligos are used for the detection of each gene. These oligos include both perfect match and mismatch oligos. The purpose of the latter is for detection of non-specific and background hybridisation, which is important for quantifying weakly expressed mRNAs.

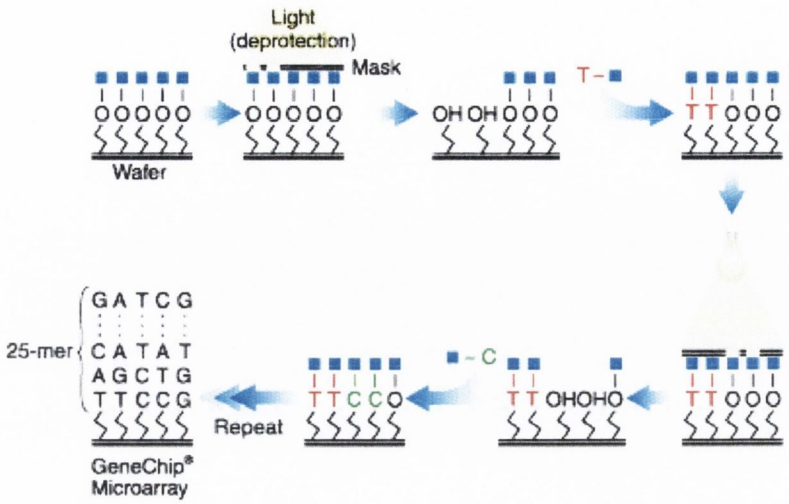

Figure 6.1 Photolithographic generation of oligonucleotide microarray

In order to detect hybridised target mRNA on an array it is necessary to label it with a fluorochrome. Early array design required control and sample RNA to be differentially labelled with two different fluorochromes and hybridised on the same array (see Fig 6.2). The Affymetrix system adopted a different approach in utilising an RT-IVT amplification and labelling step to incorporate biotin-NTPs into the resultant cRNA. Following hybridisation and appropriate washing steps the array is stained with Streptavidin-Phycoerythrin. The signal can then be amplified using goat IgG and biotinylated antibody (see Fig 6.3).

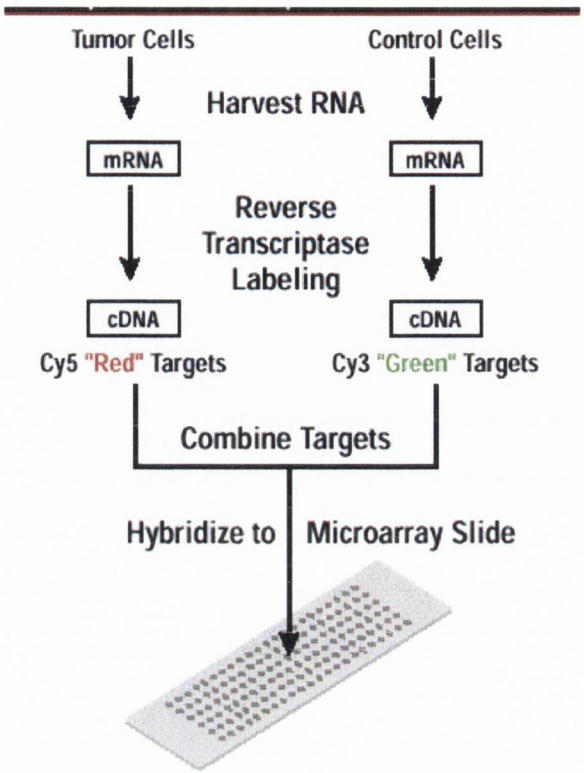

Figure 6.2 "Traditional" microarray experiment using dual labelling

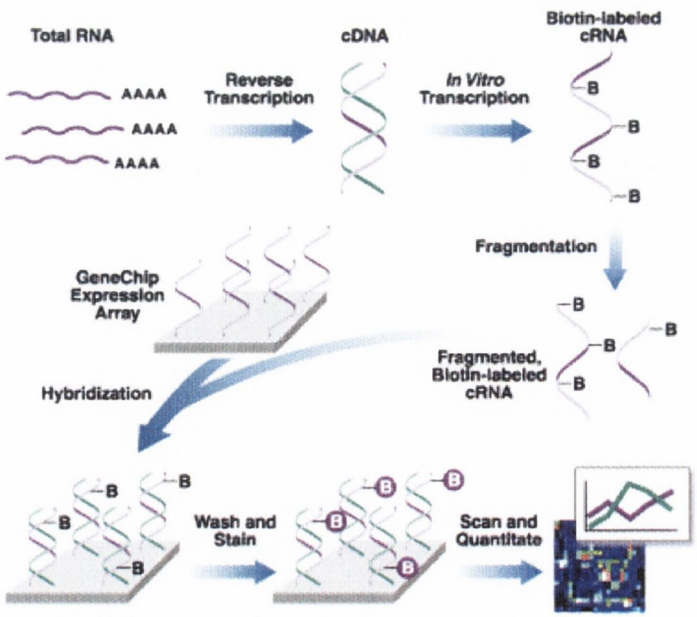

Figure 6.3 Standard Affymetrix gene expression assay

6.2.3 Spotted arrays

The other most commonly used microarrays are spotted microarrays. The array probes are manufactured separately from the arrays and can consist of cDNA, PCR products or oligonucleotides. Microscopic quantities of probe are typically spotted onto the arrays using a robotic system. Probes can be fixed to the surface in a number of ways but the most common way is by non-specific binding to polylysine-coated slides. Following robotic spotting, the remaining exposed amines of polylysine are blocked with succinic anhydride and the DNA is denatured by heating (if double-stranded).

The obvious advantage with this format is that any designed probe can be spotted on the array. Probes can be quality controlled prior to spotting making it easier to determine if probes have been correctly synthesised prior to running an experiment. One also has the choice whether to perform the experiment in a single- or dual-label format. However, spotting will not be as uniform as the *in situ* synthesised Affymetrix chips and cost can become an issue as the number of probes increase.

During the course of this study, the new Expression Array system from Applied Biosystems was used. The system relies on spotted arrays but combines chemiluminescent detection with improved probe design to provide an average sensitivity of 0.5 copies per cell, compared to the one to three copies per cell afforded by most fluorescent platforms. The reason for this is that the light used to excite the fluorescent probes can overlap with their emission spectra. A chemiluminescent reaction, however, produces light when a label binds to a substrate rather than relying on light to excite the

bound label, thereby eliminating this problem. These technologies incorporated into the Expression Array system combine to allow users to use as little as 500ng of starting total RNA and resolve genes with lower levels of expression (see chapter 2.5.5 for a detailed description of the technology). An added advantage is that Applied Biosystems also offers custom probes for subsequent real-time PCR analysis for validation work.

Figure 6.4 Applied Biosystems Expression Array System

6.2.4 Aims

Although this thesis and other studies have examined many genes that may be involved in the pathogenesis of thyroid disease, a vast number of other genes, signalling pathways and other basic mechanisms remain poorly defined. Another shortcoming remains the adequacy of diagnostic and prognostic biomarkers of disease sub-categorisation and progression.

Use of a cDNA microarray is a powerful tool for the quantitative analysis of disease-specific gene expression that can detect altered gene expression associated with the pathology or the altered biology of a disease entity. This study was undertaken as a step toward identifying previously uncharacterised molecular genetic mechanisms in thyroid carcinoma and to further understand the roles played by ret/PTC oncogenes and BRAF V600E mutation in PTC.

6.3 Materials & methods

6.3.1 Thyroid cell lines

The cell lines used in this experiment consisted of Nthy-ori 3-1, TPC-1, B-CPAP, 8505C, HTH74, KAT4 and KAT10 (see chapter 2.3.1 for detailed descriptions). All cell lines were grown in a humidified atmosphere containing 5% CO_2 at 37°C in the appropriate plating medium (see chapter 2.3.2). Cell lines were grown to approx. 80% confluence prior to RNA harvesting. RNA extraction was performed immediately on cell pellets following cell trypsinisation.

6.3.2 RNA extraction and analysis

High quantities and qualities of RNA were obtained using the RNeasy® mini kit with the added on-column DNase digestion option (Qiagen Ltd., West Sussex, UK) (see chapter 2.4.3 for detailed description).

RNA quality was assessed visually using agarose gel electrophoresis and the observation of distinct, intact bands of 28S and 18S ribosomal RNAs and the lack of genomic DNA. 260/280 absorbance ratios were used to assess levels of protein contamination. Only extracts with ratios of greater than 2 were deemed acceptable for further processing. UV spectroscopy was also used to determine the concentration of RNA extracts.

6.3.3 Microarraying

5µg of RNA was used in each microarray experiment. Chapter 2.5.5 describes the ABI microarray process in its entirety. Technical replicates (2) were performed on each RNA sample (i.e. the same RNA from a sample was processed on two different occasions). The ABI 1700 software's QC function was used to determine the reliability of results obtained from the microarrays.

6.3.4 Statistical analysis

Microarrays were analysed using a combination of Microsoft® Excel (Microsoft® Corp.), Spotfire DecisionSite™ for Functional Genomics (Spotfire AB, SE-413 28 Göteborg, Sweden) and R version 1.9.1, a free language and environment for statistical computing and graphics (R Development Core Team, 2004).

6.3.4.1 Normalisation

Biologists have long experience coping with systematic variation between experimental conditions (technical variation) that is unrelated to the biological differences they seek. Normalisation is the attempt to compensate for systematic technical differences between arrays, to see more clearly the systematic biological differences between samples. Differences in treatment of two samples, especially in labelling and in hybridisation, bias the relative measures on any two arrays.

Most approaches to normalising expression levels assume that the overall distribution of RNA numbers doesn't change much between samples, and that most individual genes

change very little across the conditions. This seems reasonable for most laboratory treatments, although treatments affecting transcription apparatus have large systemic effects, and malignant tumours often have dramatically different expression profiles. If most genes are unchanged, then the mean transcript levels should be the same for each condition. An even stronger version of this idea is that the distributions of gene abundances must be similar.

Statisticians use the term 'bias' to describe systematic errors, which affect a large number of genes. However, normalisation, like any form of data 'fiddling' adds noise (random error) to the expression measures. The true source or nature of a systemic bias is never really identified; rather some feature is identified, which correlates with the systematic error. When one 'corrects' for that feature, some error is added to those samples where the observed feature doesn't correspond well with the true underlying source of bias. Statisticians try to balance bias and noise, and their rule of thumb is that it's better to under-correct for systemic biases than to compensate fully.

Different normalisation techniques were compared on paired samples by computing fold change statistics as a function of assay signal intensity. This was achieved through the use of MA plots and a fold change histogram for each binned 10% of genes (see Fig 6.9). The 95 percentile of fold change per bin was used to compare across different normalisations and to select the appropriate method.

6.3.4.2 Filtering genes

A very basic filtering was applied initially. Flagged genes and those with a signal-to-noise ratio (S/N) of less than 3 were deemed undetectable and removed from further analysis. All control elements on the array such as hybridisation controls, RT-IVT controls, etc. were also removed prior to further analysis.

6.3.4.3 Comparing samples

When comparing samples/groups of samples, non-parametric t-tests/ANOVA were used to generate unadjusted p-values.

6.3.4.4 Adjusting p-values for multiple comparisons (FDR)

In the past methods were developed for experiments of the type n>>p (i.e. one had very few variables with a lot of replicate measures). With the advent of microarray technology the case of n<<p (thousands of genes and a very small number of biological replicates) has been adopted. In such conditions, questions raised by research scientists relate to class comparison, class prediction and class discovery problems. Concerning class comparison, the aim is to select relevant genes the transcriptional changes of which are related to a clinical or biological outcome. In such a case, a major multiplicity problem arises that leads to a renewed interest for multiple comparison procedures taking into account false positives.

The p-value (0.05 or 0.01) has been used classically to control the type I error rate (i.e. the false positive rate). Its interpretation was that from 100 tests, 5 tests would

nevertheless be significant in the case of p=0.05 (i.e. false positives). Although useful in most experiments, the use of the same p-value on a microarray with 30,000 genes would yield 1,500 false positive genes, which is an unacceptable amount. Therefore additional measures need to be taken.

Until now, statistical procedures have mostly relied on the multiple testing framework in order to control false positive conclusions. In this framework, two quantities have been considered: the Family Wise Error Rate (FWER) and the False Discovery Rate (FDR). The FWER, which is the oldest criterion considered in multiple comparisons, is defined as the probability of at least one false positive conclusion over all the true null hypotheses (a null hypothesis corresponds to the lack of relationship between gene expression measurement and a response variable). The most commonly used methods are the Bonferroni and Sidak methods. Extension of these two methods are based on step-down or step-up principles where null hypotheses are tested sequentially (Holm, 1979). In complement to the previous methods, resampling (or permutation based) procedures that make no distributional hypothesis but incorporate correlation structures and distributional characteristics have been developed and applied to microarray gene expression study (Callow et al., 2000; Dudoit et al., 2000; Ge et al., 2003).

However, as argued by Benjamini and Hochberg (1995), controlling the FWER in multiple testing settings may not always be appropriate. Indeed, in large-scale hypothesis generating studies such as microarray experiments, this criterion becomes so conservative that the probability of detecting any true association is, in some cases, almost nil. As an

alternative and less stringent concept of error control, Benjamini and Hochberg introduced the false discovery rate (FDR). The FDR is the expected proportion of erroneously rejected null hypotheses among the rejected ones. The main reason for controlling the FDR is that it controls a quantity that is relevant and leads to more powerful procedures than those relying on the FWER. Based on this concept, they initially developed a step-up procedure under the hypothesis of independence which controls FDR at a pre-specified value. Extensions to the case of dependent tests have recently been proposed by Benjamini and Yekutieli (2001).

Throughout the analysis various corrections for FDR are used depending on what and how samples were being compared and according to the appropriate level of stringency required to generate usable results.

6.3.4.5 Adjusting for fold-change noise

When comparing two samples for fold-change differences, results were adjusted for fold-change noise. This is accomplished by plotting the fold-change difference between sample 1, replicate 1 and sample 2, replicate 1 against sample 1, replicate 2 and sample 2, replicate 2 (i.e. $\log_2$(sample1, rep1 ÷ sample2, rep1) vs. $\log_2$(sample1, rep2 ÷ sample2, rep2)). From this, genes that appear upregulated in one comparison and downregulated in the other, or vice versa can then be eliminated. This method, coupled with adjusted p-values from a t-test results in a list of genes that are significantly up- or downregulated between the two samples. This list can be further reduced by restricting it to those genes with a greater than two-fold change.

6.3.4.6 Hierarchical clustering

Hierarchical clustering was performed on the generated final differential gene lists to determine whether technical replicates and cell line types grouped appropriately. Clustering was performed using the Unweighted Pair Group Method with Arithmetic Mean (UPGMA) with Euclidian distance as the similarity measure. Average value was used as the ordering function.

6.3.4.7 Analysis of gene lists

Final gene lists were manipulated and displayed using Spotfire software. For additional analyses, gene lists were exported and uploaded into PANTHER (panther.celera.com). The PANTHER database was designed for high-throughput analysis of protein sequences. One of the key features is a simplified ontology of protein function, which allows browsing of the database by biological functions. Biologist curators have associated the ontology terms with groups of protein sequences rather than individual sequences. Statistical models (Hidden Markov Models, or HMMs) are built from each of these groups. The advantage of this approach is that new sequences can be automatically classified as they become available. To ensure accurate functional classification, HMMs are constructed not only for families, but also for functionally distinct subfamilies. Multiple sequence alignments and phylogenetic trees, including curator-assigned information, are available for each family.

6.4 Results

6.4.1 RNA analysis

The quality and quantity of RNA extracted from thyroid cell lines was examined prior to its inclusion in microarray analysis. Agarose gel and UV spectroscopy results for a selection of cell lines are shown in Fig 6.5 and Table 6.1.

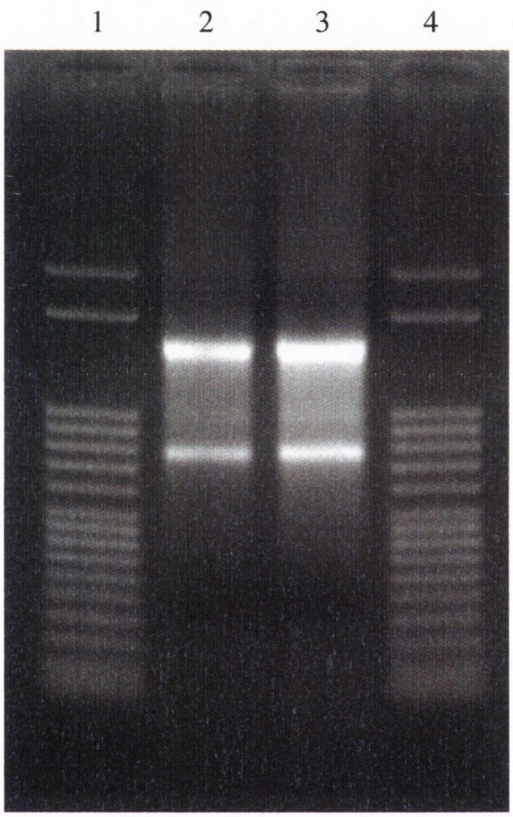

Figure 6.5 Agarose gel electrophoresis of cell line RNA samples

Typical RNA extracts electrophoresed on a 2% agarose gel containing ethidium bromide. Lanes 1 and 4: 50bp DNA ladder (used for reference only and not for sizing purposes), lane 2: Nthy-ori 3-1 RNA extract, lane 4: HTH74 RNA extract.

Cell line	RNA Concentration (ng/μl)	A260:280
KAT4	1054.9	2.183
TPC-1	349.6	2.184
HTH74	685.1	2.186
8505C	945.6	2.193
KAT10	1199.9	2.182
Nthy-ori 3-1	507.2	2.18
B-CPAP	1128.7	2.174

Table 6.1 UV spectroscopic analysis of thyroid cell lines

6.4.2 Post RT-IVT cRNA analysis

cRNA outputs from the RT-IVT reaction were analysed prior to any hybridisation. UV spectroscopy was once again used to determine nucleic acid concentration (Table 6.2) and agarose gel electrophoresis was used to determine the approximate size distribution of the labelled cRNA targets (see Fig 6.6 for example).

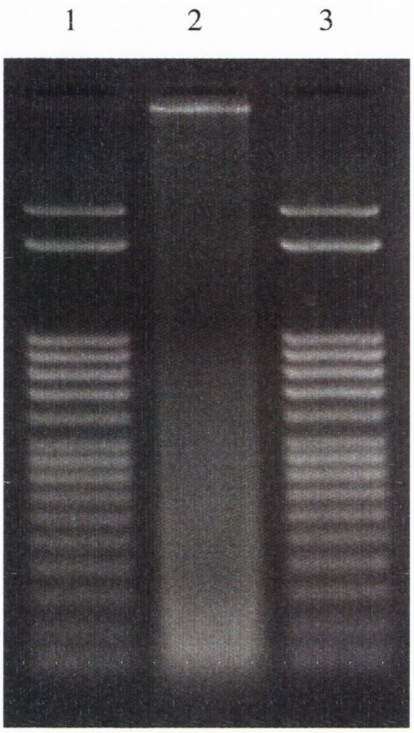

Figure 6.6 Agarose gel electrophoresis of a cRNA sample

A typical cRNA output from the RT-IVT kit electrophoresed on a 2% agarose gel containing ethidium bromide. Lanes 1 and 3: 50bp DNA ladder, lane 2: Nthy-ori 3-1 cRNA.

Cell line	cRNA Concentration (ng/μl)
KAT4	922
TPC-1	757.3
HTH74	918.9
8505C	854.1
KAT10	2962.8*
Nthy-ori 3-1	857.5
B-CPAP	468.6

Table 6.2 UV spectroscopic analysis of RT-IVT ouputs

*Judging from agarose gel electrophoresis, this result was deemed to be incorrect. KAT10 cRNA concentration appeared to be similar to other cell lines visually on the gel. As a result of this, an average of the concentration of the rest of the cell lines was used to approximate KAT10 cRNA concentration for hybridisation.

6.4.3 Microarray image capture

Images of processed microarrays were captured and processed using the ABI 1700 reader and software system. Arrays were captured in two halves and an example is displayed in Fig 6.7.

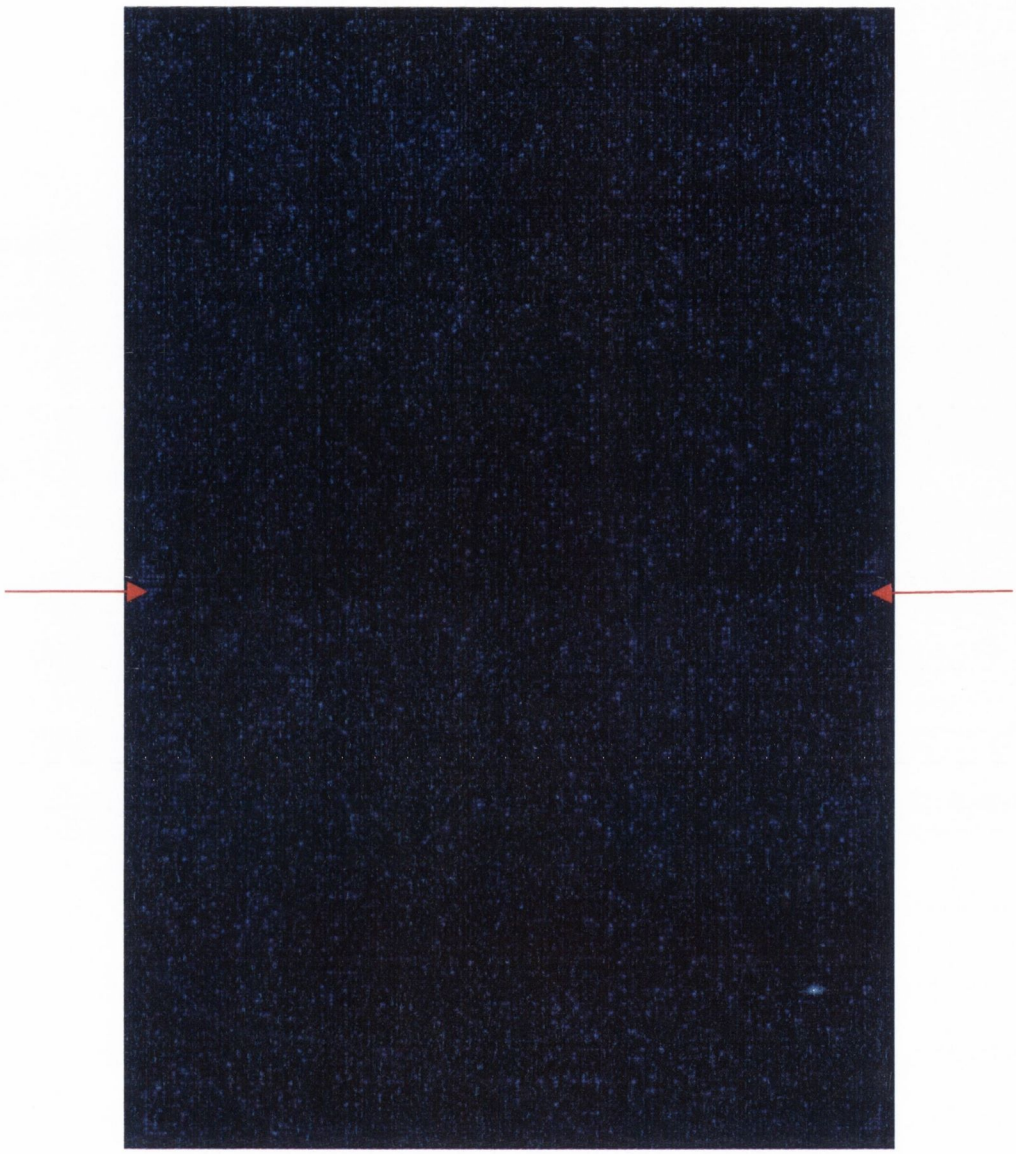

Figure 6.7 Captured image of KAT10 microarray

ABI 1700 software captures the full microarray image in two halves. The two images have been merged for the purposes of this figure but their separating fiducials are visible and are indicated by the arrows.

6.4.4 Statistical analysis

6.4.4.1 Normalisation

An appropriate normalisation method was selected through the use of MA plots and fold change analysis (see Figs 6.8 and 6.9). A 5% trimmed mean was selected as it is more powerful when analysing low signal intensity genes.

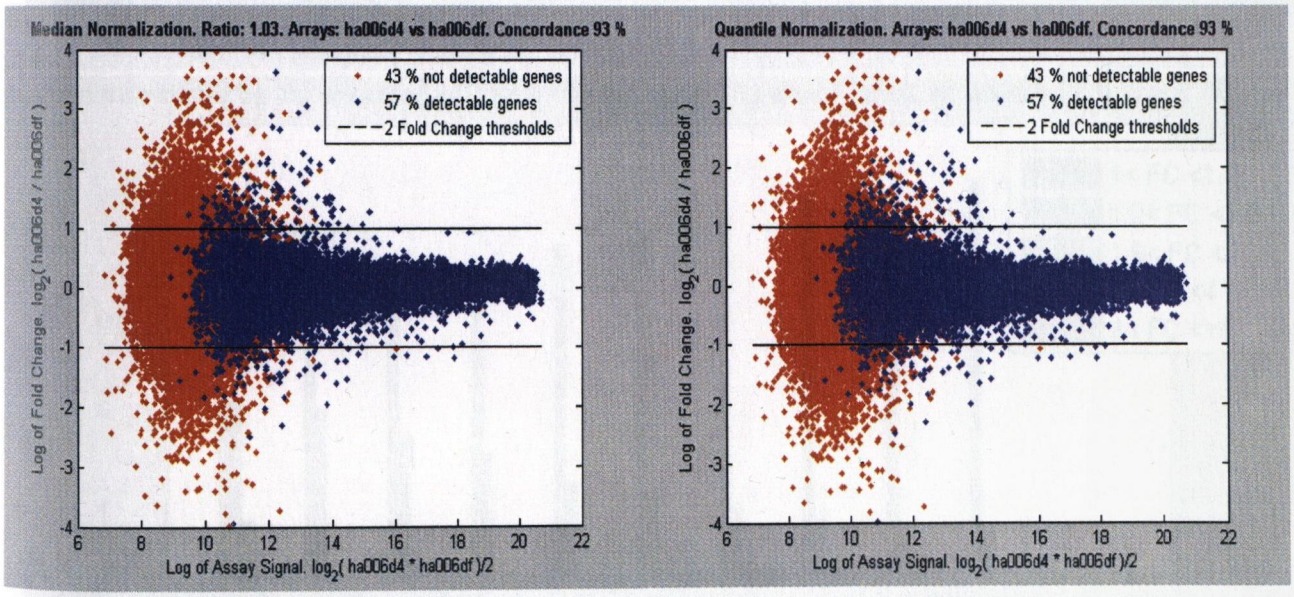

Figure 6.8 MA plots of technical replicates with different normalisation methods

This figure demonstrates the relative similarity of MA plots using median (L) and quantile (R) normalisations for two technical replicates.

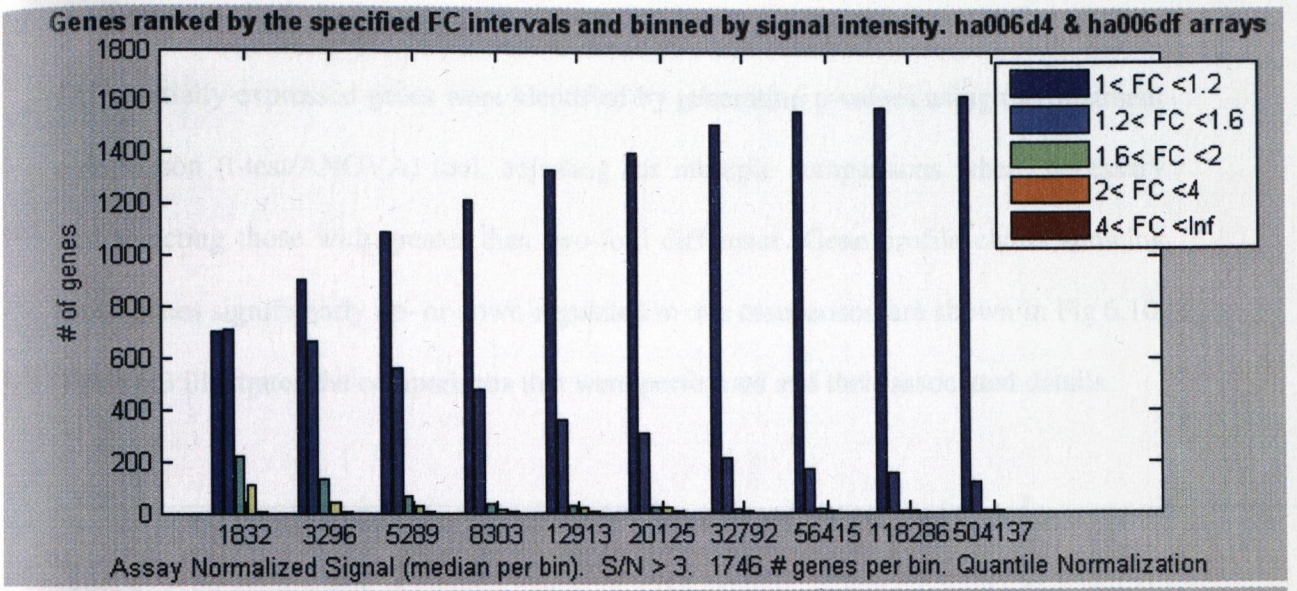

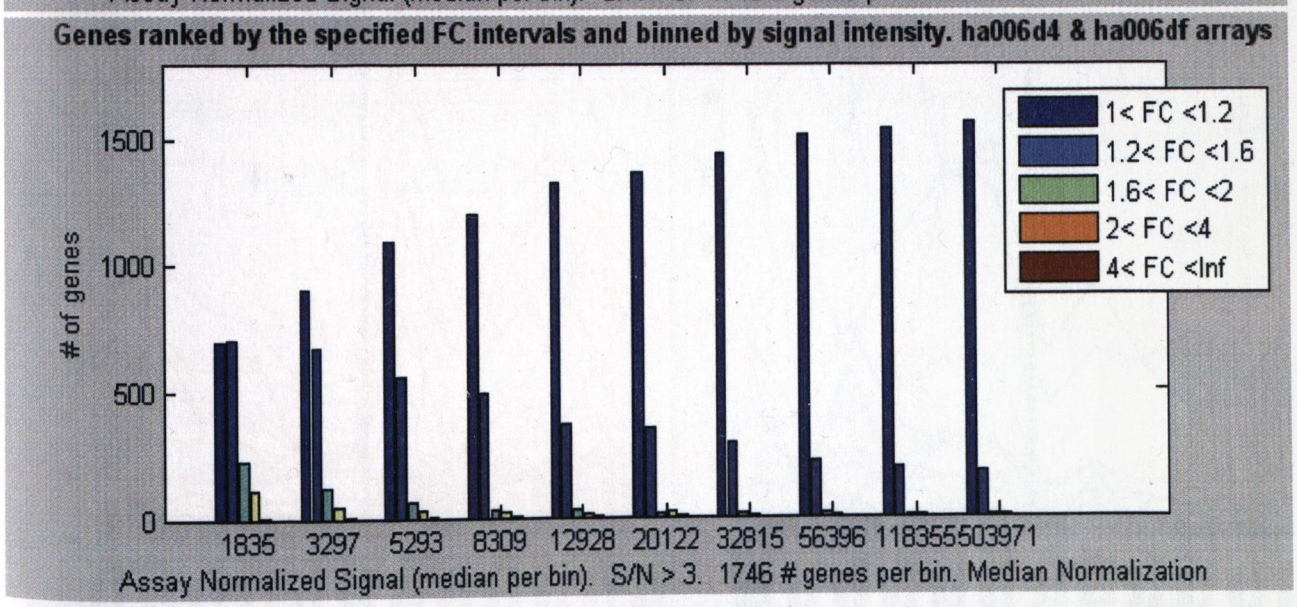

Quantile	**2.1**	**1.8**	**1.6**	**1.5**	**1.5**	**1.4**	**1.3**	**1.3**	**1.2**	**1.2**
Median	**2.1**	**1.8**	**1.6**	**1.5**	**1.4**	**1.4**	**1.3**	**1.3**	**1.3**	**1.2**
No normalization	**2.1**	**1.8**	**1.6**	**1.5**	**1.5**	**1.4**	**1.3**	**1.3**	**1.2**	**1.2**
Signal range	**1835**	**3297**	**5293**	**8309**	**12928**	**20122**	**32815**	**56396**	**118355**	**503971**

Figure 6.9 Fold change analysis

An example of fold change histograms for each binned 10% of genes are shown for median (top) and quantile (bottom) normalisations. The accompanying table displays the 95 percentile of fold change per bin and shows that different normalisation methods can be more suitable depending on signal intensities.

6.4.4.2 Treatment comparisons

Differentially expressed genes were identified by generating p-values using the treatment comparison (t-test/ANOVA) tool, adjusting for multiple comparisons where necessary and selecting those with greater than two-fold difference. Gene profile charts showing those genes significantly up- or down-regulated in one comparison are shown in Fig 6.10. Table 6.3 illustrates the comparisons that were performed and their associated details.

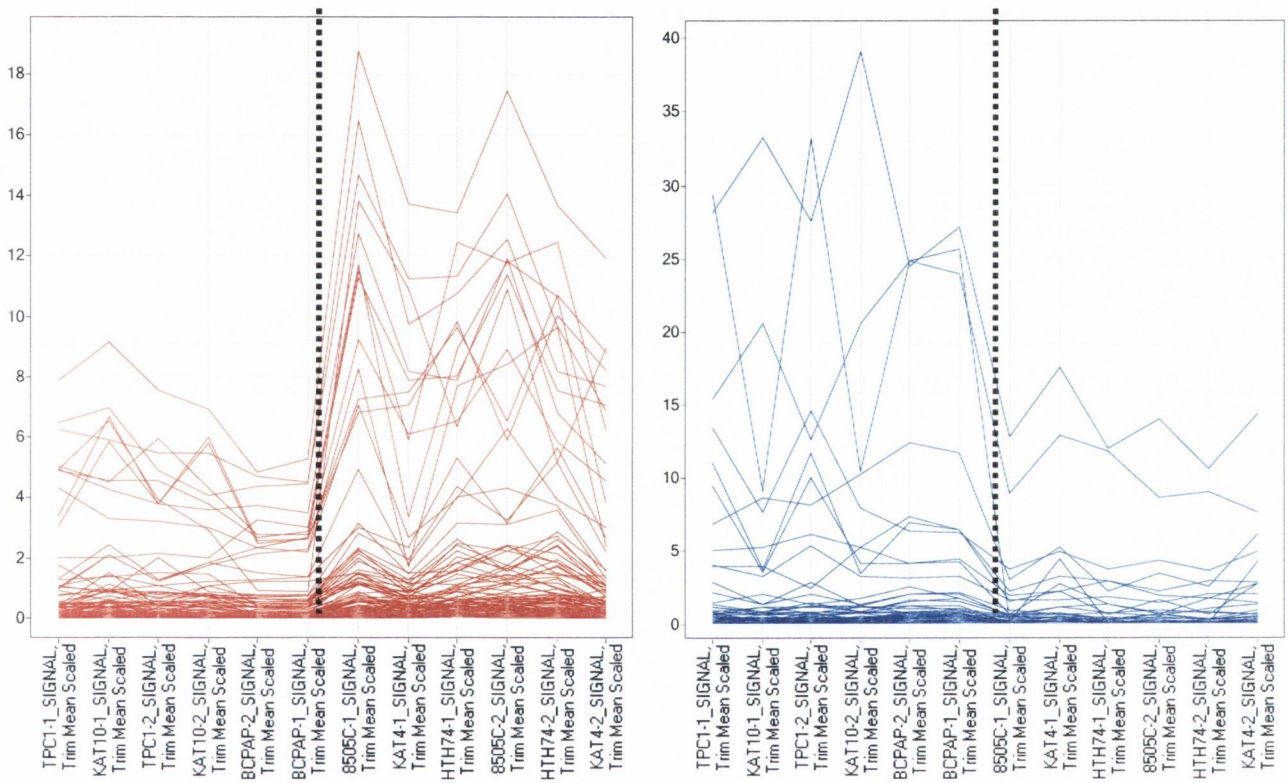

Figure 6.10 Gene profile charts

Figure displays genes that are significantly down-regulated (blue) and up-regulated (red) in ATC vs. PTC. The groups being compared are divided by a dashed line in each visualisation.

Comparison	FDR adjustment	Cut-off	No. of genes differentially expressed
ATC vs. PTC	none	p<0.01	204
BRAF mutated vs. BRAF wild-type	BY	p<0.05	234
PTC vs. Nthy-ori 3-1	Bon	p<0.05	182
TPC-1 vs. Nthy-ori 3-1	BY	p<0.05	1566
TPC-1 vs. non-ret mutated PTCs	BY	p<0.01	298

Table 6.3 Comparisons performed during the experiment

Abbreviations: BY – Benjamini and Yekutieli, Bon – Bonferroni.

6.4.4.3 Adjusting for fold change noise

Pair-wise comparisons were analysed and adjusted for fold change noise as described in chapter 6.3.4.5. Figure 6.11 shows the step-wise filtering of genes to yield a manageable number when analysing Nthy-ori 3-1 vs. TPC-1 cell lines.

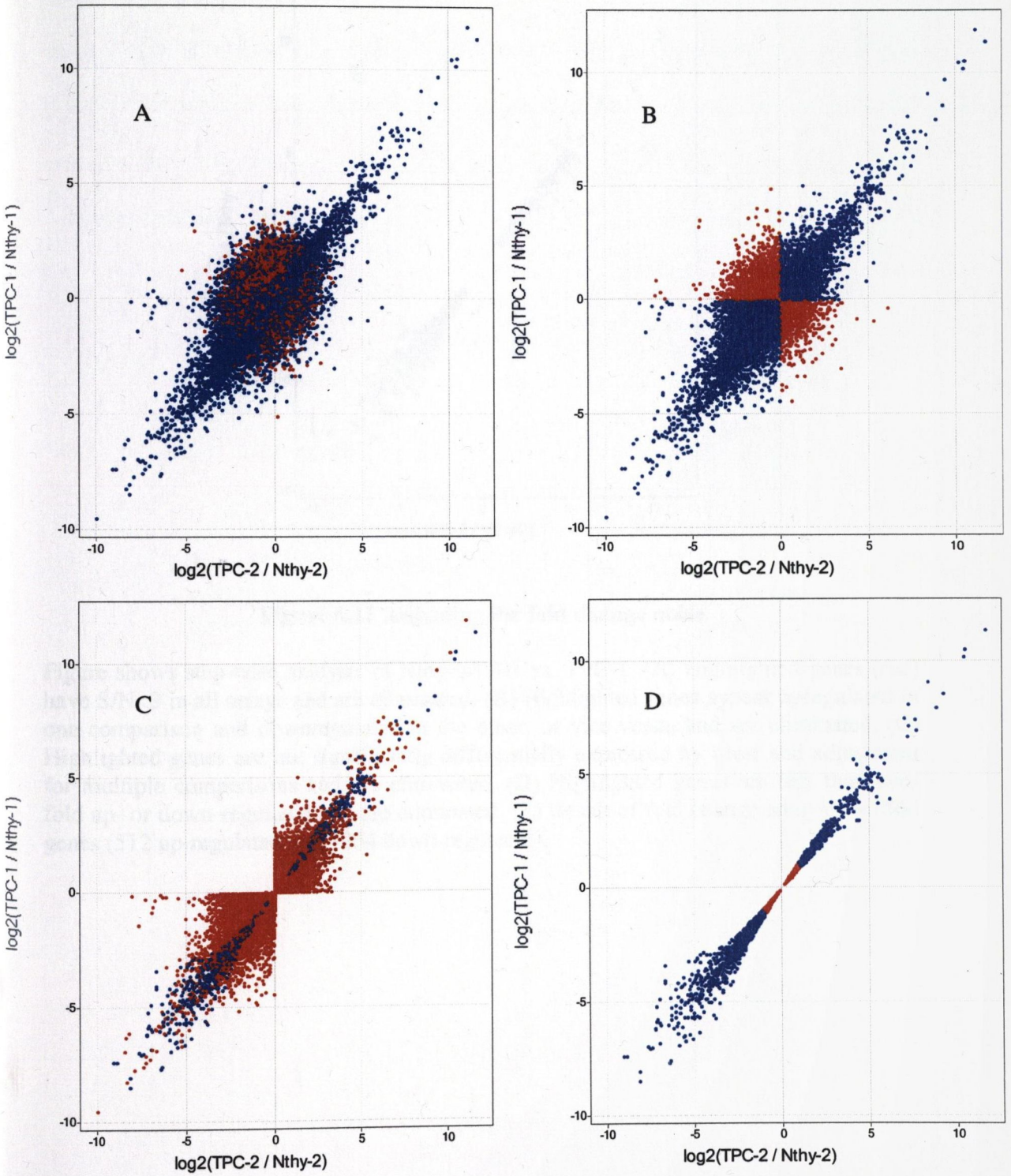
A
B
C
D
log2(TPC-1 / Nthy-1)
log2(TPC-2 / Nthy-2)
10
5
0
-5
-10

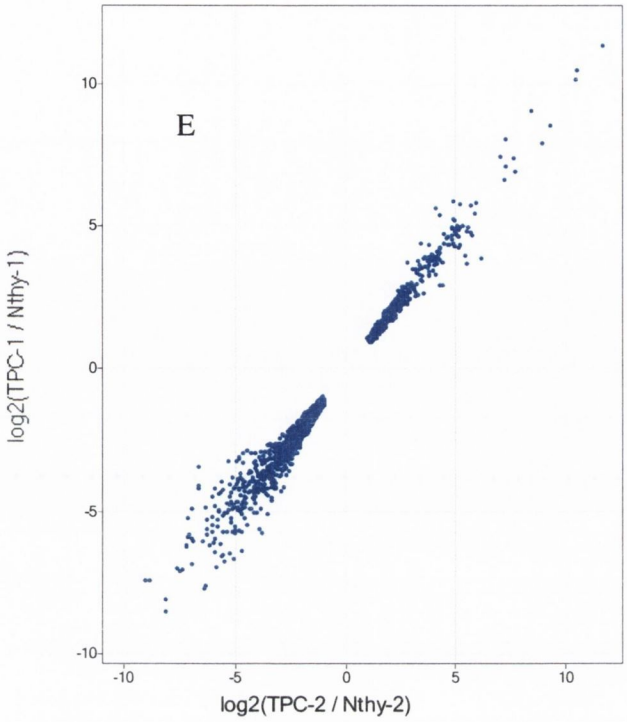

Figure 6.11 Adjusting for fold change noise

Figure shows step-wise analysis of Nthy-ori 3-1 vs. TPC-1. (A) Highlighted genes (red) have S/N<3 in all arrays and are eliminated. (B) Highlighted genes appear upregulated in one comparison and downregulated in the other, or vice versa, and are eliminated. (C) Highlighted genes are not significantly differentially expressed by t-test and adjustment for multiple comparisons and are eliminated. (D) Highlighted genes are less than two-fold up- or down-regulated and are eliminated. (E) Result of fold change analysis – 1566 genes (512 up-regulated and 1054 down-regulated).

6.4.4.4 Hierarchical clustering

Upon obtaining differentially regulated gene lists, hierarchical clustering was performed to determine whether technical replicates and cell line types grouped appropriately. An example of this clustering is shown in Fig 6.12, an analysis of BRAF mutated vs. BRAF wild-type cell lines.

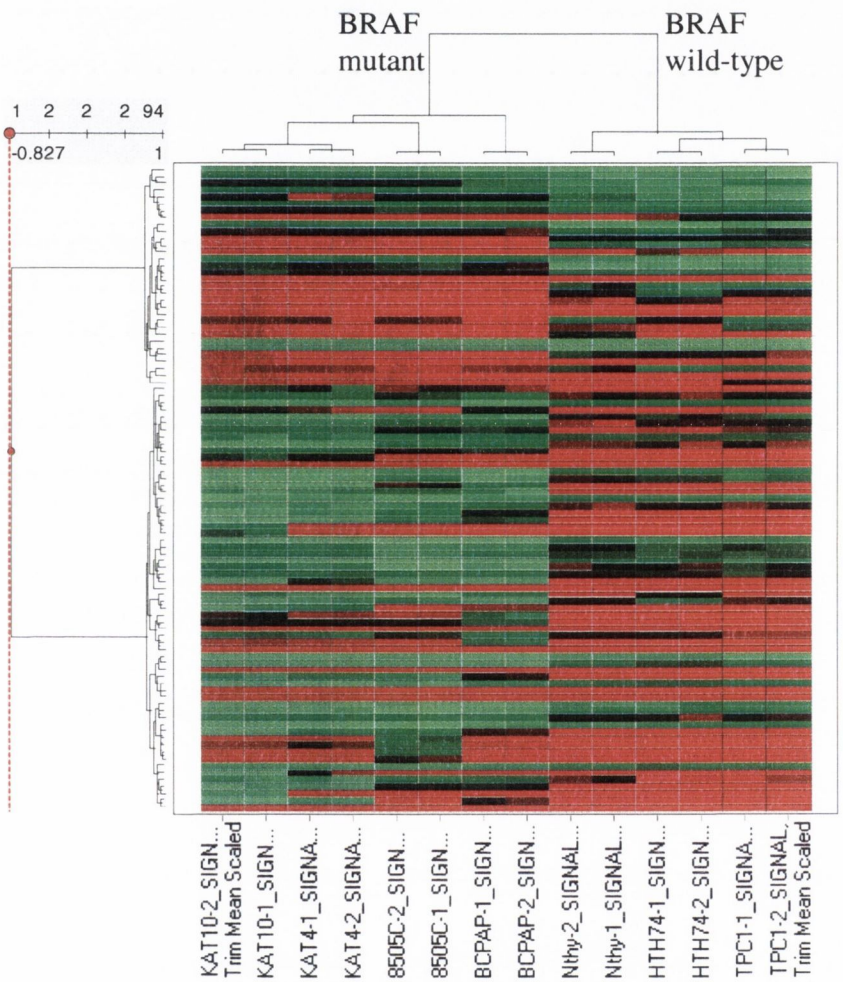

Figure 6.12 Hierarchical clustering

Hierarchical clustering of BRAF mutated and wild-type cell lines based on the gene lists obtained from treatment comparison analysis.

6.4.4.5 PANTHER

Final gene lists were uploaded and analysed in the online database known as PANTHER. Its functions include the ability to merge and differentiate genes within lists, the ability to graphically breakdown the protein families of the selected genes (see Fig 6.13) and the ability to check for over-representation of genes in a particular biological function.

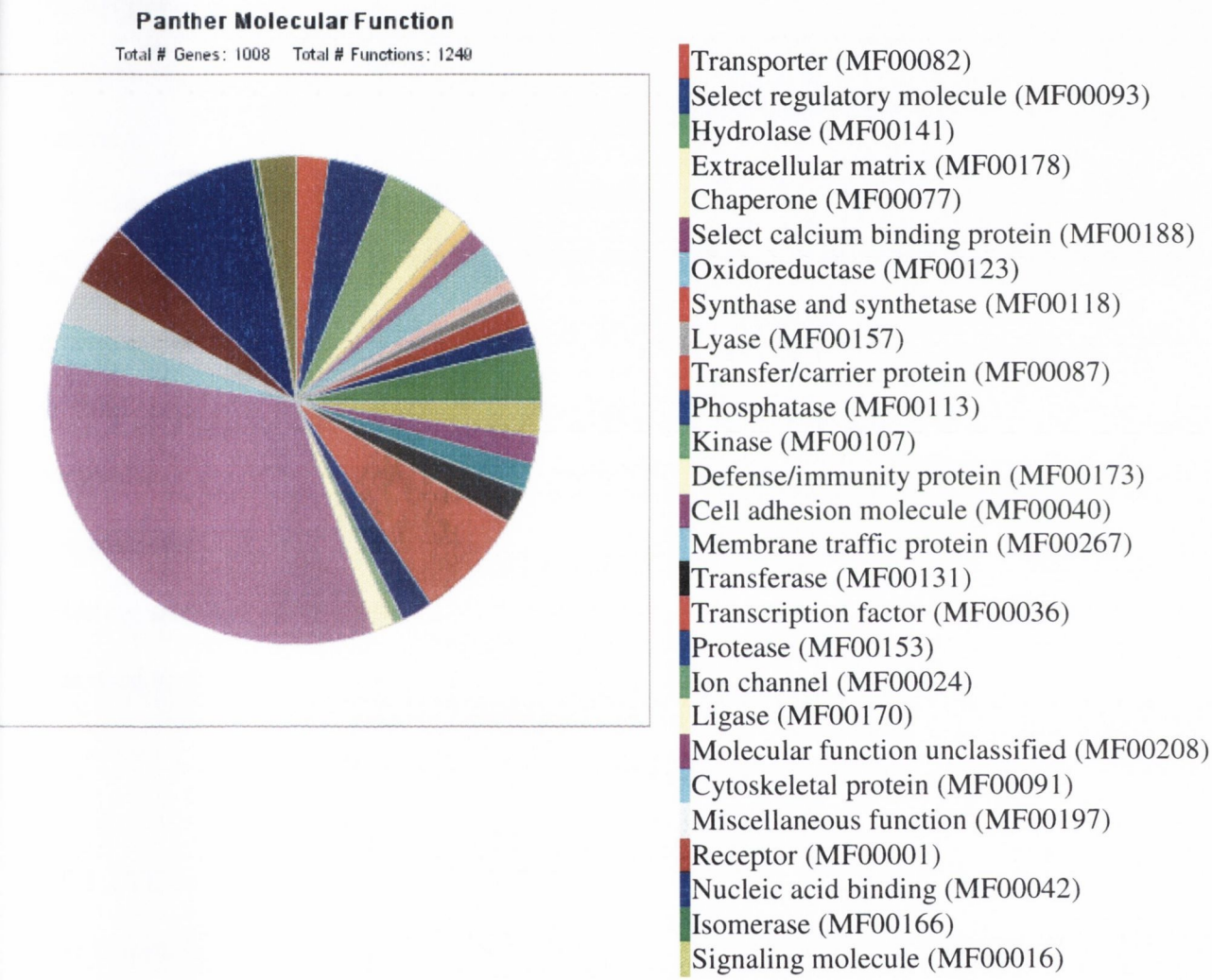

Figure 6.13 Pie chart of genes classed by molecular function

PANTHER display of the molecular function of those genes down-regulated in TPC-1 vs. Nthy-ori 3-1 cell lines.

6.5 Discussion

The vast majority of published scientific studies on thyroid carcinoma consist of the analysis of one or very few variables within a large sample group. Indeed, the previous three chapters fall into this category of study. More recently however, with the information gleaned from the human genome project and the advent of new high-throughput technological breakthroughs, this trend has been bucked towards the analysis of many (thousands of) variables in a lesser sample number, i.e. genomic expression analysis.

In this experiment, thyroid cell lines were used as *in vitro* models for biological processes/conditions that occur in human thyroid diseases. Microarray analysis was used to find genes that were differentially expressed between groups. The individual comparisons performed and the genes resulting from these comparisons are discussed in a stepwise manner below. It should be noted that it was not possible to list/discuss all genes resulting from the analyses as they run into the thousands. Instead, PANTHER analysis was used to filter out possible biologically relevant genes of interest.

6.5.1 ATC vs. PTC

The comparison of 3 ATC and 3 PTC cell lines was performed in order to investigate genes that may be involved in the progression from well-differentiated (i.e. PTC) to undifferentiated thyroid carcinoma.

- TGFB1 & TGFB2: up-regulated in ATC vs. PTC

Genes that were found to be upregulated in ATC compared with PTC included transforming growth factor beta 1 and 2 (TGFB1 & TGFB2). This finding is interesting as the RET proto-oncogene encodes for a receptor of TGFB-related neurotrophic factors, such as GDNF and neurturin. TGFB proteins are multifunctional cytokines that are involved in many cellular processes including receptor protein serine/threonine kinase signalling pathways, ligand-mediated signalling, cell cycle control and cell proliferation and differentiation. The molecules are potent inhibitors of epithelial cell proliferation and their overexpression in ATC is probably overcompensation due to a malfunction of one or more of their downstream signalling agents.

- CISH: up-regulated in ATC vs. PTC

Another gene that may be up-regulated in this manner is cytokine inducible SH2-containing protein (CISH). CISH proteins appear to provide negative regulation of cytokine signal transduction pathways such as the JAK-STAT pathway (Starr et al., 1997). They have been shown to be induced by TSH in thyroid cells previously (Park et al., 2000). Their PANTHER biological process classification indicated their functions include the inhibition of apoptosis.

- Calgizzarin: up-regulated in ATC vs. PTC

Growth inhibition by TGFB proteins has been attributed to the induction of cyclin-dependent kinase inhibitors. Calgizzarin (S100A11) has been found to be a intracellular mediator of this process (Miyazaki et al., 2004). It was originally found to be remarkably

elevated in colorectal cancers compared with that in normal colorectal mucosa (Tanaka et al., 1995) and subsequently to be a tumour suppressor gene.

Another gene downregulated was v-myb myeloblastosis viral oncogene homolog (avian)-like 2 (MYBL2). MYBL2 is another multifunctional protein involved in transcription regulation, developmental processes and cell cycle control. It is ubiquitously expressed, highly regulated throughout the cell cycle and appears to be required for cell cycle progression. Overexpression of MYBL2 has been shown to bypass p53- and $p21^{cip1}$-induced cell cycle arrest (Lin et al., 1994). Conversely, anti-sense repression of MYBL2 can induce growth arrest (Sala et al., 1992). Although it is generally thought to lack transforming activity it has been shown to induce resistance to apoptosis (Grassilli et al., 1999) and inhibit differentiation of monocytic cells (Bies et al., 1996) and retinoic acid-induced differentiation of neuroblastoma cells (Raschella et al., 1996).

- CD44: up-regulated in ATC vs. PTC

CD44 is a polymorphic family of immunologically related integral membrane glycoproteins associated with cell matrix adhesion and its associated signalling, lymphocyte activation and targeting, and tumour growth and metastasis. Although its splice variants are more often studied in thyroid cancer (Gu et al., 1998; Aogi et al., 1999), its expression has been shown to be upregulated in PTC (Gasbarri et al., 1999; Kim et al., 2002). It is widely believed to be an indicator of tumour aggressiveness in most cancers. Its up-regulation in ATC may reflect this behaviour. One thyroid study

however, found there to be no link between CD44 expression and metastasis in PTC (Kim et al., 2002).

- M-Ras: up-regulated in ATC vs. PTC

M-Ras is involved in several muscular processes such as development and contraction but more commonly in intracellular signalling cascades like the classic Ras proteins (Ha-, K-, and N-Ras). M-Ras also has transforming activities similar to its relations. Although this experiment showed its expression to be elevated in ATC, it has not previously been implicated in thyroid disease. However, epithelial cells expressing constitutively active M-Ras exhibit loss of several epithelial markers including E-cadherin and β-catenin (Ward et al., 2004) as described in chapters 3 and 4.

- CSNK1G2: up-regulated in ATC vs. PTC

Casein kinase 1, gamma 2 (CSNK1G2) is a non-receptor serine/threonine protein kinase. It has multiple functions within the cell and involved with processes such as DNA repair, endocytosis, cytokinesis, chromosome segregation and cell proliferation, differentiation and structure. It also participates in Wnt signalling and has been shown to act between Dsh and GSK-3 (see chapter 4.2.3 for a full description of Wnt signalling) in the Wnt pathway (Peters et al., 1999). Its involvement in this proliferative pathway may be the reason for its up-regulation in ATC.

- PML: down-regulated in ATC

More genes were found to be up- rather than down-regulated in ATC vs. PTC cell lines. Among those found to be down-regulated included the promyelocytic leukaemia transcription factor, PML. PML is a RING finger transcription factor thought to be involved in haematopoiesis, cell cycle control and tumour suppression. Studies have shown its expression to be lost in many tumour types but not in thyroid (Gurrieri et al., 2004), whereas others found it to be up-regulated in PTCs but not in FTCs (Yu et al., 2000). This may suggest that loss of the tumour suppressor function of PML is a relatively late event in thyroid cancer progression.

- LGALS8: down-regulated in ATC

Galectin 8 (LGALS8) is a member of the family of carbohydrate-binding proteins that act in cell adhesion. PANTHER also lists the gene under the biological process of induction of apoptosis. Studies have shown that disregulation of galectin-8 expression in neoplastic transformation seems to be correlated to the type of tumour. Although not the case for all tumour types, galectin-8 expression has been shown to be decreased in tumour tissues compared to normal in colon, pancreas, liver, skin and larynx (Danguy et al., 2001; Nagy et al., 2002). Interestingly, the closely related gene galectin-3 has been shown to be increased in thyroid tumours of follicular origin by both microarray (Huang et al., 2001) and numerous conventional analyses (Oestreicher-Kedem et al.; Saggiorato et al., 2004), suggesting an important role for the galectins in thyroid neoplastic transformation.

- ANKRD3: down-regulated in ATC

Ankyrin repeat domain 3 (ANKRD3) or DIK/RIP4 is another non-receptor serine/threonine protein kinase that was found to be down-regulated in ATC. It has been shown to both activate NFκB and induce apoptosis in a kinase-independent manner. Holland et al. (2002) showed ANKRD3 to be essential for differentiation in keratinocytes. This gene may therefore be one of the those responsible for the final progression from differentiated to anaplastic thyroid carcinoma.

6.5.2 BRAF mutated vs. BRAF wild-type cell lines

These two groups of cell lines were compared in order to obtain information on possible downstream effectors/results of aberrant RAF kinase signalling in thyroid cancer. For statistical purposes no distinction was made between homozygous and heterozygous V600E mutations as the heterozygous mutation is exclusively observed and sufficient to cause disease *in vivo*.

- Non-motor actin binding proteins: up-regulated in V600E cell lines

The lists of genes were compared to the whole genome on the basis of their molecular function/biological process. The significance of the over- or under-representation of a particular PANTHER functional category was tested using the binomial distribution. In the over-expressed list non-motor actin binding proteins were found to be over-represented ($p=3.15 \times 10^{-3}$). Members of this subset of genes over-expressed in V600E

cell lines included coronin, actin binding proteins, 1B and 2A (CORO1B & CORO2A) and bullous pemphigoid antigen 1 (BPAG1). These proteins in general are responsible for cell communication, adhesion, cell cycle control, proliferation and differentiation, and cell structure. Another unrelated structural protein found to be up-regulated was kinesin family member 9 (KIF9), a microtubule binding motor protein. These findings coupled with the fact that BRAF mutations are almost exclusively found in classic PTC, suggest that these genes might be involved in the manifestation of the signature characteristics of this PTC subtype, i.e. branching papillae with a characteristic core and epithelium with orderly, cuboidal to columnar cells.

- Histones: up-regulated in V600E cell lines

By far the most over-represented group in the BRAF mutated cell lines was that of the histones. Their over-representation was highly significant ($p=2.12 \times 10^{-11}$) with their members including histone 1H2ab, histone 1H2ae, histone 1H2aj, histone 1H2ak, histone 2H2ab and histone 3H2a. Histone over-expression has recently been reported in a microarray study in PTC in general (Yano et al., 2004), in particular, the H2A histone family. As histones are involved in chromatin packaging and remodelling, it is interesting to speculate that their over-expression may be responsible for the features observed in the nuclei of PTC such as finely dispersed chromatin condensed at the nuclear membrane and longitudinal grooving and inclusions. However these nuclear features are observed in other PTC subtypes that are inconsistent with BRAF mutation.

- GRB14: up-regulated in V600E cell lines

Growth factor receptor-bound protein 14 (GRB14) functions as a transmembrane receptor regulatory/adaptor protein and has been shown to inhibit several receptor tyrosine kinases such as insulin receptor (Bereziat et al., 2002) upon binding. In this regard, it may be a compensatory effect similar to the over-expression of CISH and TGFB1 & 2 observed in ATC.

Several transcription factors were also found to be over-expressed. An example of these is zinc finger protein 323 (ZNF323), a KRAB box transcription factor thought to be involved in embryonic organogenesis (Pi et al., 2002).

Interestingly, among the genes found to be down-regulated in V600E cell lines, actin family cytoskeletal proteins, non-motor actin binding proteins and cytoskeletal proteins were all found to be over-represented ($p=1.22 \times 10^{-4}$, 7.06×10^{-4} and 2.92×10^{-3} respectively). Examples of such genes include vinculin (VCL), stomatin (STOM) and synaptopodin (SYNPO). As discussed above, these genes are implicated in cellular adhesion, structure and motility. The fact that these classes of genes are over-represented in both the up- and down-regulated lists suggests that mutated Raf kinases may indeed play an important and complex role in influencing the morphology of thyroid carcinomas.

- CDKN1A: down-regulated in V600E cell lines

Cyclin-dependent kinase inhibitor 1A (CDKN1A) (p21, Cip1) plays a role in cell cycle control (G_1 arrest), cell proliferation and differentiation and functions as a tumour

suppressor. It was found to be under-expressed in the BRAF mutated group and studies have shown it to induce or enhance apoptosis in thyroid cancer lines following treatment by a variety of growth inhibitory agents (Yang et al.; Podtcheko et al., 2003; Hakulinen et al., 2002). Its down-regulation in the V600E cell lines may therefore represent a means of escape from cell cycle arrest and/or apoptosis.

- Inducers of apoptosis: down-regulated in V600E cell lines

Although unrelated gene family-wise, and therefore missed following PANTHER functional category testing, many genes were observed in the under-expressed list that are involved in apoptosis, in particular its induction. Caspase recruitment domain family, member 10 (CARD10) was among these genes. It has been shown to activate NFκB via BCL10 and IKK. Similarly under-expressed was death effector filament-forming Ced-4-like apoptosis protein (DEFCAP/CARD7). DEFCAP has the ability to form cytoplasmic structures termed death effector filaments. It enhances APAF1 and cytochrome c-dependent activation of pro-caspase-9 and consecutive apoptosis.

- Tumour necrosis factor receptors: down-regulated in V600E cell lines

Other genes that were also down-regulated were tumour necrosis factor receptor superfamily, members 10b and 6, or Fas (TNFRSF10B & TNFRSF6). Both genes are involved in cytokine and chemokine mediated signalling pathways. TNFRSF10B and TNFRSF6 are receptors for TNF-related apoptosis-inducing ligand (TRAIL, also known as Apo2L) and Fas ligand (FasL) respectively. Both induce apoptosis in a wide range of tissues. Fas has been shown to be widely expressed in most thyroid carcinomas, both *in*

vivo and *in vitro* (Mitsiades et al., 2000), and might even be upregulated in neoplastic thyroid cells compared to normal thyrocytes (Arscott et al., 1999). It has however never been studied in context with BRAF mutations and suggests another means with which this subtype of PTC may escape normal cell control.

6.5.3 ret/PTC positive vs. ret/PTC negative cell lines

This comparison, and those following, consist of one single cell line compared with one or several others. Acknowledging that this is a statistically weaker position from which to draw conclusions, more stringent adjustments were made by way of compensation (Table 6.3) to reduce the numbers of genes in the resulting lists to manageable numbers. Despite this however, some of the lists were quite extensive and as a result the single genes or groups of genes discussed below are far from comprehensive. Comparison of ret/PTC positive vs. negative cell lines was performed to investigate the possible effects of ret/PTC oncogene expression in thyroid carcinoma cell lines.

- RET: up-regulated in ret/PTC positive vs. negative cell lines

The first gene that was apparent in the up-regulated list was RET itself. This finding demonstrates that the probe for RET on the microarray must originate from the tyrosine kinase domain of the gene as this is the only native domain that the chimeric ret/PTC-1 oncogene possesses. PANTHER did indeed confirm that the RET probe was located at the far 3' end of the gene. In this regard, it functions as a convenient positive control and internal validation measure.

- FGF2: up-regulated in ret/PTC positive vs. negative cell lines

Fibroblast growth factor 2 (FGF2), a wide-spectrum mitogenic, angiogenic, and neurotrophic factor was over expressed in the TPC-1 cell line. It is involved in cell cycle control, cell proliferation/differentiation and cell surface receptor mediated signal transduction via the MAPKKK cascade. Studies have shown FGF2 to be over-expressed not only in well-differentiated thyroid carcinoma (Boelaert et al., 2003), but possibly in thyroid hyperplasia also (Shingu et al.; Thompson et al., 1998). Its over-expression seems to be an early event in thyroid cancer progression and may therefore be related to ret/PTC oncogene activation.

- LCP: up-regulated in ret/PTC positive vs. negative cell lines

Lymphocyte cytosolic protein 1/LCP1 (L-plastin) is a non-motor actin binding protein thought to be involved in cell structure and oncogenesis. It was over-expressed in the ret/PTC positive cell line and has been shown previously to be likewise expressed in a multitude of human cancers including ovarian, breast, pancreatic, melanoma and liposarcoma (Lin et al., 1993). It has not previously been linked with thyroid carcinoma.

- RAB18: up-regulated in ret/PTC positive vs. negative cell lines

The RAS proteins are G-proteins that function in signal transduction pathways. They are quite common and potent oncogenes and have been identified in a large percentage of all human cancers. They are discussed in chapter 1.5.3. With regard to thyroid cancer, they are more frequently observed in FTC rather than PTC but their presence in PTC is thought to signify a poor prognosis. One of the genes on the over-expressed list was

RAB18, a small GTPase and member of the RAS oncogene family. It is therefore possible that ret/PTC may exert influence through RAB18's intracellular signalling cascades in a similar manner to that exerted by RAS itself.

- MAP17: up-regulated in ret/PTC positive vs. negative cell lines

Membrane-associated protein 17 (MAP17) is expressed at significant levels in only a single epithelial cell population: the proximal tubular epithelial cells of the kidney. However, it was found to be up-regulated in the TPC-1 cell line. Relatively little is known about the gene or its protein product and PANTHER lists its molecular function as unclassified. It is however thought to be involved in oncogenesis due to the fact that it is markedly upregulated in various human carcinomas originating from the kidney, colon, lung, and breast, as compared with normal epithelial cell populations (Kocher et al., 1996). The fact that wild-type RET is expressed in the developing kidney suggests that there may be links between ret/PTC, MAP17 and the process of thyroid tumorigenesis.

- CDKN2A: up-regulated in ret/PTC positive vs. negative cell lines

Cyclin-dependent kinase inhibitor/CDKN2A (p16) was also over-expressed in the ret/PTC cell line. p16 functions as a tumour suppressor gene in cell cycle control by inhibiting cyclin dependent kinase 4 and 6, which phosphorylate the Rb (Retinoblastoma) protein. A reciprocal relationship between p16 and Rb expression has been observed suggesting the presence of a negative feedback loop allowing Rb to limit levels of p16. Thus, reduced or absent Rb function should result in enhanced p16 levels. p16 expression is down regulated in a variety of human tumours. Thyroid cancers are no exception to this

and p16 expression has been shown to be reduced by various means including mutation (Elisei et al., 1998), methylation (Boltze et al., 2003) and deletion (Jones et al., 1996). Despite this, overexpression of p16 has been observed in precancerous and malignant cervical lesions. Up-regulation of p16 in cervical lesions is believed to be a consequence of functional inactivation of Rb by HPV E7 protein (Sakaguuchi et al., 1996). Although p16 is a tumour suppressor protein its growth inhibitory effect is evaded because of E7 mediated inactivation of Rb in the cervix (Giarre et al., 2001). The ret/PTC oncogene or more likely one of its downstream effectors may therefore have to ability to inactivate or influence Rb in the thyroid resulting in the over-expression of p16.

- TOB1: down-regulated in ret/PTC positive vs. negative cell lines

TOB1 (transducer of ERBB2, 1), a transcription cofactor involved in receptor protein tyrosine kinase signalling pathways was down-regulated in TPC-1. It was initially identified as a protein that interacts with ERBB2 and its exogenous over-expression has been found to aggressively suppress the growth of NIH/3T3 cells and induce G_0/G_1 arrest (Matsuda et al., 1996). Moreover, mice lacking the TOB1 gene developed tumours including lung, liver, and lymph node (Yoshida et al., 2003). It has been shown to be under-expressed in various human cancers and in particular lung (Yoshida et al.; Iwanaga et al., 2003). Its under-expression in conjunction with ret/PTC activation provides further insight into the mechanisms of action of this oncogene.

- MNT: down-regulated in ret/PTC positive vs. negative cell lines

MAX binding protein (MNT) is a transcription cofactor involved in cell cycle control, proliferation and differentiation. Studies have shown that MNT knockout triggers many targets typical of the "Myc" response and is sufficient to transform primary fibroblasts in conjunction with Ras (Nilsson et al., 2004). LOH has been demonstrated in breast cancer (Nigro et al., 1998). This behaviour is consistent with that of a tumour suppressor gene. Its under-expression in the TPC-1 cell line is the first reported instance in thyroid disease.

6.5.4 TPC-1 vs. Nthy-ori 3-1

This comparison was performed as a continuation of the ret/PTC positive vs. negative cell line comparison discussed in the previous section. The reason it was performed was to reduce possible artefacts from the results that may have been caused by comparing the TPC-1 cell line to other PTCs. Genes may have been falsely included in the lists due to the fact that some of the cell lines were anaplastic in origin or that some had additional genetic defects such as BRAF mutations. The TPC-1 cell line was therefore compared to the "normal" cell line with a view to removing these unknown falsely differentially regulated genes. Although not a ideal comparison due to the fact that their origins are quite diverse and that Nthy-ori 3-1 is SV40 transformed, their comparison would be nonetheless better than the previous comparison in examining the effects of ret/PTC oncogene activation. Unfortunately, due to the nature of comparing just one sample to another, even with replicates, the number of differential genes was quite large. Even applying the most stringent FDR method resulted in far too many genes to discuss in this

thesis. As a result the only meaningful results that can be discussed are those obtained from the PANTHER functional category binomial testing.

Those groups that were up-regulated in the TPC-1 cell line compared with the "normal" cell line included actin family cytoskeletal proteins ($p=1.77 \times 10^{-4}$), non-motor actin binding proteins ($p=2.14 \times 10^{-4}$), cytoskeletal proteins ($p=4.75 \times 10^{-4}$) and other cytoskeletal proteins ($p=4.95 \times 10^{-3}$). These groups are all involved in cell structure and motility and once again are over-represented in one of the gene lists. Their consistent presence in the gene lists overall must be far from a coincidence and suggests that their over- and under-expression may be involved in thyroid carcinogenesis and especially thyroid cancer morphology.

Among genes down-regulated were kinases ($p=7.51 \times 10^{-4}$) and protein kinases ($p=1.88 \times 10^{-3}$). The interferon receptors were under-expressed ($p=9.6 \times 10^{-3}$) including interferon receptor gamma 2 and alpha 2 (IFNGR2 & IFNAR2). Likewise were extracellular matrix proteins ($p=2.8 \times 10^{-3}$) such as MMP11 and various collagens further underlining the potential structural changes in thyroid cancer. Once again, genes involved in the induction of apoptosis were significantly under-expressed ($p=7.07 \times 10^{-3}$). Individual members of this group included BAD, DEFCAP, TRAF4, APAF1, IFNGR2 and IFNAR2. The constant down-regulation of genes involved in the promotion of apoptosis over most comparisons is probably to be expected due to the fact that it is a consistent theme in cancer. It is interesting to speculate that the evasion of apoptosis in a tissue

normally associated with a low mitotic index may be an important element not only in PTC but thyroid cancer in general.

6.5.5 PTC cell lines vs. Nthy-ori 3-1

In the last comparison, all PTC cell lines were compared with the normal regardless of their known genetic aberrations. The reasoning behind this comparison was to obtain possible markers for PTC in general. Following t-testing and FDR adjustment the only genes found to be differentially regulated were all under-expressed in PTC. Ideally if one were looking for potential biomarkers of PTC they would preferably be those that were over-expressed in the disease state. This is because potential assays, be they PCR based or immunohistochemistry based, are easier to design if the diagnostic test is looking for the presence rather than the absence of a marker. Nonetheless, some of the genes found to be down-regulated in PTC are discussed below.

Similar groups were again found to be over-represented in this gene list. Extracellular matrix proteins were highly over-represented ($p=5.64 \times 10^{-6}$). Genes in this category included MMP11, various collagens and glypican 1 and 2 (GPC1 & GPC2). Cell adhesion molecules were over-represented ($p=1.09 \times 10^{-3}$), including beta 2 integrin (ITGB2) and various cadherin-related genes. The morphological significance of these families in PTC has been discussed previously.

Genes not found in other lists included large tumour suppressor, homolog 2 (LATS2), a putative non-receptor serine/threonine protein kinase involved in cell proliferation and differentiation and cycle control. It exerts its tumour suppressor function by down-regulating cyclin E and inhibiting the G1/S and (Li et al., 2003) and/or G2/M transition (Kamikubo et al., 2003). It has also recently been shown to induce apoptosis through downregulation of Bcl-2 and Bcl-x(L) (Ke et al., 2004). On a similar note, nerve growth factor receptor (NGFR) was under-expressed in PTC. NGFR, a member of the TNFR superfamily, functions in the JNK and NFκB cascade and is thus ultimately an inducer of apoptosis. Therefore the down-regulation of LATS2 and NGFR may confer a significant growth advantage to PTC.

6.5.6 Conclusion

As shown in the many studies of various cancers, expression microarrays can provide insights that were hard to obtain in the past when single genes or pathways were examined. This experiment has shown that thyroid carcinoma is no exception by making comparative analyses of microarray expression data for thyroid carcinoma cell lines using several variables including known mutations/oncogenes and carcinoma subtype.

The use of cell lines for this purpose may not be ideal but provided a readily available source of genetic material that may be a suitable *in vitro* model for what occurs in the human thyroid. Nevertheless, this study provides a wealth of data, some of which confirmed previous knowledge whereas others are novel.

If validated in larger independent panels including clinical samples, these genes, together with known tumour-specific chromosomal translocations, could prove to be a powerful molecular adjunct to thyroid tumour pathology for the purpose of general diagnosis and/or differentiating histologic subtypes of thyroid carcinoma.

6.6 References

Aogi K, Kitahara K, Urquidi V, Tarin D, Goodison S. Comparison of telomerase and CD44 expression as diagnostic tumor markers in lesions of the thyroid. Clin Cancer Res 1999; 5: 2790-7.

Arscott PL, Stokes T, Myc A, Giordano TJ, Thompson NW, Baker JR Jr. Fas (CD95) expression is up-regulated on papillary thyroid carcinoma. J Clin Endocrinol Metab 1999; 84: 4246-52.

Benjamini Y, Hochberg Y. Controlling the false discovery rate: a practical and powerful approach to multiple testing. J R Stat Soc Ser B 1995; 57: 289-300.

Benjamini Y, Yekutieli D. The control of the false discovery rate in multiple testing under dependency. Ann Stat 2001; 29: 1165-1188.

Bereziat V, Kasus-Jacobi A, Perdereau D, Cariou B, Girard J, Burnol AF. Inhibition of insulin receptor catalytic activity by the molecular adapter Grb14. J Biol Chem 2002; 277: 4845-52.

Bies J, Hoffman B, Amanullah A, Giese T, Wolff L. B-Myb prevents growth arrest associated with terminal differentiation of monocytic cells. Oncogene 1996; 12: 355-63.

Boelaert K, McCabe CJ, Tannahill LA, Gittoes NJ, Holder RL, Watkinson JC, Bradwell AR, Sheppard MC, Franklyn JA. Pituitary tumor transforming gene and fibroblast growth factor-2 expression: potential prognostic indicators in differentiated thyroid cancer. J Clin Endocrinol Metab 2003; 88: 2341-7.

Boltze C, Zack S, Quednow C, Bettge S, Roessner A, Schneider-Stock R. Hypermethylation of the CDKN2/p16INK4A promotor in thyroid carcinogenesis. Pathol Res Pract 2003; 199: 399-404.

Callow MJ, Dudoit S, Gong EL, Speed TP, Rubin EM. Microarray expression profiling identifies genes with altered expression in HDL-deficient mice. Genome Res 2000; 10: 2022-2029.

Danguy A, Rorive S, Decaestecker C, Bronckart Y, Kaltner H, Hadari YR, Goren R, Zick Y, Petein M, Salmon I, Gabius HJ, Kiss R. Immunohistochemical profile of galectin-8 expression in benign and malignant tumors of epithelial, mesenchymatous and adipous origins, and of the nervous system, Histol Histopathol 2001; 16: 861-8.

Dudoit S, Yang Y, Callow M, Speed T. Statistical methods for identifying differentially expressed genes in replicated cDNA microarray experiment. Statistica Sinica 2000; 12: 111-139.

Elisei R, Shiohara M, Koeffler HP, Fagin JA. Genetic and epigenetic alterations of the cyclin-dependent kinase inhibitors p15INK4b and p16INK4a in human thyroid carcinoma cell lines and primary thyroid carcinomas. Cancer 1998; 83: 2185-93.

Elkins R, Chu F.W. Microarrays: their origins and applications. Trends Biotechnol 1999; 17: 217-218.

Gasbarri A, Martegani MP, Del Prete F, Lucante T, Natali PG, Bartolazzi A. Galectin-3 and CD44v6 isoforms in the preoperative evaluation of thyroid nodules. J Clin Oncol. 1999; 17: 3494-502.

Ge Y, Dudoit S, Speed T. Resampling-based multiple testing for microarray data analysis. TEST 2003; 12: 1-44.

Giarre M, Caldeira S, Malanchi I, Ciccolini F, Leao M, Tommasino M. Induction of pRb degradation by Human Papillomavirus Type 16 E7 Protein is Essential To Overcome p16INK4A-imposed G1 Cell Cycle Arrest. Journal of Virology 2001; 75: 4705-4712.

Grassilli E, Salomoni P, Perrotti D, Franceschi C, Calabretta B. Resistance to apoptosis in CTLL-2 cells overexpressing B-Myb is associated with B-Myb-dependent bcl-2 induction. Cancer Res 1999; 59: 2451-6.

Gu J, Daa T, Kashima K, Yokoyama S, Nakayama I, Noguchi S. Expression of splice variants of CD44 in thyroid neoplasms derived from follicular cells. Pathol Int 1998; 48: 184-90.

Gurrieri C, Capodieci P, Bernardi R, Scaglioni PP, Nafa K, Rush LJ, Verbel DA, Cordon-Cardo C, Pandolfi PP. Loss of the tumor suppressor PML in human cancers of multiple histologic origins. J Natl Cancer Inst 2004; 96: 269-79.

Hakulinen P, Kosma VM, Komulainen H. Expression of p53 and p21 Ki-ras proteins in rat thyroid gland tumors induced by 3-chloro-4-(dichloromethyl)-5-hydroxy-2(5H)-furanone (MX). Anticancer Res 2002; 22: 703-6.

Holland P, Willis C, Kanaly S, Glaccum M, Warren A, Charrier K, Murison J, Derry J, Virca G, Bird T, Peschon J. RIP4 is an ankyrin repeat-containing kinase essential for keratinocyte differentiation. Curr Biol 2002; 12: 1424-8.

Holm S. A simple sequentially rejective multiple test procedure. Scand J Stat 1979; 6: 65-70.

Huang Y, Prasad M, Lemon WJ, Hampel H, Wright FA, Kornacker K, LiVolsi V, Frankel W, Kloos RT, Eng C, Pellegata NS, de la Chapelle A. Gene expression in papillary thyroid carcinoma reveals highly consistent profiles. Proc Natl Acad Sci U S A 2001; 98: 15044-9.

Iwanaga K, Sueoka N, Sato A, Sakuragi T, Sakao Y, Tominaga M, Suzuki T, Yoshida Y, K-Tsuzuku J, Yamamoto T, Hayashi S, Nagasawa K, Sueoka E. Alteration of expression or phosphorylation status of tob, a novel tumor suppressor gene product, is an early event in lung cancer. Cancer Lett 2003; 202: 71-9.

Jones CJ, Shaw JJ, Wyllie FS, Gaillard N, Schlumberger M, Wynford-Thomas D. High frequency deletion of the tumour suppressor gene P16INK4a (MTS1) in human thyroid cancer cell lines. Mol Cell Endocrinol 1996; 116: 115-9.

Kamikubo Y, Takaori-Kondo A, Uchiyama T, Hori T. Inhibition of cell growth by conditional expression of kpm, a human homologue of Drosophila warts/lats tumor suppressor. J Biol Chem 2003; 278: 17609–17614.

Ke H, Pei J, Ni Z, Xia H, Qi H, Woods T, Kelekar A, Tao W. Putative tumor suppressor Lats2 induces apoptosis through downregulation of Bcl-2 and Bcl-x(L). Exp Cell Res 2004; 298: 329-38.

Kim JY, Cho H, Rhee BD, Kim HY. Expression of CD44 and cyclin D1 in fine needle aspiration cytology of papillary thyroid carcinoma. Acta Cytol 2002; 46: 679-83.

Kocher O, Cheresh P, Lee SW. Identification and partial characterization of a novel membrane-associated protein (MAP17) up-regulated in human carcinomas and modulating cell replication and tumor growth. Am J Pathol 1996; 149: 493-500.

Lander ES, Linton LM, Birren B, et al. Initial sequencing and analysis of the human genome. Nature 2001; 409: 860-921. Erratum in: Nature 2001; 412: 565. Nature 2001; 411: 720.

Li Y, Pei J, Xia H, Ke H, Wang H, Tao W. Lats2, a putative tumor suppressor, inhibits G1/S transition. Oncogene 2003; 22: 4398-405.

Lin CS, Park T, Chen ZP, Leavitt J. Human plastin genes. Comparative gene structure, chromosome location, and differential expression in normal and neoplastic cells. J Biol Chem 1993; 268: 2781-92.

Lin D, Fiscella M, O'Connor PM, Jackman J, Chen M, Luo LL, Sala A, Travali S, Appella E, Mercer WE. Constitutive expression of B-myb can bypass p53-induced Waf1/Cip1-mediated G1 arrest. Proc Natl Acad Sci USA 1994; 91: 10079-10083.

Lockhart D, Winzeler E. Genomics, gene expression and DNA arrays. Nature 2000; 405: 827-836.

Matsuda S, Kawamura-Tsuzuku J, Ohsugi M, Yoshida M, Emi M, Nakamura Y, Onda M, Yoshida Y, Nishiyama A, Yamamoto T. Tob, a novel protein that interacts with p185erbB2, is associated with anti-proliferative activity. Oncogene 1996; 12: 705-13.

McPherson JD, Marra M, Hillier L, et al. A physical map of the human genome. Nature 2001; 409: 934-41.

Mitsiades N, Poulaki V, Tseleni-Balafouta S, Koutras DA, Stamenkovic I. Thyroid carcinoma cells are resistant to FAS-mediated apoptosis but sensitive tumor necrosis factor-related apoptosis-inducing ligand. Cancer Res 2000; 60: 4122-9.

Miyazaki M, Sakaguchi M, Akiyama I, Sakaguchi Y, Nagamori S, Huh NH. Involvement of interferon regulatory factor 1 and S100C/A11 in growth inhibition by transforming growth factor beta 1 in human hepatocellular carcinoma cells. Cancer Res 2004; 64: 4155-61.

Nagy N, Bronckart Y, Camby I, Legendre H, Lahm H, Kaltner H, Hadari Y, Van Ham P, Yeaton P, Pector JC, Zick Y, Salmon I, Danguy A, Kiss R, Gabius HJ. Galectin-8 expression decreases in cancer compared with normal and dysplastic human colon tissue and acts significantly on human cancer cell migration as a suppressor. Gut 2002; 50: 392-401.

Nigro CL, Venesio T, Reymond A, Meroni G, Alberici P, Cainarca S, Enrico F, Stack M, Ledbetter DH, Liscia DS, Ballabio A, Carrozzo R. The human ROX gene: genomic structure and mutation analysis in human breast tumors. Genomics 1998; 49: 275-82.

Nilsson JA, Maclean KH, Keller UB, Pendeville H, Baudino TA, Cleveland JL. Mnt loss triggers Myc transcription targets, proliferation, apoptosis, and transformation. Mol Cell Biol 2004; 24: 1560-9.

Oestreicher-Kedem Y, Halpern M, Roizman P, Hardy B, Sulkes J, Feinmesser R, Stern Y. Diagnostic value of galectin-3 as a marker for malignancy in follicular patterned thyroid lesions. Head Neck 2004 Aug 26 [Epub ahead of print].

Park ES, Kim H, Suh JM, Park SJ, Kwon OY, Kim YK, Ro HK, Cho BY, Chung J, Shong M. Thyrotropin induces SOCS-1 (suppressor of cytokine signaling-1) and SOCS-3 in FRTL-5 thyroid cells. Mol Endocrinol 2000; 14: 440-8.

Peters JM, McKay RM, McKay JP, Graff JM. Casein kinase I transduces Wnt signals. Nature 1999; 401: 345-350.

Pi H, Li Y, Zhu C, Zhou L, Luo K, Yuan W, Yi Z, Wang Y, Wu X, Liu M. A novel human SCAN/(Cys)2(His)2 zinc-finger transcription factor ZNF323 in early human embryonic development. Biochem Biophys Res Commun 2002; 296: 206-13.

Podtcheko A, Ohtsuru A, Tsuda S, Namba H, Saenko V, Nakashima M, Mitsutake N, Kanda S, Kurebayashi J, Yamashita S. The selective tyrosine kinase inhibitor, STI571, inhibits growth of anaplastic thyroid cancer cells. J Clin Endocrinol Metab 2003; 88: 1889-96.

R Development Core Team (2004). R: A language and environment for statistical computing. R Foundation for Statistical Computing, Vienna, Austria. ISBN 3-900051-00-3, URL http://www.R-project.org.

Raschella G, Negroni A, Pucci S, Amendola R, Valeri S, Calabretta B. B-myb transcriptional regulation and mRNA stability during differentiation of neuroblastoma cells. Exp Cell Res 1996; 222: 395-9.

Saggiorato E, Aversa S, Deandreis D, Arecco F, Mussa A, Pulighedu B, Cappia S, Conticello S, Papotti M, Orlandi F. Galectin-3: presurgical marker of thyroid follicular epithelial cell-derived carcinomas. J Endocrinol Invest 2004; 27: 311-7.

Sakaguchi M, Fujii Y, Hirabayashi H, Yoon HE, Komoto Y, Oue T, Kusafuka T, Okada A, Matsuda H. Inversely Correlated expression of p16 and Rb protein in Non-Small Cell Lung Cancers: An immunohistochemical study. Int J Cancer 1996; 65: 442-445.

Sala A, Calabretta B. Regulation of BALB/c 3T3 fibroblast proliferation by B-myb is accompanied by selective activation of cdc2 and cyclinD1 expression. Proc Natl Acad Sci USA 1992; 89: 10415-10419.

Schena M, Shalon D, Davis RW, Brown PO. Quantitative monitoring of gene expression patterns with complementary DNA microarray. Science 1995; 270: 467-470.

Shingu K, Fujimori M, Ito K, Hama Y, Kasuga Y, Kobayashi S, Itoh N, Amano J. Expression of fibroblast growth factor-2 and fibroblast growth factor receptor-1 in thyroid diseases: difference between neoplasms and hyperplastic lesions. Endocr J 1998; 45: 35-43.

Starr R, Willson TA, Viney EM, Murray LJL, Rayner JR, Jenkins BJ, Gonda TJ, Alexander WS, Metcalf D, Nicola NA, Hilton DJ. A family of cytokine-inducible inhibitors of signaling. Nature 1997; 387: 917-921.

Tanaka M, Adzuma K, Iwami M, Yoshimoto K, Monden Y, Itakura M. Human calgizzarin: one colorectal cancer-related gene selected by a large scale random cDNA sequencing and northern blot analysis. Cancer Lett 1995; 89: 195-200.

Thompson SD, Franklyn JA, Watkinson JC, Verhaeg JM, Sheppard MC, Eggo MC. Fibroblast growth factors 1 and 2 and fibroblast growth factor receptor 1 are elevated in thyroid hyperplasia. J Clin Endocrinol Metab 1998; 83: 1336-41.

Venter JC, Adams MD, Myers EW, et al. The sequence of the human genome. Science 2001; 291: 1304-51. Erratum in: Science 2001; 292:1838.

Ward KR, Zhang KX, Somasiri AM, Roskelley CD, Schrader JW. Expression of activated M-Ras in a murine mammary epithelial cell line induces epithelial-mesenchymal transition and tumorigenesis. Oncogene 2004; 23: 1187-96.

Yang HL, Pan JX, Sun L, Yeung SC. p21 Waf-1 (Cip-1) enhances apoptosis induced by manumycin and paclitaxel in anaplastic thyroid cancer cells. J Clin Endocrinol Metab 2003; 88: 763-72.

Yano Y, Uematsu N, Yashiro T, Hara H, Ueno E, Miwa M, Tsujimoto G, Aiyoshi Y, Uchida K. Gene expression profiling identifies platelet-derived growth factor as a diagnostic molecular marker for papillary thyroid carcinoma. Clin Cancer Res 2004; 10: 2035-43.

Yoshida Y, Nakamura T, Komoda M, Satoh H, Suzuki T, Tsuzuku JK, Miyasaka T, Yoshida EH, Umemori H, Kunisaki RK, Tani K, Ishii S, Mori S, Suganuma M, Noda T, Yamamoto T. Mice lacking a transcriptional corepressor Tob are predisposed to cancer. Genes Dev 2003; 17: 1201-6.

Yu E, Lee KW, Lee HJ. Expression of promyelocytic leukaemia protein in thyroid neoplasms. Histopathology 2000; 37: 302-8.

Chapter 7

General discussion, conclusions and future work

This thesis examined a series of potential biomarkers of disease biology and progression in thyroid neoplastic and inflammatory tissues. The molecular pathogenesis of thyroid carcinoma is poorly characterised with only a few chromosomal or genetic abnormalities being described. The assessment was carried out using molecular techniques including TaqMan® PCR for both expression and genotyping, and microarray technology.

7.1 E-cadherin

In chapter 3, E-cadherin expression in a variety of thyroid tissue types (both neoplastic and non-neoplastic) was studied. Although previous studies have shown reduced E-cadherin expression levels in thyroid carcinomas in general, its association with ret/PTC oncogenes has not previously been investigated. Its role in the thyroid autoimmune disease Hashimoto thyroiditis was also unknown. The study was undertaken to further elucidate the expression profile of E-cadherin in thyroid in association with ret/PTC-1 activation in thyroid tissue and to determine if a link exists between expression of the chimeric transcript and cellular adhesion.

In accordance with previous studies on the molecule, variable down-regulation of E-cadherin among carcinomas was demonstrated with a gradual reduction from normal to well-differentiated carcinomas to its absence in anaplastic lesions. More interestingly, ret/PTC-1 positive PTC cases had consistently lower E-cadherin expression levels than the corresponding ret/PTC-1 negative papillary carcinomas suggesting an association between ret activation and the loss of cellular adhesion.

An immediate question arising from this observation is how is this possible? It may be the case that down-regulation of E-cadherin expression is an ultimate consequence of the aberrant kinase signalling of ret/PTC. The relationship between tyrosine kinase signalling and reduced cellular adhesion is well known. Studies such as Behrens et al. (1993) have shown that disturbance of intercellular adhesion and induction of *in vitro* invasion of MDCK cells by tyrosine kinases such as v-src is accomplished by tyrosine phosphorylation of the E-cadherin/catenin complex. Both epidermal growth factor (EGF) (Hoelting et al., 1994) and transforming growth factor-α (TGF-α) (Haugen et al., 1993) have additionally been shown to increase migration, invasion and general tumorigenicity in PTC, presumably by similar means. Due to the fact that ret/PTC is also a tyrosine kinase, the tyrosine phosphorylation-dependent checkpoints that regulate cell adhesion, locomotion and tissue morphogenesis in the thyroid are likely to be important factors that contribute to converting the aberrant expression of a tyrosine kinase into the pathological phenotype of PTC.

Indeed, even in those differentiated tumours that show normal E-cadherin mRNA levels; its function may nonetheless be abolished by similar biochemical modifications. Additionally, due to the reversibility of phosphorylation reactions, differentiated epithelial structures such as thyroid follicles could reform in the metastases following appropriate dephosphorylation of the E-cadherin/catenin complex. However, further immunohistochemical studies will be required to investigate these theories fully.

Yap et al. (1995) showed that E-cadherin is essential for initial thyroid cell adhesion and follicular reorganisation. During thyroid follicular morphogenesis, E-cadherin mediates cell-cell adhesion and recruits other specialised proteins to the cell surface such as ZO-1 and Na^+/K^+-ATPase. Machado et al. (1999) suggested that inactivation of E-cadherin may be responsible for the characteristic growth pattern of diffuse gastric carcinomas. It may be therefore fair to say that in human cancers such as thyroid that reduced or absent E-cadherin expression is directly related to histological features as well as invasion and metastasis. Could this imply that the ret/PTC oncogene influences tumour morphology to the extent of the distinctive characteristics of PTC indirectly via E-cadherin? It is possible and perhaps even more so due to the fact that the study also revealed significantly different E-cadherin expression levels between PTC and FTC with the latter being much lower.

One of the more important discoveries was the fact that ret/PTC-1 positive Hashimoto thyroiditis cases also had significantly reduced E-cadherin expression levels compared to those in normal samples and in both ret/PTC-1 negative HT and PTC. This finding not only suggested an association between ret activation and the loss of cellular adhesion, but also more significantly provided further evidence that Hashimoto thyroiditis may represent a pre-neoplastic lesion of papillary thyroid carcinoma.

It has been suggested that tumour morphology reflects the function of cell adhesion molecules. It is possible therefore that immunohistochemical analyses could provide an early indicator of unstable E-cadherin expression, even at a time when this instability has

not yet resulted in a change in histomorphological features. This would be especially interesting to see in those cases of HT mentioned above.

Among the remaining outstanding questions are can E-cadherin down-regulation play a role in the initiation of tumorigenesis and perhaps even more importantly for therapeutic consideration, can E-cadherin down-regulation in tumours be effectively blocked?

7.2 The catenins

As a natural progression from E-cadherin, catenin expression was subsequently investigated in chapter 4. The objective was to measure the levels of E-cadherins ligands, β- and γ-catenin, in the same thyroid tissue types once again in the context of ret/PTC-1 positivity in order to establish if any further link exists between expression of the chimeric transcript and cellular adhesion in thyroid autoimmune disease and thyroid neoplasia.

Similar to E-cadherin, β-catenin was shown to decrease in conjunction with cancer progression, i.e. normal → PTC → ATC. γ-catenin was under-expressed in the ATC cohort but not so in PTC. The well-differentiated thyroid carcinomas showed varying levels of catenin expression. FTC showed significantly lower levels of catenin expression than PTC. No association was found between catenin levels and ret/PTC-1 presence. These results suggest that although the catenins may play a role in the progression of

thyroid cancer in general, they do not appear to be associated with ret/PTC-1 modulated pathways.

The apparent disparity between β- and γ-catenin expression in PTC may be accounted for by the fact they may differ in their potency as agents of transformation. A study by Zhurinsky et al. (2000) showed that the formation of γ-catenin-LEF/TCF-DNA complex in vitro is inefficient compared to a likewise complex containing β-catenin. Even in γ-catenin transfected cells, endogenous β-catenin (whose levels are elevated by γ-catenin transfection) is more readily recruited in the LEF/TCF-DNA complex.

Interestingly though, Kolligs et al. (2000) suggested that both catenins have different effects on TCF/LEF target genes. They found that even wild-type β-catenin had a two-fold greater effect on gene expression activation than wild-type γ-catenin in a model c-Fos promoter construct. In contrast wild-type γ-catenin was shown to more efficient at activating c-Myc promoter constructs than wild-type and even mutated β-catenin.

The differential transcriptional specificity that exists between β- and γ-catenin has yet to be fully understood. While both appear to be potent transactivators interacting with LEF/TCF factors, their specificities in binding and regulating target genes in mammalian cells are unknown. As signalling by them is thought to result from their transactivation potential, unravelling the nature of their target genes is of utmost importance. The relationships between the two molecules have yet to be fully characterised. Being so similar and sharing molecular partners, changes in the relative levels of the two can

trigger a variety of direct and indirect responses. Better understanding of these aspects and their physiological relevance depends on both direct characterisation of the affinities of the two proteins towards their different cytoplasmic and nuclear partners and the cellular mechanisms that may selectively modulate such interactions.

Of the components in the E-cadherin complex, β- and γ-catenin stand out as astonishing molecules whose functions extend well beyond those of more conventionally regarded regulators for E-cadherin. It is now known that they are involved in numerous signalling complexes including the Wnt pathway, growth factor receptor signalling and the TCF-LEF pathway. In addition to their binding to E-cadherin and members of the cytoskeleton, they interact with an ever-increasing number of molecules. Because of this, they can exert numerous functions from cell growth and death and cell migration to gene transcription. They therefore play key roles in tumorigenesis, development and many other physiological and pathological processes.

Further studies with larger numbers of samples are required to fully establish the clinical relevance and value of these molecules in thyroid cancer. Furthermore, it will be essential to examine E-cadherin/catenins in conjunction with their associated molecules such as TCF/LEF, GSK3β, APC and axin for example. It may be necessary to study the pattern of the expression of these molecules in primary as well as metastatic tumours, as they may play different roles at different stages of tumour development. Comparing the effects of both catenins on transcription, defining new potential target genes for both molecules through microarray technology and studies with transgenic mice employing tissue-

specific elimination of catenins will provide further insight into the roles played by these molecules in thyroid cancer.

7.3 BRAF

The earlier chapters investigated the possible effects of ret/PTC oncogene activation on members of the adherens junctions, namely E-cadherin and the catenins. Originally thought to be exclusively present in PTCs, our group demonstrated that Hashimoto thyroiditis cases could also harbour ret/PTC oncogene activation (Sheils et al., 2000).

BRAF, as a member of the Ras/Raf/MEK/ERK pathway has been implicated in a variety of human neoplasms including thyroid. While ret/PTC oncogenes are accountable for genetic aberrations leading to some PTCs, the purpose of this study was to assess BRAF T1799A mutation rates in various thyroid tissues and to investigate if concomitant mutations with ret/PTC activation occurred in inflammatory and/or neoplastic lesions.

The T1799A mutation was detected in 15 of 34 (44%) PTC samples and in none of the remaining thyroid tissue types (ATC, HT and FA/NORM) examined. This detection rate is comparable to the literature's 29-69% detection rate in PTC. T1799A mutation was mainly restricted to the classic morphological subtype of PTC. There was no significant statistical association between BRAF mutation and ret/PTC oncogene detection.

As stated by Lima et al. (2004), "the Chernobyl accident resulted in the highest number of a specific type of human cancer (PTC) that occurred as a consequence of a single event in a single place, at a specific time, ever recorded". The dramatic increase in the occurrence of thyroid carcinoma in areas of Belarus, Ukraine and the Russian Federation, following Chernobyl, has provided unique opportunities to study the molecular pathology of thyroid cancer.

By far the most intriguing, and perhaps disturbing, results to be gained from this study were those pertaining to temporal trends. It was speculated in chapter 5 that our results could indicate a progression from the potentially radiation-induced ret/PTC positive papillary carcinomas in the period 1991-96 to a more normally distributed, spontaneously BRAF mutated variety from 1996 to date. This observation begs the question how is this possible?

Other studies have shown increased thyroid cancer rates in distant geographical areas at the same time as the previously mentioned ret/PTC "spike" in this study. A recent report by the Committee Examining Radiation Risks of Internal Emitters (CERRIE) in the UK has shown the risks of getting cancer from tiny amounts of radioactivity could be higher than previously thought.

As discussed in chapter 5, several studies have shown that BRAF mutation rates in PTC from Ukraine are comparable to those found in American series. At the time of writing this, further studies have been published showing that the frequency of BRAF mutation is

significantly lower in post-Chernobyl PTC than in adult sporadic PTC (Lima et al., 2004). The low frequency of BRAF mutations in post-Chernobyl PTC may reflect the nature of the etiological agent. Ionising radiation is well known to be effective at causing DNA double-strand breaks as opposed to point mutations. Numerous studies have suggested the possibility that the major mechanism of thyroid carcinogenesis in radiation-induced thyroid carcinomas is the formation of rearrangements, such as ret/PTC oncogenes, because of direct double-strand breakage of DNA resulting in illegitimate reciprocal recombination favoured by spatial juxtaposition of the relevant loci during interphase. Therefore, unlike ret/PTC rearrangements, BRAF mutations seem to be inherently associated with PTC in a portion of patients, irrespective of geographical location or radiation exposure of the patient. In fact in the study by Xing et al. (2004) they found no BRAF mutations in FTC and benign adenomas from Ukraine patients with radiation exposure. This, coupled with the finding that a high prevalence of BRAF mutations is associated with a low rate of ret/PTC rearrangements in adult sporadic PTC further supports the hypothesis that BRAF mutation is not a radiation susceptible one, but a mutation that is caused by some other unknown event(s) that occurs specifically in PTC and not in other types of thyroid neoplasms.

Therefore, a similar bias towards ret/PTC rearrangements from 1991-3 exists in both this study and similar ones performed on material obtained from irradiated patients following Chernobyl. Similarly, reduced or non-elevated BRAF mutation rates were reported in the irradiated samples. A comparable phenomenon was reported in this current study cohort. The full health legacy of the Chernobyl nuclear disaster may not be known for many

more years. The major adverse health effect, namely increased thyroid cancer in the younger local population following the accident, has been well documented. The data presented in chapter 5 suggests a statistical link between exposure to Chernobyl fallout and thyroid molecular pathology in geographically distant populations exposed to lower levels of radionuclides, including adults.

It is now well recognised that aberrant activation of effectors along the ret/PTC-RAS-BRAF signalling pathway plays a prominent role in the pathogenesis of PTC. The relative lack of overlap between ret/PTC, RAS and BRAF mutations provides strong genetic evidence for the requirement of this signalling pathway for transformation to PTC. Despite this, specific phenotypic differences are evident between PTCs harbouring mutations of the different genes. For instance BRAF mutation is associated with the classic morphological variant of PTC and RAS mutation with the follicular variant. It is possible that the different oncoproteins may have different downstream effectors or even be involved in alternative pathways.

The high frequency of BRAF mutations found in PTC and their specificity to PTC or less differentiated tumours arising from PTC make BRAF a potentially important marker for tumour diagnosis and prognosis. The testing for BRAF mutations in thyroid tumours is further simplified by the fact that the vast majority are restricted to the T1799A mutation. There are several methodologies that could be applied for detection and some could be used not only at the time of surgery but also for preoperative diagnosis of thyroid FNA specimens. Some methods are even appropriate for use on archived samples, as shown in

this study. BRAF mutation analysis may prove useful in the future in assisting with the final diagnosis of cases that cannot easily be distinguished as either papillary or follicular carcinomas.

Early detection of BRAF mutations in PTC and especially in poorly differentiated or anaplastic carcinomas could be important in planning appropriate therapy. Attempts have been made to develop anticancer agents that target Raf proteins. However most of these agents such as antisense constructs and kinase inhibitors have been developed to target RAF-1 rather than BRAF.

BRAF is likely to be involved in tumour development primarily through deregulation of ERK activity. Therefore, anticancer agents targeted against BRAF must be effective in inhibiting MEK/ERK activation. For example, agents that can inhibit kinases that phosphorylate BRAF at serine 445, threonine 598 and serine 601 may be effective in reversing or tempering constitutive BRAF activation. High levels of RKIP may be effective in inhibiting BRAF accessibility to MEK, as is the case with RAF-1 (Yeung et al., 1999). Alternatively, the answer may lie with pre-existing chemical inhibitors of MEK. Inhibition of MEK represents a particularly suitable target for therapy due to its substrate specificity. Namba et al. (2003) showed that U0126, which inhibits phosphorylation of MEK1/2, could suppress cell growth in BRAF mutated cell lines. The targeting of MEK has also been shown to be effective *in vivo*. Sebolt-Leopold et al. (1999) used small molecule inhibitors of MEK1/2 as therapeutic agents in colon tumours and found one to exert strong growth inhibition. Another chemical inhibitor, CI-1040, is

already at the advanced stage of testing in clinical trials for many types of cancers. It is possible that inhibitors as described above may be used orally as non-cytotoxic agents in the clinical management of patients with advanced thyroid tumours in the future. Regardless of the agent or methodology used, pharmacological intervention along the BRAF-MEK-ERK axis is likely to provide a very powerful way of disrupting tumour progression due to the nature of this pathway.

The disparity in publications on RAF-1 and BRAF is astounding when one considers the importance of BRAF mutation in cancer – especially melanoma and thyroid carcinoma. As of writing, a PubMed search for BRAF yields 273 hits whereas a similar search for RAF-1 yields 1485 results. Despite the fact that it was the original Raf kinase discovered and that studies of RAF-1 have contributed vital insights into Raf kinase biology, more study needs to be devoted to the closely related BRAF, namely its mutation frequency (especially in radiation-related tumours) and its role in thyroid cancer and cancer as a whole.

7.4 Microarrays

Papillary thyroid carcinoma is the most common thyroid malignancy, with an incidence of <100 cases per year in Ireland and 16,000 cases per year in the U.S. The incidence is on the rise with a global estimate of half a million new cases this year. However, benign thyroid nodules are far more frequent and distinguishing between them and malignant nodules is a common diagnostic problem. It is estimated that 5-10% of people will develop a clinically significant thyroid nodule during their lifetime. Although the introduction of fine needle aspiration (FNA) 30 years ago made identifying PTC more reliable, clinicians often have to make decisions regarding patient care on the basis of equivocal information. This diagnostic dilemma can be further compounded in the evaluation of more problematic nodules such as fvPTC.

The molecular pathogenesis of PTC is poorly characterised with only a few chromosomal or genetic abnormalities being described. Although this thesis and innumerable other studies have examined a great many genes involved in the pathogenesis of thyroid disease, a vast number of other genes, signalling pathways and other basic mechanisms remain poorly defined. Another shortcoming is the insufficiency of diagnostic and prognostic biomarkers. This study was undertaken as a step toward identifying previously uncharacterised molecular genetic mechanisms of carcinogenesis in thyroid carcinoma and to further understand the roles played by ret/PTC oncogenes and BRAF V600E mutation in said disease.

A vast number of genes were found to be differentially expressed across groups and individual cell lines and are discussed in chapter 6. Some genes were found to be exclusive to certain comparisons whereas others were found to be present in many comparisons. The same could be said of molecular pathways following PANTHER analysis. The over-expression of genes such as CD44, casein kinases, p16 and FGF2 may lead to tumour invasiveness and metastasis formation and shift the balance from apoptosis to cell survival and proliferation. Likewise, the under-expression of tumour suppressor genes such as TOB1 and MNT may also contribute to the genesis and promotion of thyroid cancer.

In order to investigate fully the genes discussed in chapter 6, it will be necessary to conduct validation of these differentially expressed genes. These validations will have to be conducted using techniques such as quantitative PCR on the original samples to narrow down possible candidate genes. Genes surviving this initial scrutiny could then be used in validation of fresh or even formalin-fixed samples using a PCR technique or even immunohistochemistry.

Although the use of cell lines in the experiment was convenient with regard to the amount and availability of suitable material with the required mutations, it is probably not an ideal reflection of what occurs *in vivo*. This does not mean that the obtained results are wrong per se, but rather that there may be some discrepancies if compared to actual clinical specimens. Although there was an unlimited supply of genetic material when using cell lines, there were very few biological replicates due to the simple fact that it is

difficult to obtain several cell lines with a similar genotype. This also reduces statistical power somewhat. An ideal study would consist of a collection of numerous surgical samples with both diverse genotypes (BRAF and ret/PTC mutations) and phenotypes (fvPTC, tall cell variant, etc.). Initially, one would generate a differential gene list for a suitable comparison (i.e. benign vs. malignant or follicular variant vs. classic PTC) and supervised clustering would be performed based on these differential genes. Following this training phase, unknown samples can then be tested and fitted to the diagnostic groups predicted during the training. Once the unknown sample(s) have been tested, they then automatically become a part of the predictor model. This would be a perpetual process and could ultimately lead to an unrivalled diagnostic tool consisting of hundreds or even thousands of samples.

Many studies exist that have tried to identify markers for thyroid carcinoma that can distinguish benign from malignant lesions preoperatively. These include, among others: galectin-3 (LGALS3), telomerase, MET, HBME-1, TPO and p53. Although many of these candidates initially prove promising, many have often been revealed to be simply not specific enough for use as biomarkers and a single gene or even list of genes has yet to be translated into a clinically useful marker(s).

Molecular classification of tumours is an emerging technology that will undoubtedly change the way patients are managed. Follicular lesions of the thyroid are one group of neoplasms that may benefit greatly from molecular analysis as a part of the diagnostic process. It is currently possible to determine the levels of gene expression by PCR on

RNA isolation from as few as 10 cells from an FNA biopsy (Winzer et al., 1998) and from paraffin-embedded material as shown throughout this thesis. A recent study has investigated the FNA technique for preoperative diagnosis of MTC (Takano et al., 1999).

This study has shown that molecular analysis reveals genes that can distinguish between "normal" thyroid, PTC and ATC *in vitro*. It also revealed genes and pathways that are significantly associated with the different signature mutations commonly found in thyroid cancer. These data provide insight into the molecular pathogenesis of thyroid carcinoma and may provide insights into new treatments. Although an emerging technology, further work on clinical specimens may provide a molecular basis for the classification of thyroid tumours that are problematic diagnostically for even the most experienced pathologist. It will prove useful in deciding both the necessity and extent of surgery in patients with nodules. The number of benign thyroid nodules that are unnecessarily operated on will be reduced accompanied with a corresponding reduction in the number of malignant lesions that escape the attention of the surgeon. Furthermore, decisions regarding postoperative treatment will be able to be made with greater confidence. Although there is some degree of resistance to the integration of high-throughout genome-wide techniques into the clinical setting from traditionalists, there is little doubt they will play ever increasing roles in the future. As Arthur C. Clarke said: "Any sufficiently advanced technology is indistinguishable from magic".

7.5 References

Behrens J, Vakaet L, Friis R, Winterhager E, Van Roy F, Mareel MM, Birchmeier W. Loss of epithelial differentiation and gain of invasiveness correlates with tyrosine phosphorylation of the E-cadherin/beta-catenin complex in cells transformed with a temperature-sensitive v-SRC gene. J Cell Biol 1993; 120: 757-66.

Haugen DR, Akslen LA, Varhaug JE, Lillehaug JR. Demonstration of a TGF-alpha-EGF-receptor autocrine loop and c-myc protein over-expression in papillary thyroid carcinomas. Int J Cancer 1993; 55: 37-43.

Hoelting T, Siperstein AE, Clark OH, Duh QY. Epidermal growth factor enhances proliferation, migration, and invasion of follicular and papillary thyroid cancer in vitro and in vivo. J Clin Endocrinol Metab 1994; 79: 401-8.

Kolligs FT, Kolligs B, Hajra KM, Hu G, Tani M, Cho KR, Fearon ER. gamma-catenin is regulated by the APC tumor suppressor and its oncogenic activity is distinct from that of beta--catenin. Genes Dev. 2000; 14: 1319-31.

Lima J, Trovisco V, Soares P, Maximo V, Magalhaes J, Salvatore G, Santoro M, Bogdanova T, Tronko M, Abrosimov A, Jeremiah S, Thomas G, Williams D, Sobrinho-Simoes M. BRAF mutations are not a major event in post-Chernobyl childhood thyroid carcinomas. J Clin Endocrinol Metab 2004; 89: 4267-71.

Machado JC, Soares P, Carneiro F, Rocha A, Beck S, Blin N, Berx G, Sobrinho-Simoes M. E-cadherin gene mutations provide a genetic basis for the phenotypic divergence of mixed gastric carcinomas. Lab Invest 1999; 79: 459-65.

Namba H, Nakashima M, Hayashi T, Hayashida N, Maeda S, Rogounovitch TI, Ohtsuru A, Saenko VA, Kanematsu T, Yamashita S. Clinical implication of hot spot BRAF mutation, V599E, in papillary thyroid cancers. J Clin Endocrinol Metab 2003; 88: 4393-7.

Sebolt-Leopold JS, Dudley DT, Herrera R, Van Becelaere K, Wiland A, Gowan RC, Tecle H, Barrett SD, Bridges A, Przybranowski S, Leopold WR, Saltiel AR. Blockade of the MAP kinase pathway suppresses growth of colon tumors in vivo. Nat Med 1999; 5: 810-6.

Takano T, Miyauchi A, Matsuzuka F, Liu G, Higashiyama T, Yokozawa T, Kuma K, Amino N. Preoperative diagnosis of medullary thyroid carcinoma by RT-PCR using RNA extracted from leftover cells within a needle used for fine needle aspiration biopsy. J Clin Endocrinol Metab 1999; 84: 951-5.

Winzer R, Schmutzler C, Jakobs TC, Ebert R, Rendl J, Reiners C, Jakob F, Kohrle J. Reverse transcriptase-polymerase chain reaction analysis of thyrocyte-relevant genes in fine-needle aspiration biopsies of the human thyroid. Thyroid 1998; 8: 981-7.

Xing M, Vasko V, Tallini G, Larin A, Wu G, Udelsman R, Ringel MD, Ladenson PW, Sidransky D. BRAF T1796A transversion mutation in various thyroid neoplasms. J Clin Endocrinol Metab 2004b; 89: 1365-8.

Yap AS, Stevenson BR, Keast JR, Manley SW. Cadherin-mediated adhesion and apical membrane assembly define distinct steps during thyroid epithelial polarization and lumen formation. Endocrinology 1995; 136: 4672-80.

Yeung K, Seitz T, Li S, Janosch P, McFerran B, Kaiser C, Fee F, Katsanakis KD, Rose DW, Mischak H, Sedivy JM, Kolch W. Suppression of Raf-1 kinase activity and MAP kinase signalling by RKIP. Nature 1999; 401: 173-7.

Zhurinsky J, Shtutman M, Ben-Ze'ev A. Differential mechanisms of LEF/TCF family-dependent transcriptional activation by beta-catenin and plakoglobin. Mol Cell Biol 2000; 20: 4238-52.